EXPERIMENTAL RESEARCH ON SEISMIC RETROFITTING OF R/C EXTERIOR BEAM-COLUMN-SLAB JOINTS UPGRADED WITH CARBON FIBER REINFORCED POLYMER (CFRP) SHEETS

by

Erdal Gökgöz

B.S. in Civil Engineering, Boğaziçi University, 2005

Submitted to the Institute for Graduate Studies in

Science and Engineering in partial fulfillment of

the requirements for the degree of

Master of Science

Graduate Program in Civil Engineering

Boğaziçi University

2008

EXPERIMENTAL RESEARCH ON SEISMIC RETROFITTING OF R/C EXTERIOR BEAM-COLUMN-SLAB JOINTS UPGRADED WITH CARBON FIBER REINFORCED POLYMER (CFRP) SHEETS

APPROVED BY:

Asst. Prof. Cem Yalçın
(Thesis Supervisor) .....

Assoc. Prof. Azadeh Parvin
(Thesis Co-Supervisor) .....

Prof. Uğur Ersoy .....

Asst. Prof. Kutay Orakçal .....

Asst. Prof. Şevket Özden .....

DATE OF APPROVAL: 17.01.2008

To my father, whom I owe my engineering abilities to.

ACKNOWLEDGEMENTS

I would like to gratefully acknowledge my thesis supervisors, Asst. Prof. Cem Yalçın and Assoc. Prof. Azadeh Parvin, for their invaluable guidance and support during the experimental research. I would also like to thank to the other members of examining committee, Prof. Uğur Ersoy, Asst. Prof. Şevket Özden and Asst. Prof. Kutay Orakçal for their helpful suggestions and valuable comments.

I would like to express my special gratefulness to my friends and colleagues, Ibrahim Topcu, Osman Kaya and Selçuk Altay for their help and suggestions during the construction and testing of the specimens, to the assistants of Structures Laboratory, Savaş Atmaca and Serap Altın, and to the technicians, Hasan Şenel and Hamdi Ayar, for their help in the experimental phase of this research.

I want to state my pleasure to my colleagues, Onur Ertaş, Nurihan Amuce and Rahman Shahshenas, for their valuable supports in my thesis study.

My special gratitude goes to my fiancée, Gökçe, for her patience, faithful companionship and continuous encouragement.

Special thanks are due to my family, my mother and brother, for their encouragement, help, and continuous support during every phase of my education.

This research has been financially supported by the U.S. National Science Foundation through grant OISE-0535294; the Scientific and Technological Research Council of Turkey (TUBITAK) through grant ICTAG-I597-NSF (103I026) and Boğaziçi University Scientific Research Project, under Grant No. 05A401. I would also like to acknowledge the BASF-YKS, the Chemical Company, and Akçansa Hazırbeton A. Ş. due to their support in material supply. The conclusions and recommendations presented in this report are solely those of the author and do not necessarily represent the views of the sponsor.

ABSTRACT

EXPERIMENTAL RESEARCH ON SEISMIC RETROFITTING OF R/C EXTERIOR BEAM-COLUMN-SLAB JOINTS UPGRADED WITH CARBON FIBER REINFORCED POLYMER (CFRP) SHEETS

Under seismic action, the most critical part of R/C structures, which were built in the United States before 1970, is beam-column joints. Common deficiencies of these joints could be summarized as; widely spaced column ties, no transverse reinforcement in joint region, inadequate lap splicing in column and insufficient embedment length of positive beam reinforcement in the joint. This research investigates the actual behavior of such joints with an inclusion of transverse beams and a floor slab. Moreover, CFRP wrapping methodologies are developed to improve the seismic behavior of such deficient joints.

In order to investigate the effect of CFRP retrofitting on the behavior of exterior beam-column joints, four 2/3-scaled reinforced concrete beam-column subassemblies were produced and tested under constant axial load and reversed cyclic loading. Three of the specimens had floor slabs and one specimen had only transverse beams (without the slab). The specimen that had no floor slab and one of the other specimens with floor slab were tested as control specimens without the CFRP application. The remaining two specimens with floor slabs were retrofitted with CFRP sheets and then tested.

Experimental results demonstrated that torsional cracks on the transverse beams and shear deformations within the joint core turned out to be critical especially when the floor slab was included. Slippage of the positive beam reinforcement in the joint region was another significant deficiency observed in the control specimens. CFRP retrofitted specimens exhibited superior behavior in terms of load carrying capacities. Slippage of the positive beam reinforcement was successfully prevented. Beams and columns were also confined by CFRP sheets and their performance was enhanced in terms of shear and torsional strength.

ÖZET

DÖŞEMELİ BETONARME KENAR BİRLEŞİM BÖLGELERİNİN KARBON FİBER TAKVİYELİ POLİMER MALZEMELERLE SİSMİK GÜÇLENDİRİLMESİ

Amerika Birleşik Devletleri'nde, 1970 öncesinde yapılan betonarme binalar incelendiğinde, kolon–kiriş birleşim noktalarının deprem etkisi altında en kritik bölgeler olduğu gözlenmiştir. Kolon etriyelerinin geniş aralıklarla yerleştirilmesi, kolon-kiriş birleşim bölgesinde etriye bulunmaması, kolon donatısı bindirme boyunun kısa olması ve kiriş donatılarının yetersiz ankraj edilmesi, birleşim noktalarındaki ortak detaylandırma hatalarıdır. Bu araştırma, döşeme ve yükleme yönüne dik yönde yer alan kirişlerin etkisi altında, belirtilen birleşim noktalarının davranışını incelemektedir. Bu yetersizliklere sahip birleşim noktaları için, CFRP ile sargılama teknikleri geliştirilmektedir.

CFRP sargılama ile güçlendirmenin, kolon-kiriş birleşim noktası davranışına etkisi, dört, 2/3 oranlı, betonarme kolon-kiriş birleşim noktası numunesi üretilip, sabit eksenel yük altında, tersinir yatay kuvvetler ile test edilerek incelenmiştir. Bu numunelerden üçü, döşeme ve yükleme yönüne dik yönde yer alan kirişlere sahipken, biri sadece yükleme yönüne dik yönde yer alan kirişlere sahiptir. Döşemesiz numune ve döşemeli numunelerden biri kontrol numunesi olarak, CFRP uygulanmadan test edilmiş, kalan iki numune ise, CFRP ile güçlendirildikten sonra test edilmişlerdir.

Deneysel sonuçlar göstermiştir ki, kesme ve burulma kuvvetleri altındaki deformasyonlar, özellikle döşemeli numunelerde oldukça kritik seviyelerdedir. Yetersiz ankraj edilmiş kiriş donatılarının sıyrılması, kontrol numunelerinde gözlenen bir diğer önemli sorundur. CFRP ile güçlendirilmiş numuneler, taşıma gücü bakımından oldukça üstün bir performans sergilemişlerdir. Kiriş donatılarındaki sıyrılma problemi başarıyla çözülmüş, kirişler ve kolonlar sarılarak, kesme ve burulma dayanımları arttırılmıştır. Güçlendirilmiş numunelerin enerji sönümleme kapasitelerinde de artış gözlenmiştir.

TABLE OF CONTENTS

LIST OF FIGURES

LIST OF TABLES

LIST OF SYMBOLS / ABBREVIATIONS

A_g	Cross-sectional area of column
$b_{f,\ max}$	Maximum flange thickness
$b_{f,\ overhanging}$	Overhanging flange thickness
C_b	Internal horizontal compression force
d	Depth of beam
Ø	Diameter of rebar
f_c'	Compressive strength of concrete
γ	Joint shear strength factor
h	Height of column
h_c	Height of column
L	Span length
l_c	Lenght of column
L1	Length of first strip
L2	Length of second strip
L3	Length of third strip
M	Moment
M_r	Moment strength ratio
$M_{ultimate}$	Ultimate moment
M_{yield}	Yielding moment
N	Axial load
P	Load
T_b	Internal horizontal tension force
t_{min}	Minimum slab thickness
V	Shear force
V_b	Beam shear force
V_c	Column shear force
w	Distributed load
x	Distance from support
z_b	Distance between beam longitudinal bars

ACI	American Concrete Institute
CFRP	Carbon fiber reinforced polymer
EQ	Earthquake
GFRP	Glass fiber reinforced polymer
GLD	Gravity load designed
LVDT	Linear variable differential transformer
NSM	Near-surface mounted
R/C	Reinforced concrete
2-D	Two dimensional
3-D	Three dimensional

1. INTRODUCTION

1.1. General

Recent earthquakes catastrophically show that reinforced concrete structures, especially constructed before 1970 are highly susceptible to damage under seismic action. Potential hazard of such buildings can put pressure on people who live in these buildings. Today, there are millions of buildings which are vulnerable under moderate to strong seismic activity. Although, replacement of such buildings with the new ones is a radical solution, its implications are not economical and practical. Rehabilitation of such structures seems the only way in most cases to save these buildings.

In the last three decades, researchers have investigated deficiencies of the reinforced concrete frame structures, which were damaged during the earthquakes, and consequently developed retrofitting measures for these seismic deficiencies. There is no doubt that numerous methods have been developed using different approaches. However, the most critical part of these reinforced concrete frame structures appears to be the beam-column joints according to failure type of buildings under seismic action.

Figure 1.1. Joint failure from 1999 Kocaeli EQ (Sezen *et al.*, 2000)

In seismic actions, beam-column connection, as one of the most critical structural sub-assemblages, transfers the forces from the beams to the columns and vice versa. In order to have a uninterrupted force transfer between the beams and columns, joints should have sufficient shear strength. Joints, that are designed for only gravity loads do not have such strength. Besides of shear strength, the performance of the joint depends on the some other main parameters, namely, confinement of the joint core, anchorage of the longitudinal reinforcement bars and strength ratios of column to beam as well. Geometry of the members and their directions are also effective in seismic behavior of beam-column joints.

Recent earthquakes confirm that there is a strong need for retrofitting the beam-column joints in order to maintain the integrity of the existing buildings after a detrimental earthquake. Among various retrofitting methods, researchers have already investigated steel or reinforced concrete jacketing and epoxy injection. They demonstrated their positive effects with experimental studies.

Polymer technologies have made a significant progress in the last two decades and fiber reinforced polymers (FRP) have become an important alternative for Civil Engineering application. Among them, carbon fiber reinforced polymer (CFRP) sheets are widely-used materials and they are very efficient for retrofitting R/C structures offering advantages such as resistance to corrosion, ease of application and low unit weight.

1.2. Research Objectives and Scope

The main objectives of this experimental research are to:

- Develop an advanced seismic retrofitting strategy for 3-D Beam-Column joints using CFRP sheets.
- Understand the effects of floor slabs and transverse beams on response of Beam-Column joint.
- Determine the effect of CFRP wrapping on behavior of 3-D Beam-Column joint.
- Investigate the applicability of CFRP sheets on such joints.
- Compare and evaluate experiment results with 2-D test results.

In the experimental program, four 2/3-scale reinforced concrete beam-column subassemblies were tested under constant axial load and reversed cyclic loading following a predefined displacement history.

The specimens were three dimensional and consisted of top and bottom columns, two beams in the transverse directions and one beam in the longitudinal direction. All of the specimens had the same dimensions and details and they were designed according to pre-1970's ACI 318 codes and design practice of that time.

Three of the specimens had floor slabs and one specimen had only transverse beams without the slab. The specimen, which had no floor slab and one of the other specimens with floor slab were tested as control specimens without the CFRP application. The remaining two specimens which had floor slabs were retrofitted with CFRP sheets.

The performance of the joints was evaluated by examining the lateral load versus story drift response, cracking pattern, joint shear response, beam and column rotations, strain values in longitudinal and transverse reinforcement and also CFRP sheets, energy dissipation capacity and stiffness deterioration.

In this research, carbon fiber reinforced polymer sheets were used to retrofit beam-column joint with floor slabs and transverse beams. Whereas many researchers have proposed design guidelines of FRP applications without including the effects of transverse beams and slabs, difficulty in applying the CFRP sheets onto 3-D concrete surface and comparing its effectiveness is another parameter most researchers omit. Consequently, this is an important inspiration of the research.

1.3. Report Outline

This experimental investigation on the seismic behavior of reinforced concrete beam-column-slab connections and retrofitting of these connections by using CFRP sheets is presented on this thesis.

Chapter 1 provides brief information about the behavior of the joint under seismic action and the objectives of this research. Literature review and previous research results are summarized and some details of the key researches were emphasized on the second chapter. In chapter 3, all the details of the experimental study are shown with construction techniques and testing phases. Experimental results are presented with graphical data in chapter 4. Discussion and comparison of test results including 3-D versus 2-D test results are also presented in this chapter. Chapter 5 gives a summary of findings and recommendations for further research in this area.

2. LITERATURE REVIEW

2.1. Introduction

Recent earthquakes evidently confirm once again that the behavior of beam-column connections is very crucial for seismic resistance of reinforced concrete structures. In other words, the most critical part of the reinforced concrete structure is the beam-column joint. In order to understand the behavior of beam-column joints, number of experimental and analytical studies has been held since the 1960's. Today, sufficient experimental and analytical data on seismic response of joints were derived from these studies and furthermore, parameters governing joint behavior and the principal mechanism for joint failure could be described clearly.

Figure 2.1. Damage on beam-column joint during Kocaeli EQ (Sezen *et al.*, 2000)

R/C framing systems, designed primarily for gravity loads, with little or no attention given to lateral load effects, are typically characterized by non-ductile reinforcing details in the joint regions and in the members. Beres *et al.* (1996) conducted a comprehensive research on the seismic response of connection regions for gravity load designed frames in order to evaluate these frames and to properly plan repair and retrofit strategies.

Today, there is a strong need for strengthening of such seismically deficient joints. However, there are many difficulties in methods and their applications. Undoubtedly, efficiency of these techniques is the most important and critical factor. These strengthening methodologies are not only applied to the joints, but also applied to members and/or overall framing systems as well. The most common methods for strengthening are the construction of R/C jackets and steel jackets or steel cages. These methods require intensive labor and detailing and therefore their applications need too much time and effort.

In the last two decades, a new technique for strengthening structural elements has become very popular. Today, the use of fiber reinforced polymers as externally bonded reinforcement in critical regions of R/C elements is widely used for strengthening a variety of R/C members, namely beams, columns and non-structural walls in order to increase the capacities of these members under flexural, shear and compressive forces.

2.2. Design Philosophy of Beam-Column Joints

Simple analysis of moment-resisting frame of a typical R/C structure is very practical in order to understand the design philosophy of the joints. Fundamentally, there are two different types of forces which are applied to the structures; lateral and vertical forces. Vertical forces are applied to structure as gravity loading and moment distribution of R/C structure subjected to this loading may be described as in Figure 2.2a. On the other hand, horizontal forces consists of wind and earthquake loads and the latter one is more critical for R/C structures. Figure 2.2b illustrates the moment distribution of such frame subjected to earthquake loading.

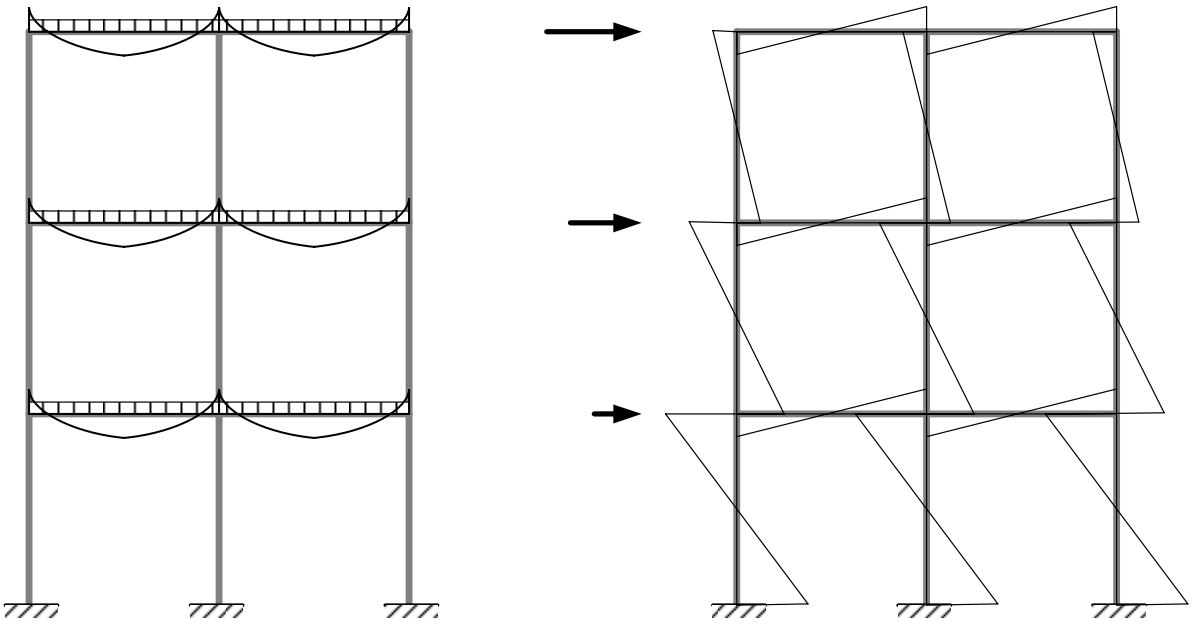

Figure 2.2. Moment diagrams of a frame under a) Gravity loads, b) EQ loads

Almost all structures can resist their own weight and therefore they can stand as if there is no lateral loading; namely earthquake loading. For that reason, the critical moment diagram is evident under earthquake loading. Forces acted on any exterior joints under lateral loading can be seen in Figure 2.3. Moment reversals on the joint are very sharp and this circumstance generate highly considerable shear forces, both in vertical and horizontal directions. Shear failure in the joint may originated from these shear forces. Shear failure is extremely undesired, because it causes very sudden failure of structure without dissipating required energy during the earthquake.

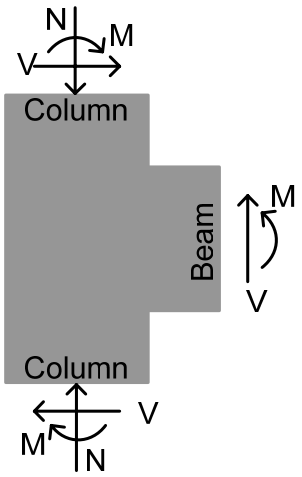

Figure 2.3. Forces acted on an exterior beam-column joint

Another common type of failure in the joint region could be seen as bond slip of the longitudinal reinforcement bars in both beams and columns due to suddenly changing boundary conditions under reversed moments. This event triggers a sudden decrease in the capacity of the joint strength and therefore less energy can be dissipated.

Failure modes of the joint have been investigated by many researchers and they were classified according to Meinheit and Jirsa (1981) as (a) beam hinging, (b) column hinging, (c) joint concrete crushing, (d) reinforcing bar anchorage failure, and (e) joint shear failure. Figure 2.4 illustrates these failure modes. According to design philosophy of the R/C structures, desired failure of the moment resisting frame should occur at the beam. In other words, yielding hierarchy should be satisfied as first yielding occurs at the beam and last yielding occurs at the column.

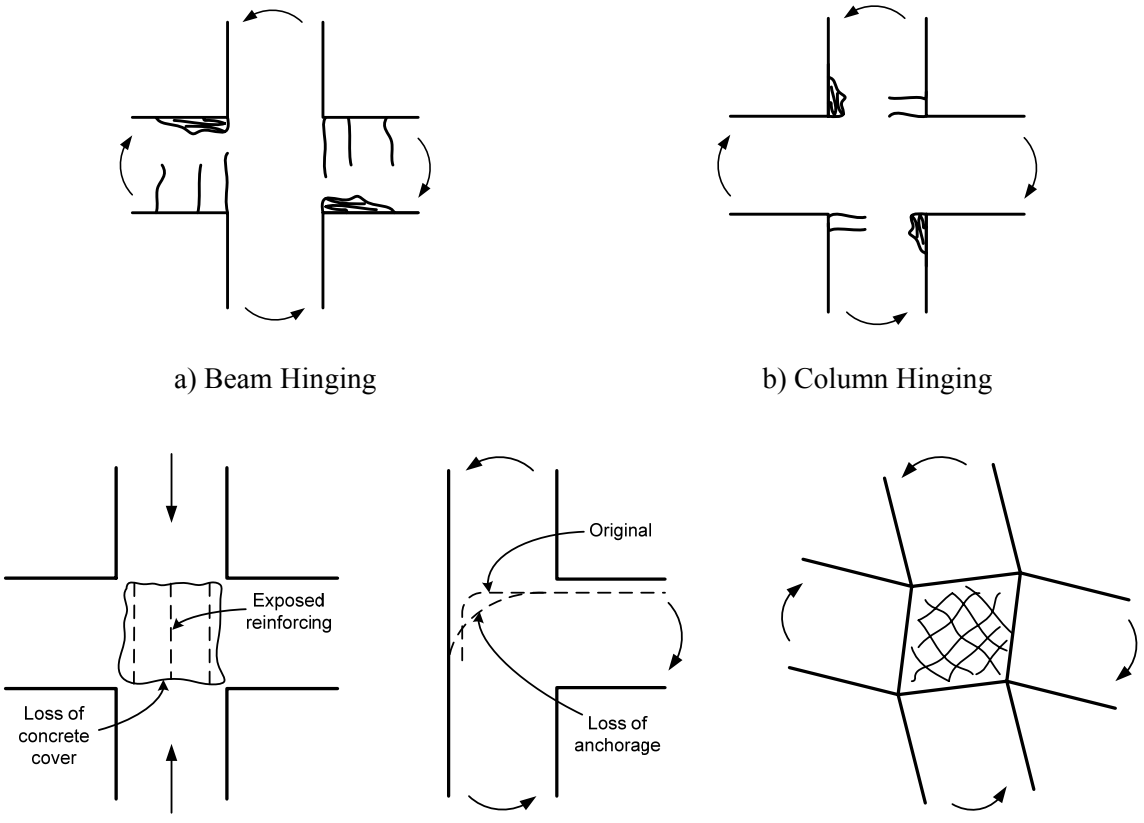

a) Beam Hinging

b) Column Hinging

c) Column Crashing

d) Reinforcing Bar Anchorage

e) Connection Shear

Figure 2.4. Failure modes of typical beam-column joints

During a strong earthquake, R/C frames need large displacement capacities. There are two possibilities to supply this demand; by using displacement capacities of members and joints. This condition is described in terms of ductility. Ductility is defined as the ability of a structure to undergo large amplitude cyclic deformations in the elastic range without a substantial reduction in strength (Park, 1989).

According to design philosophy, R/C beams should have required ductility; otherwise, joints are forced to meet these displacement needs. However, joints cannot supply these demand since their behavior is governed by shear and bond-slip mechanism, both of which typically exhibit poor hysteretic properties. A poor hysteretic behavior is also obvious evidence of less energy dissipation capacity of the joint.

Current design codes emphasize the importance of yielding hierarchy of the moment resisting R/C frames. According to this common approach, beam should be hinged before the joint failure occurs. In order to maintain this yielding, strength of beams should be limited and ductility of beams should be increased. By this way, the deformations of the joint can be prevented and sustain large displacement capacities for frames.

The buildings which were designed and constructed before 1970 in the United States have been investigated by numerous researchers. Some typical details of structures were identified by Beres *et al.* (1996) through a review of detailing manuals (ACI 315) and design codes (ACI 318) from the past five decades, and in consultation with practicing structural engineers. The following details were found typical and judged to be potentially critical towards the safety of gravity load designed (GLD) R/C structures in an earthquake.

- Longitudinal reinforcement ratio of the columns does not exceed 2%.
- Lapped splices of column reinforcement at the maximum moment region just above the construction joint at the floor level.
- Widely spaced column ties that provide little confinement to the concrete.
- Little or no transverse reinforcement within the beam-to-column joint.
- Discontinuous positive beam reinforcement with a short embedment length.
- Construction joints below and above the beam-column joint.
- Columns with bending moment capacity less than that of the beams.

2.3. Key Parameters Affecting the Behavior of Beam-Column Joints

There are many parameters which affect the behavior of beam-column joints, but some of them seem more severe. ACI 352R-02 (Recommendation for the Design of Beam-Column Connections in Monolithic Reinforced Concrete Structures) defines these critical factors that significantly influence the seismic performance of a beam-column joint as follows: (i) the relative column versus beam flexural strength, (ii) the joint stress, (iii) the anchorage of the reinforcement in the joint region, and (iv) the confinement of the joint core. Besides of these factors, axial load, presence of transverse beams and floor slab, and type and direction of loading should also be accepted as main parameters which define definite behavior of R/C beam-column joint. Surely, dimensions of the R/C members and the reinforcement bars (rebars), material properties of concrete and rebars, details of the reinforcement are effective in the behavior of such connections.

2.3.1. Column versus Beam Moment Strength Ratio

Flexural strength ratio of columns versus beams is very important parameter that affects the behavior of joints. This ratio also defines the hinging process of the joint; namely, it describes when the first yielding occurs. This ratio is calculated from the sum of flexural strength of columns at both top and bottom of the joint divided by sum of beams on both sides of the joint. The column to beam moment strength ratio (M_r) should be computed in both direction of loading separately. While calculating the ratio, moment capacity of the columns is calculated under the factored axial load.

According to the design philosophy of the R/C moment resisting frames, yielding hierarchy should be satisfied as weak beam-strong column concept. Therefore, sum of moment capacities of columns should be higher than those of beams. It means that the moment strength ratio should definitely be greater than 1.0. According to current ACI codes, the ratio must be higher than 1.2. Besides, ACI 352R-02 recommended that this should be much more than 1.2 to prevent yielding in any column. However, this ratio of 1.2 could not be satisfied in the buildings which were constructed before 1970s and the ratio is typically around 1.0 or even less for such structures. (Beres *et al.*, 1996)

For the exterior joints, the flexural strength ratio is mostly higher than 1.2, because only one beam was taken into account in the calculation. This ratio becomes less for the interior joints due to the same consideration and therefore the yielding hierarchy could not be supplied all the times.

Contribution of the floor slab is another important concern in the calculation of the flexural strength ratio. Numerous researchers (Ehsani and Wight, 1985a, Durrani and Wight, 1987, French and Moehle, 1991, Di Franco *et al*., 1995, Pantazopoulou and French, 2001, etc.) investigated how much floor slabs contribute to the beam flexural strength when the beam-column connections were subjected to lateral loading. They concluded that the actual effective slab width mainly depends on imposed lateral drift, transverse beam stiffness, loading history, boundary conditions, slab panel aspect ratio (the aspect ratio is the length of the longest side of a panel divided by the length of the shortest side), and reinforcement distribution. They also indicated that all reinforcement in a slab might effectively contribute to the beam moment strength when subjected to large lateral drifts.

According to the current ACI code, effective width of the slab can be calculated by a certain formula. ACI 352R-02 recommended that the beam flexural strength should be determined by considering the slab reinforcement within an effective flange width, in addition to the beam's longitudinal tension reinforcement within the web. Forces introduced to the joint should be based on beam flexural strength considering the effective slab reinforcement contribution for negative bending moment (slab in tension). Slab reinforcement should be considered to act as beam tension reinforcement having strain equal to that occurring in the web at the depth of the slab steel.

2.3.2. Shear Resisting Mechanism in Beam-Column Joint

It is possible to summarize the shear forces acted on beam-column joint region with different approaches. One of the widely used approaches is the one which use direction of the forces subjected to the beam-column region; namely, horizontal and vertical shear forces. Most of the case, magnitudes of the shear forces on the joint region are higher than those within the adjacent beams and columns. Therefore, the beam-column joint should be carefully detailed for shear in order to prevent this possible failure.

Figure 2.5 illustrated the formation of horizontal shear forces and their institutional factors. An exterior column extending between points of contraflexure, at approximately half-story heights may be isolated as a free body, as shown in 2.5(a). Internal horizontal tension T_b, compression C_b and beam shear force V_b can be seen in the figure. In order to maintain equilibrium in the section, compression force on the concrete is assumed to be equal to the tension force on the reinforcement. By this assumption and symmetry of the system, horizontal shear force could be derived basically as:

$$V_c = (T_b z_b + V_b h_c) / l_c \quad (1)$$

The moment and the shear forces on the column can be seen in Figure 2.5(b) and 2.5(c). Horizontal shear force, V_{jh}, can be derived from these figures as:

$$V_{jh} = T_b - V_c = [V_c (l_c - z_b) - (V_b h_c)] / z_b \quad (2)$$

According to Paulay and Priestley (1992), V_{jh} is typically four to six times larger than that across the column between adjacent joints, V_c. This ratio clearly shows the how the shear stresses are effective in the joint with respect to shear forces in the members themselves. In Figure 2.5(b), variation of the internal tension forces along the column can be seen. This figure also explains the changes in tensile stresses through the section and critical section due to these tensile forces.

Basic mechanism of shear transfer for the exterior joint is shown in Figure 2.6. The mechanism, which was derived from the experimental and analytical studies, consists of two main parts, namely; concrete strut and truss mechanisms. Diagonal strut mechanism consists of forces, those generated in the concrete as in Figure 2.6a. Otherwise, other forces, transmitted to the joint core from beam and column bars by means of bond, necessitate a truss mechanism as shown in Figure 2.6b (Hwang and Lee, 1999).

To prevent shear failure by diagonal tension, usually along a potential corner to corner failure plane, both horizontal and vertical shear reinforcement is required. Such reinforcement enables a diagonal compression field to be mobilized, as shown Figure 2.6, which provides a feasible load path for both horizontal and vertical shearing forces. The

amount of horizontal joint shear reinforcement required may be significantly more than would normally be provided in column in the form of ties or hoops, particularly when axial compression on columns is small (Paulay and Priestley, 1992).

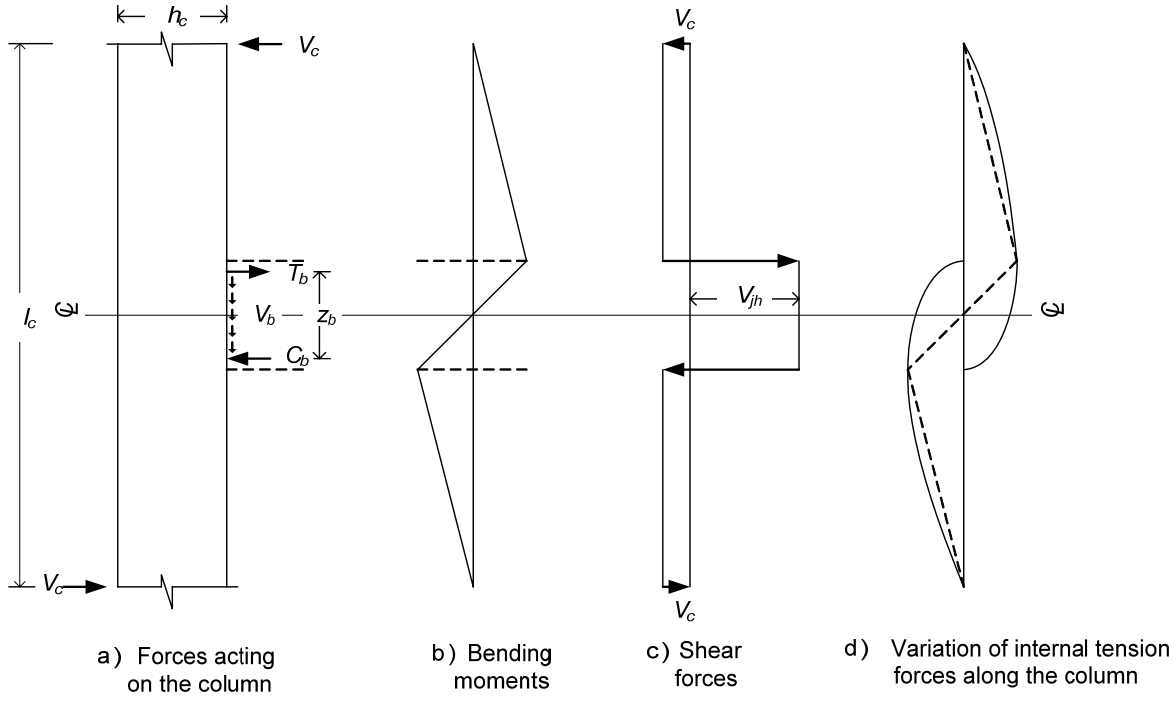

Figure 2.5. Characteristics of column and joint behavior

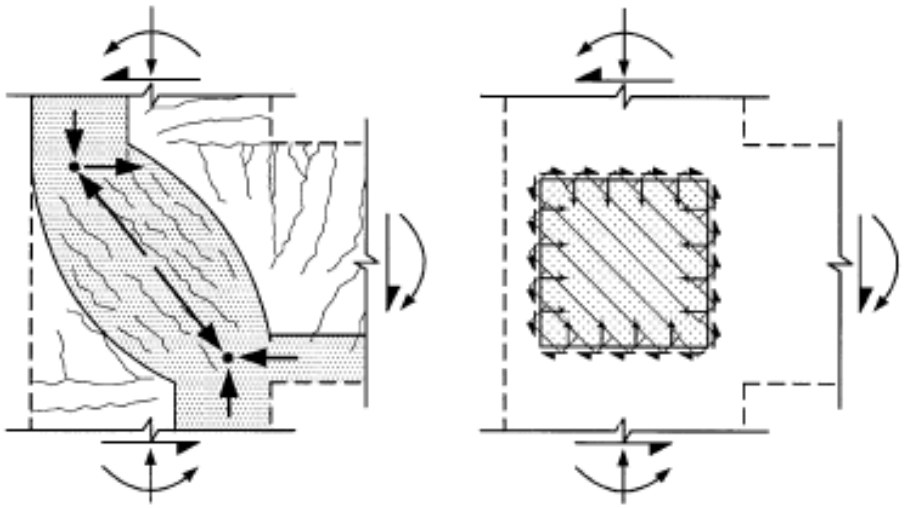

a) Concrete Strut mechanism b) Truss mechanism

Figure 2.6. Mechanism of shear transfer (Hwang and Lee, 1999)

For the buildings which were designed and constructed before 1970's in the United States, typically, there is little or no transverse reinforcement within the beam-column joint (Beres *et al.*, 1996). Therefore, the truss mechanism explained above, could not be maintained properly. Besides of this phenomenon, discontinues positive beam reinforcement with short embedment length into the column can cause the bond failure before even the joint reaches its shear capacity with insufficient detailing.

Recent earthquakes, namely; Turkey (1999) and Taiwan (1999), clearly demonstrated that predicting shear forces on the beam-column joints is very crucial in order to prevent sudden and catastrophic failures of the buildings. Therefore, numerous analytical studies have been conducted on the determination of joint shear forces and deformations through a comprehensive experimental database of previous tests. Bonacci and Pantazopoulou (1993) investigated parametric dependence of joint behavior, and underscores diversity in experimental techniques used in various countries by using a database of 86 beam-column joint tests compiled from published literature. Kim and LaFave (2007) made a very comprehensive research using an extensive database of beam-column test. They investigated different types of joints with parameters of material property, joint panel geometry, reinforcement confinement, column axial load and reinforcement bond condition. They concluded that the most important influence parameters on joint shear behavior were found to be somewhat different by connection type and failure mode sequence. However, concrete compressive strength was the most common governing parameter on joint shear behavior for all groups in the constructed database. In addition, joint shear cracking stresses and strains were investigated by simple equations. Finally, the design checks recommended by ACI 352R-02 were also examined for the specimens within the constructed database.

2.3.3. Anchorage of the Reinforcing Bars in Joint Region

Anchorage of longitudinal steel bars is one of the most important subjects, together with shear transfer capacity, for seismic design of beam-column joints in R/C frames. Joint size / bar diameter ratio, development length, geometry of bent bar, column axial force level and transverse reinforcement in the joint region seem the most important parameters which affect the bond and anchorage of reinforcement bars.

Consequences of bond deterioration along the longitudinal beam or column bars in a joint were summarized by Kaku and Asakusa (1991a) as follows:

- Pinching in force-story drift hysteresis curve and inevitable loss of the energy absorbing capacity of the beam-column subassemblage.
- Increasing the slip deformations at the beam-column interface, which sometimes becomes excessive and difficult to repair.
- Changing the shear transfer mechanism in the joint core from truss action to concrete compression strut action.
- Decreasing the moment resisting capacity of the plastic hinge region of adjoining members.

Paulay *et al.* (1978) investigated beam-column joints under seismic actions and they arrived some conclusions regarding the bond deterioration. They recommended that the diameter of beam bars passing through the joint core should not be excessive if slip of bars through the joint core due to bond failure is to be avoided. In design, slip can be avoided by limiting the beam bar diameter to a certain proportion of the column depth or limiting the average bond stress on the beam bars. Goto *et al.* (1988) made an investigation on the effectiveness of the transverse reinforcement on the bond performance. They showed that the transverse reinforcement was effective to reduce the beam bar slip at the beam-column interface, namely, the bond deterioration in the joint. According to Leon (1991), the comparison of experimental and analytical data indicated that if short anchorage length (20 bar diameters) and large shear stresses are used simultaneously, large losses of bond transfer capacity and stiffness will occur.

Kitayama *et al.* (1991) concluded that column axial stress smaller than 0.3 f_c' does not exhibit beneficial effect on the bond resistance along the beam reinforcement within a joint, and that smaller than 0.5 f_c' does not influence the joint shear strength as a result of experimental studies.

Altay *et al.* (2007) investigated the bond-slip behavior of inadequately embedded beam bars with experimental and analytical studies. The experimental results had revealed that drift capacity of the test specimen mainly depended on the anchorage capacity of the

shortly embedded beam bottom longitudinal reinforcement bars into the column. Comparisons are made between experimental results, and an existing bond stress-slip model in the literature. Based on the observed behavior, in general, analysis results using the developed backbone curve for bond stress-slip relationship pertaining only to this study was in good agreement with experimentally obtained moment-slip rotation results.

2.3.4. Confinement of Joint Core

Beam-column joint should be confined in order to transfer the shear forces through the joint by concrete strut mechanism, provide required anchorage for the longitudinal beam bars and prevent buckling of column longitudinal bars due to axial load. It is possible to summarize the contributors of confinement of joint core in three major ways; joint transverse reinforcement, longitudinal column bars and transverse members framing into the joint.

For the buildings of pre-1970's, there is no or limited transverse reinforcement in the joint region. (Beres *et al.*, 1996) Therefore, confinement by the stirrups cannot be observed for such joints. Where the longitudinal column bars are always taken into account, the effect of transverse members framing into the joints cannot be observed for the exterior and corner joints.

Kitayama *et al.* (1991) conducted an experimental study with different joint reinforcement details- one with the usual closed hoops and the others with legged cross ties parallel and normal to the loading direction (see Figure 2.7). Ties parallel to the loading direction, indicated by circle 1 in Figure 2.7a and 2.7c, would resist joint shear by the truss mechanism and confine joint core concrete to that direction, whereas transverse ties, indicated by circle 2, would restrain the expansion of core concrete normal to the loading direction. Usual closed hoops were placed in specimen B2, which would resist shear and also confine the core concrete. The normal legged cross ties showed increasing strains resulting from their confining role, but strains in the normal legged cross ties were smaller than those in the parallel legged cross ties that participated in joint shear resistance as well as confinement.

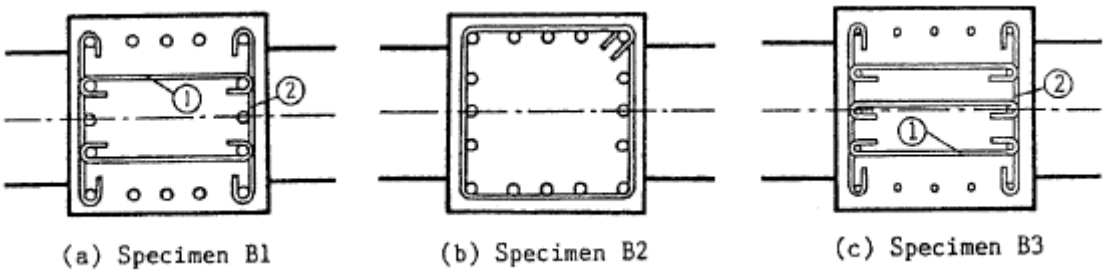

Figure 2.7. Different joint reinforcement details (Kitayama *et al.*,1991)

Cheung *et al*. (1991) expressed that there was no evidence during the tests to indicate that presence of floor slabs or beams in two directions provided significant confinement to the joint cores during bidirectional seismic loading.

2.3.5. Axial Load

Axial load on columns may be different depending on location of column in the structure. The axial load is higher in the first stories, and decreases gradually towards upper floors. However, axial load is generally around 30% of the axial load capacity of the column. The compressive stress of any section of the column can be calculated under both compression and flexure.

How the axial load affects the behavior of joints is a questionable topic. Therefore, during the experimental studies on beam-column connections, the axial load effects were investigated as a parameter. Beres *et al.* (1996) investigated the effects of axial load on the behavior of joints under cyclic loading. According to results of these experiments, a strength increase of 15-20% was detected when higher column axial load was used. These test results showed the beneficial effect of higher levels of axial load on the column. They changed the level of axial force from 100 kips (445 kN) to 350 kips (1557 kN) and compare the test results. In all cases, the specimens with higher axial load delays the onset of critical shear cracking and also helps to provide better confining action to the embedded bars, delaying their pullout. In a building subjected to the overturning effects during an earthquake, the columns on the compressed side of the buildings would perform better than those on the other side. For moderately slender buildings, where the columns do not even approach going into tension from overturning, it is suggested that a conservative estimate

of base shear capacity be obtained using the joint shear capacities for the 100 kip axial load, ignoring the beneficial capacity increase from columns on the compression side of the building. These results cannot be extrapolated to very slender frames where the column compression load may essentially disappear from severe overturning effects.

Ichinose (1991) expressed that the column axial force increases the width of the strut action. This results in smaller demands of horizontal hoop action and better anchorage of beam bars.

Bonacci and Pantazopoulou (1993) suggested that axial load has no discernible coherent influence on the strength of beam-column joints. Kitayama *et al.* (1991) expressed that column axial load does not seem to influence the joint shear strength. Higher axial compression load in a column, however, accelerates the strength decay in the diagonal compression failure of the joint core concrete after beam flexural yielding.

Besides of these, research on comparison between interior and exterior R/C beam-column joint behavior indicated that whereas the increase of column axial load level gave no influence on the ultimate strength of the interior joints, such level of increase in column load improved the shear strength nearly 11%. (Fujii and Morita, 1991)

2.3.6. Presence of Transverse Beams and Floor Slab

As it was explained comprehensively in the previous section named as “column versus beam moment strength ratio”, design codes require that the columns should be stronger than the beams, thus ensuring a desirable hierarchy of yielding. The determination of the flexural strength of the beams is one of the important issues in ensuring the correct hierarchy of yielding. In determining the flexural resistance of a beam in negative bending, it is necessary to estimate the contribution of the slab reinforcement as well. The current ACI Code specifies an effective slab width to be used when calculating the negative and positive moment resistance of the beams framing into the joint. However, this effective slab width was not taken into account for the structures built before 1970’s. Also, codes from different countries assume different effective slab width.

According to these design approaches, some of the important parameters affecting the contribution of the slab reinforcement do not take into account. For instance, at exterior joints, the size and strength of the spandrel beams play an important role in affecting the effective slab width in negative bending. Di Franco *et al.* (1995) expressed that the effective slab width influences a number of key parameters as follows:

- The flexural strength ratio between the columns and beams may be underestimated when the effective slab width is not taken into account in design.
- The hierarchy of yielding between beams and columns to ensure "weak beams" and "strong columns" may be jeopardized if the slab contribution is not properly assessed.
- The ductility and energy dissipating capacities of the beams may be significantly reduced by the increase in negative moment capacity due to the contribution of the slab bars.
- A larger effective slab width would result in larger shears in both the joint and in the beam that could result in premature shear failures.

Ehsani and Wight (1985a, 1985b) conducted experimental study on exterior concrete beam-column subassemblies having floor slabs and spandrel beams as well as specimens having columns and main beams only. The slab reinforcement parallel to the main beam was found to contribute significantly to the negative flexural moment capacity of the beam. In the design of the specimens, they assumed that only the first set of slab bars adjacent to the beams would contribute. However, they observed that all of the reinforcement across the full width of the slab yielded in tension. They concluded that the flexural strength ratio may be overestimated if the slab reinforcement is neglected in design. They proposed that the slab bars within an effective slab width, at least equal to the width of the beam on each side of the column be included. They also recommended that the ratio of M_r be no less than 1.4.

According to results of experimental studies which were conducted by Durrani and Zerbe (1987), the presence of the slab reinforcement increased the negative flexural capacity of the beam by as much as 70%. For transverse beams that reached their torsional yielding capacity during the test, the effective width of slab contributing to flexure was determined to be equal to the column width plus twice the depth of the transverse beam.

French and Boroojerdi (1987) made experimental studies and found that the specimens with increased torsional stiffness of the spandrel beam had greater effective slab participation. However, they also concluded this effect decreased with increased deformations and the slab participation may decrease in frames subjected to skew earthquakes.

Cheung *et al*. (1991) tested full-scale beam-column-slab assemblies under seismic actions. They found that the slab contribution was greatly decreased due to earlier yielding and stiffness loss of the loaded transverse beams as compared to unidirectional loading. They recommended that the effective width of slabs at exterior joints with transverse beams be taken as the lesser of: one quarter of the span of the transverse edge beam on each side of the column centerline; or one quarter of the span of the main beam taken on each side of the column centerline.

Bonacci and Pantazopoulou (1993) made a parametric investigation on presence of transverse beams using a database of 86 beam-column joint tests compiled from published literature, and from the results of a simple mechanical model developed using equilibrium, kinematic and material considerations. They expressed that shear failures were clustered in the group of specimens with no transverse beams, and, to a smaller extend, in the group with a single transverse beam provided on one side of the connection. No specimen was reported to have failed in joint shear when beams framed into all vertical faces of the joint. It was evident that the transverse beams confine the joint by means of their longitudinal reinforcement, which was anchored inside the joint in the transverse direction (and therefore prevented partially the lateral expansion of the joint core), as well as by effectively increasing the volume of joint concrete that actively participated in the joint shear-resisting mechanism. Beres *et al.* (1996) implied that the presence of transverse beams resulted in slower strength degradation but no increase in capacity.

2.3.7. Type and Direction of Loading

Structural behavior of beam-column joints is directly affected by the type and the direction of the loading. Undoubtedly, experimental methods which simulate the seismic action were described by the help of previous researches. Park (1989) prepared a detailed

report on evaluation of ductility of structures and structural subassemblages from laboratory testing.

Shake table testing, pseudo-dynamic testing and quasi-static cyclic load testing could be described as widely accepted seismic load testing methods. Whereas shake table test can be seen as more realistic, because real earthquake data were used, often only scale models can be tested and scaling of the earthquake record may also be necessary. In pseudo-dynamic testing experimental measurements are made of the restoring forces of the structure at each step during the testing, and this direct experimental feedback is used to calculate by inelastic dynamic computer analysis the displacements to be imposed on the structure in the next step by hydraulic actuators to closely resemble those that would occur if the structure was subjected to the ground shaking of a particular earthquake (Park, 1989).

Quasi-static cyclic load testing is a widely used method of experimental testing of structures and structural assemblages. The load is applied by hydraulic actuators and load pattern is not attempted to follow the strain rate or the specific displacement history imposed by a particular earthquake. Instead the structure is subjected to predetermined number of displacement or load controlled quasi-static loading cycles. The slow strain rate means that the test may take several days to conduct.

Quasi-static load testing gives conservative estimates of the real strength of the structure or structural assemblage, since real earthquake loads are dynamic and an increase in the strain rate results in an increase in the strength of the materials. However, there are no significant differences between the shapes of the hysteresis loops which are obtained from quasi-static and dynamic loading tests. The effect of loading velocity on the energy dissipation of R/C columns was not significant for displacements of 4 times that at first yield of the longitudinal reinforcement, but at higher displacements the energy dissipation capability was appreciably larger when the loading velocity was 100 cm/sec than when the loading velocity was 10 cm/sec.

In quasi-static load testing, the displacement history does not follow in detail the complex response of a structure to an actual earthquake. Instead a more simple displacement history is applied to enable an assessment to be made as to whether the

structure is tough enough to be likely to perform satisfactorily during a severe earthquake. Unfortunately, investigators in the past have used a range of displacement histories, and various definitions of yield and ultimate deformations, which have made the comparison of results of different investigations difficult. As a result, values for ductility factor obtained from experimental tests have sometimes been misused in judging the likely performance of structures during severe earthquakes. Agreement is needed for appropriate definitions of the main parameters describing inelastic behavior for quasi-static load testing, so that performance obtained from analytical and experimental investigations can be properly assessed and compared in terms of their application to the design of structures for earthquake resistance.

It has been suggested by some investigators that the imposed deformation history should be based on the level of interstorey drift rather than on the level of displacement ductility factor. The interstorey drift is obtained by dividing the interstorey horizontal displacement by the storey height. Interstorey drift is commonly used in quasi-static loading tests. For example, in the United States, if the test structure or structural subassemblage can withstand imposed displacement cycles with interstorey drifts of up to ±3% without substantial loss in strength, the structure is satisfactory. In Japan interstorey drifts of up to ±2% are commonly imposed in tests. Loss in strength is generally defined as horizontal load carrying capacity reducing by more than 20% (Park, 1989).

The concept of using interstorey drift as a test criterion has considerable merit since it avoids the difficulty of the definition of the yield displacement. However, care should be taken in the use of interstorey drift as a test criterion since the level of imposed interstorey drift should depend on the stiffness of the structure and the level of displacement ductility factor to be imposed, as found from dynamic analysis. Hence, the imposed interstorey drift should depend on the stiffness of the structure and on the required ductility. Also, measured interstorey drifts do not give an indication of the available ductility factor of the structural assemblage. Ideally, hysteretic responses measured in quasi-static load tests when plotted should have marked on them both the displacement ductility factor and the interstorey drift.

2.4. Strengthening of Reinforced Concrete Structures

Strengthening of R/C structures is made effectively only if the behavior of structural systems and members can be understood clearly. Therefore, numerous experimental studies have been conducted on these structural systems and subassemblies. Besides of these, effects of material properties and loading have also been investigated. Tests of such structural members and systems and therefore the behavior knowledge of them were given in the previous part under the light of theoretical and experimental data.

Behaviors of structures during a strong earthquake show that the majority of buildings in regions of high seismicity do not meet current seismic code requirements and many of these buildings are vulnerable to damage and collapse in an earthquake. Concerns for seismic rehabilitation of existing buildings grew considerably in the last three decades and resulted in several research programs to identify and mitigate seismic risks. During this period of time, earthquakes provided significant new impetus for seismic rehabilitation of buildings in 1990's. Today, earthquakes in all over the world provide continuous reminder of the need for seismic mitigation programs supported by research to demonstrate their effectiveness and improve the efficiency. The objectives of the seismic rehabilitation researches were to provide information for evaluation of the vulnerability of existing structures for various levels of seismicity, and to develop economical construction techniques for repairing and strengthening hazardous structures. Moreover, seismic rehabilitation guidelines have been developed using these research outcomes.

Buildings constructed prior to 1970 in the US commonly have significant deficiencies in configuration and detailing. It is possible to say that the same detailing can be seen on the buildings, which were designed only gravity loads taken into account. Typical frame details are also identified by Moehle, 2000. Longitudinal reinforcement in beams commonly was discontinuous, and that in columns normally was lap-spliced with short length just above the floor level. Transverse reinforcement generally was not proportioned to prevent shear or lap failures, and details usually included wide spacing, open stirrups, and hoops with 90-degree bends. Joint transverse reinforcement was uncommon. All these details can lead to performance with inadequate lateral displacement ductility as well as inadequate protection against vertical collapse.

The most significant failures of R/C buildings in the past earthquakes have been attributed to column failures. Causes have included column shear distress, spalling of column end regions, buckling of column longitudinal reinforcement, and formation of soft stories. Several collapse of one or more stories of buildings have been attributed to column failures (see Figure 2.8a). Failures of beam-column connections also have been observed. Figure 2.8b depicts an example from the Northridge earthquake. Failure of slab-column connections have been observed in the past earthquakes, in some cases leading to building collapse. The example shown in Figure 2.8c indicates typical failure of column-slab connection. Other examples of solid slabs, reinforced and prestressed, have been reported. Damage to shear walls and to coupling beams, while costly and disruptive, generally have not resulted in building collapse, and therefore have received less attention than have columns, joints, and slab-column connections.

a) Typical Column Failure b) Typical Joint Failures c) Typical Slab-Column Connection Failure

Figure 2.8. Failure Types of Buildings (Moehle, 2000)

Whereas some failures in structures can be attributed to specific details, structures mostly fail due to more systematic causes. Attachment of architectural elements, such as the parapet walls in the parking structure, can increase stiffness of components in specific locations of a building resulting in overload a premature failure. Weak-column/strong-beam systems are prone to story failures, especially frames having columns with widely-

spaced excessive flexibility in frames, as well as in frame-wall structures with flexible foundations may result in failure of framing components owing to excessive drift.

For a seismic rehabilitation project, two general approaches usually are considered; global modification of the structural system or local modification of isolated components of the structural and nonstructural systems. In the first approach, the modifications to the structural system are designed so that the design demands, often denoted by target displacement, on the existing structural and nonstructural components are less than their capacities. Common approaches include addition of structural walls, steel braces, or base isolators. Passive energy dissipation schemes are not common for R/C frames because the displacements required for them to be effective often are beyond the displacement capacities of the existing components. Active control is rarely used. Another approach involves local modification of isolated components of the structural and nonstructural system. In this approach, the objective is to increase the deformation capacity of deficient components so that they will not reach their specified limit state as the building responds at the design level. Common approaches include addition of concrete, steel, or fiber reinforced polymer composite jackets. Generally, global modification schemes are more common than local modification schemes. However, difficulties in developing accurate models of foundation flexibility and conservative acceptance criteria for existing components require use of some combination of the two approaches (Moehle, 2000).

Many researchers have been investigated numerous strengthening methods and some of them were proven to be effective methods, shown by experimental investigations. Consequently, some retrofitting techniques have been popular by the time and used widely to strengthen seismically deficient structures. Today, these common methods can be summarized as steel and concrete jacketing, prestressing cables and application of fiber reinforced polymers.

Strengthening of R/C joints is a challenging task that poses major practical difficulties. A variety of techniques applicable to concrete elements have also been applied to joints with the most common ones being the construction of reinforced concrete or steel jackets (Alcorer and Jirsa, 1993). R/C jackets and some forms of steel jackets, namely steel cages, require intensive labor and artful detailing. Moreover, concrete jackets increase the

dimensions and weight of structural elements. Plain or corrugated steel plates have also been tried (Beres *et al.,* 1992; Ghobarah *et al.,* 1997). In addition to corrosion protection, these elements require special attachment through the use of either epoxy adhesives combined with bolts or special grouting (Antonopoulos and Triantafillou, 2003).

Today, fiber reinforced polymers are very popular in seismic rehabilitation of existing structures. Like R/C or steel jacketing and prestressing cables, they are used for retrofitting of existing structures, and fiber reinforced polymer (FRP) sheets are much admired with special characteristics like resistance to corrosion, ease of application and low unit weight. However, how it can be applied is not certainly defined. It is a new material and therefore the new methods of application should be developed. For that reason, many experimental studies have been conducted on the retrofitting of seismically critical R/C regions with FRP sheets. These studies consist of test of R/C specimens like columns and beams, structural subassemblages like frames with or without infill walls and beam-column joints. Contribution of the slab and transverse beams on behavior of beam-column joints is another important concern of the seismic performance of R/C structures. For that reason, many experimental researches were conducted and their results present important and useful outputs on behavior of structures under seismic action.

2.5. FRP Strengthening of Reinforced Concrete Structures

Use of FRP for strengthening of the R/C structures is mainly for local modification of structural components, which have deficiencies. Therefore, FRP strengthening methods were investigated according to members, retrofitted by such methods. As structural members, strengthening of beams and columns and also strengthening of beam-column joint were summarized in the following part.

2.5.1. Strengthening of Beams

There are mainly two kinds of methods for strengthening of R/C beams: Flexural strengthening, and, torsional and shear strengthening. Both of methods were investigated by experimental and analytical studies.

Numerous researchers presented their studies on flexural strengthening of R/C beams (Teng, 2001) and the experimental results demonstrate clearly the excellent performance of this strengthening technique, especially when compared to other traditional strengthening methodologies. This technique was found to be simple, easy and quick to install. It requires essentially unqualified labor, although it is necessary an appropriate site supervision to ensure its quality. Its thickness allows very little cross sectional increases while providing the concrete element a significant increase in strength and stiffness. This technique is particularly effective for R/C beams with a relatively low original flexural reinforcement ratio. The concrete strength may also affect the stiffness and ultimate load capacity of the plated beam, especially when related to concrete cover separation type of failure.

Experimental and theoretical studies confirm that the shear strength of R/C beams can be increased effectively by bonding closed-loop FRP strips in their shear region. The strength increment is related to the external FRP reinforcement ratio, but has no distinct relation with shear-span ratio. Consequently, the higher external FRP reinforcement ratio, the greater the increment can be achieved. Moreover, the complete wrap of the torsion zone of a R/C beam is more effective in strengthening the torsional resistance than a beam strengthened using strips of various configurations. It was observed that the beam's ductility was significantly enhanced. When a beam is strengthened using vertical fiber strip, the failure is delayed but inevitably occurs in the unwrapped space between the strips (Teng, 2001).

Due to non-ductile behavior of shear and torsional failure of the beam, shear and torsional strengthening is more critical than the flexural strengthening. It is also possible to say that shear strengthening is more complex than flexural strengthening. Therefore, many researches have been held on strengthening of beams in the last three decades. A series of 12 concrete beams were tested by Chajes *et al.* (1995) to study the effectiveness of composite fabrics applied externally to improve the member's shear capacity. Carbon, glass, and aramid FRP were used to study the influence of stiffness and strength of these materials. An increase in the beam's ultimate strength of 60–150% was achieved. In a study performed by Triantafillou (1998), experimental and analytical results were compared with externally strengthened beams. The failure of these beams was due to composite delamination from the concrete surface, at very low composite strain levels (in

the range of 0.05–0.17%). Malek and Saadatmanesh (1998) made an analytical study of R/C beams strengthened with web-bonded fiber reinforced plastic plates or fabrics.

2.5.2. Strengthening of Columns

Some existing R/C columns do not have enough shear strength and ductility against a severe earthquake shock. Therefore, new seismic retrofitting methods for columns have been developed during the last decades. These techniques have improved the earthquake-resistant capacity of the columns as follows; increase in shear strength, improvement of ductility, and, increase in compressive capacity.

Gergely *et al.* (2000) summarized the extensive research on retrofit of columns which was performed at the University of California, and they expressed that circular, square, and rectangular bridge columns have been strengthened externally using continuously wrapped CFRP composites and steel jacketing. Confinement, ductility, and shear effects were studied, and design guidelines were developed. An experimental investigation was conducted by Saadatmanesh *et al.* (1996) to study the seismic performance of R/C columns retrofitted with composite straps. The retrofitted columns had a superior ductility (up to 6) compared to the low ductility level of 1.5 observed for the baseline specimens.

Teng (2001) investigated numerical models, experimental results and new design approaches on FRP strengthening of columns. It has been demonstrated that advanced composite column retrofit jacket systems can be structurally just as effective as conventional steel jacketing in improving the seismic response characteristics of substandard R/C columns. Design models for the composite jackets show that the required jacket thickness decreases with increasing jacket modulus in the hoop direction for shear and lap splice retrofits. For flexural plastic hinge confinement even lower modulus jackets can be very efficient as long as they exhibit large failure strain capacities. The effectiveness and accuracy of the established design models has been validated by large scale bridge column model tests for all three possible column failure modes of shear, plastic hinge confinement, and lap splice debonding for both circular and rectangular column geometries and different levels of column reinforcement ratios. The large scale

laboratory validation tests have shown that both the advanced composites retrofit concepts and the developed design guidelines are ready for actual column retrofit project application. Advantages of these methods are as follows.

- It is easy to provide required shear and ductility capacity;
- Retrofit works do not influence the stiffness of the retrofitted columns;
- It is possible to minimize increase in weight accompanied with retrofitting;
- It is easy to control the quality of construction.

2.5.3. Strengthening of Slab-Column Connections

Numerous techniques were explored for strengthening slab–column connections against punching shear failure. These techniques include the use of transverse reinforcement prestressed against the slab surface, the use of structural steel beams attached to the column face and bottom surface of the slab to act as a column capital, or the use of a combination of steel plates glued to the top and bottom faces of the slab and transverse prestressed steel bolts for simultaneously improving the flexural and shear strength of the slab (Harajli *et al.*, 2006).

Strengthening of slab-column connections using externally bonded FRP composite sheets has evolved over the last two decades as a practical alternative to traditional strengthening methods such as externally bonded steel plates, steel or concrete jacketing, or external post-tensioning. In application of FRP composite sheets for slabs, a number of experimental studies have explored the idea of using FRP for strengthening slab–column connections (Harajli *et al.*, 2006). All of these studies reported enhancement of the punching shear strength as a result of using FRP. A recent test conducted by Harajli and Soudki (2003) on interior slab–column connections demonstrated clearly that the use of carbon fiber-reinforced polymer (CFRP) sheets in the critical negative moment region of the slab increases the flexural stiffness of the connection, delays the formation and growth of tensile flexural and shear cracks by increasing the flexural strength of the slab in the vicinity of the column and, consequently, improves the two-way shear capacity of the connection. Combining CFRP sheets and steel bolts, a more effective system was developed for strengthening slab-column connections in both shear and flexural modes by

El-Salakawy *et al.* (2004). Harajli *et al.* (2006) used FRP sheets and steel bolts to extend the technique proposed by El-Salakawy *et al.* (2004).

2.5.4. Strengthening of Beam-Column Joints

Strengthening of beam-column joints is very difficult task which has many difficulties in practice. Whereas many strengthening methods have been developed during the last decade, a new technique of strengthening of beam-column joints was emerged more than a decade ago. The technique occupied the use of FRP materials as externally bonded reinforcement in critical regions of R/C elements. Bridge pier retrofitting is also included the topic of beam-column joint retrofitting due to its similarity by the methods of application and usage.

The strengthening practice of beam-column joints started with the application of carbon fiber composite jackets for the three columns joining with cap beam of an existing concrete bridge pier by Gergely *et al*. (1998). A displacement-based approach was used to design the carbon fiber composite wrap for the bridge bent and four full-scale specimens were tested. They confirmed that retrofit of a bridge pier for gravity load and seismic improvement of the performance of a typical bridge was feasible. Columns, cap beams, and cap beam-column joints could benefit from the retrofit with carbon fiber composite materials and increase both the shear capacity and the ductility of the concrete pier. They also performed pushover analysis and found good agreement between the experimental and theoretical load versus displacement responses. The procedures used to design the retrofit for the pier of this bridge can be used as a prototype for the retrofit of other bridges with similar deficiencies. Full-scale experiments of existing bridges would be valuable for verification of the results presented here.

Gergely *et al.* (2000) investigated a retrofit technique based on externally applied CFRP composite sheets. In order to study the behavior of concrete T-joints, they designed, built, and tested 14 1/3-scale exterior beam-column joint specimens. There were four control specimens tested in as-built condition. The remaining specimens were externally reinforced using composite woven sheets. The following variables have been considered: the composite curing process, the CFRP layout, and the surface preparation of the concrete

specimens. The experimental results were also compared with the analytical findings. Based on the increase in the strength of the specimens and by analyzing the joint shear stresses, a design equation is given for the retrofit of beam-column joints. The analytical findings from the T-joint specimens were also used in the retrofit of a bridge bent. In conclusion, it is obvious that externally bonded CFRP composite sheets greatly enhance the joint's shear capacity. In addition, they improve the overall damage control, and the joints proved to have a minimal residual strength at the end of the test sufficient to support dead load. Failure of the baseline specimens was identical, with extensive diagonal tension cracks in the joint region, which extended into the beam at the level of the bottom longitudinal reinforcement. The FRP reinforced specimens reached their peak load, but as the composite delaminated, this load level could not be sustained. This caused specimen failures at lower loads and corresponding bending moments more than the element's capacity.

Prota *et al.* (2000) focused on a new technique for the seismic upgrade of R/C beam-column connections in gravity load-designed (GLD) frames by the application (combined or not) of FRP rods and laminates. The FRP rods provide flexural strengthening, whereas the lay-up laminates provide confinement and shear strengthening. Along with the modeling of such upgraded connections to assess the increase of strength and/or ductility provided by the composite reinforcement, an experimental program was planned and it was being undertaken. The results of an experimental program confirmed that the combined action by FRP jacketing and near surface mounted FRP rods can be a promising and flexible retrofit technique for beam-column connections in GLD buildings.

Granata and Parvin (2001) conducted an experimental study on FRP strengthening of beam-column joint. This study was performed specifically for evaluating the moment capacity of the beam-column connections wrapped with Kevlar fiber composite fabric. Experimental results demonstrated significant improvement of flexural capacity of beam-column connections and provided certain guidelines for the proper FRP fabric thickness. It was also concluded that the addition of FRP overlays to the bottom of the beam-column connections provided the mechanism for shear transfer between the beam and column elements.

Ghobarah and Said (2002) constructed and tested several R/C exterior beam-column joints in order to develop effective selective rehabilitation schemes for R/C beam-column joints using advanced composite materials. The joints were designed to simulate non-ductile detailing characteristics of pre-seismic code construction. The control specimens showed joint shear failure when subjected to cyclic loading at the beam tip. Different fiber-wrap rehabilitation schemes were applied to the joint panel with the objective of upgrading the shear strength of the joint. The tested rehabilitation techniques were successful in improving the shear resistance of the joint and in eliminating or delaying the shear mode of failure.

El-Amoury and Ghobarah (2002) tested three exterior beam-column joint specimens that were built in accordance to pre-1970s' practice. Specimens consisted of a control specimen and two rehabilitated specimens and they were tested under quasi-static load until failure. The objective of the rehabilitation was to upgrade the shear strength of these joints and reduce the potential for bond-slip of the bottom bars of the beam. Glass fiber-reinforced polymer (GFRP) sheets were wrapped around the joint to prevent the joint shear failure. GFRP sheets were attached to the bottom beam face to replace the inadequately anchored steel bars. The control specimen showed combined brittle joint shear and bond failure modes while the rehabilitated specimens showed a more ductile failure mode. A simple design methodology for the rehabilitation scheme was also proposed.

Antonopoulos and Triantafillou (2003) examined the role of various parameters on the effectiveness of FRP through 2/3-scale testing of 18 exterior R/C beam-column joints. These parameters included area fraction of FRP (the cross sectional area of FRP divided by member's cross sectional area); distribution of FRP between the beam and the column; column axial load; internal joint (steel) reinforcement; initial damage; carbon versus glass fibers; sheets versus strips; and effect of transverse beams. The results of a comprehensive experimental program, demonstrate the important role of mechanical anchorages in limiting premature debonding, and they provide important information on the role of various parameters. The tests also demonstrated that the externally bonded FRP reinforcement is a viable solution towards enhancing the strength, energy dissipation, and stiffness characteristics of poorly detailed (in shear) R/C joints subjected to simulated seismic loads. Relatively low FRP area fractions increased both the strength and the

cumulative dissipated energy up to about 70–80%. The increase in stiffness varied with the imposed displacement level and reached values in the order of 100%.

Mukherjee and Joshi (2005) investigated on the performance of R/C beam-column joints under cyclic loading. Joints had been cast with adequate and deficient bond of reinforcements at the beam-column joint. FRP sheets and strips had been applied on the joints in different configurations. Both glass and carbon composite materials could be efficiently used for seismic retrofitting as well as rehabilitation of R/C joints. Joints exhibited enhanced strength regardless of reinforcement detailing and damage state. Considerable increase in yield load could be achieved by use of these materials. Yield load and initial stiffness depended on numbers of overlays provided in the joint area. Specimens strengthened using CFRPs exhibited stiffer behavior than GFRP strengthened specimens. Energy dissipation capacity could be increased with the use of small amount of composites. Tests on rehabilitated specimen suggest that FRP not only restores its original strength but also add considerable enhancement in its yield load, initial stiffness and energy dissipation capacity.

Ghobarah and El-Amoury (2005) investigated two main parameters of deficient joint; anchorage failure of beam bottom steel bars by bond slip and shear failure of joint through examination of six exterior beam-column subassemblies with nonductile reinforcement detailing. The first three specimens had inadequate anchorage length of the bottom beam rebars. Two of them were strengthened using carbon-fiber-reinforced polymer sheets attached to the bottom beam face and then tested. The other three specimens did not have ties in the joint zone, in addition to inadequate anchorage length of the beam rebars. Two of the beam-column joints were strengthened by glass-fiber-reinforced polymer jackets of the joint zone and steel rods or plates. They concluded that the rehabilitation techniques eliminated the brittle joint shear and steel bar bond-slip failure modes, and ductile beam hinging instead occurred.

Balsamo *et al.* (2005) studied on the repair of full-scale R/C frame structure by using CFRP laminates. The repair was characterized by a selection of different fiber textures depending on the main mechanism controlling each component. The experimental tests confirmed that CFRP composites allowed the repaired structure to withstand the

displacement demand under seismic action with moderate damage above the foundation. The repaired structure also showed a large displacement capacity without exhibiting any loss of strength and was able to provide energy dissipation very similar to that of the original configuration. The cyclic behavior of the repaired structure was stable and no significant effect of cumulative damage was observed on the strengthened elements. Regarding the local deformability of joints and the shear walls, the rotations of CFRP repaired joints always overcame those of original joints under the design earthquake. The presence of CFRP laminates over the entire height of the shear walls reduced the deformability of such members at any earthquake intensity.

Aidoo *et al.* (2006) conducted an experimental investigation on the behavior of eight full-scale R/C bridge girders taken from a demolished Interstate bridge, and retrofitted with three different CFRP systems. Specimens were subjected to monotonic cyclic loading. In all cases, the retrofits provided an increase in the girder capacity. Conventional adhesives were applied and near-surface mounted (NSM) CFRP systems behaved well under monotonic cyclic loads, although the NSM exhibited significantly greater ductility due to the improved bond characteristics of this type of retrofit.

2.6. Rationale for the Experimental Study

Numerous methods were investigated in the literature regarding the retrofitting methodologies. Limited experimental data on the behavior of beam-column joints with transverse beams and floor slab is apparently noticed. Especially, a few experimental studies have been conducted on retrofitting methodologies of such beam-column joints. This research will guide to understand the actual behavior of 3-D beam-column joint under seismic action.

Herein presented experimental results are expected to be employed for the development of design guidelines for seismic retrofitting of beam column joints upgraded with externally bonded CFRP sheets.

By comparison of the test results between 2-D and 3-D beam-column joints, advanced retrofitting methodologies can also be developed.

3. EXPERIMENTAL INVESTIGATION

3.1. General Description of Experimental Program

Seismic deficiencies of exterior beam-column joints with transverse beams and with or without floor slabs were investigated experimentally. These joints were designed for gravity load according to pre-1970 USA practices. Strengthening methodology for joints using CFRP sheets was also investigated during the research. One exterior beam-column joint with only transverse beams, and three exterior beam-column joints with transverse beams and floor slabs were designed, constructed and tested in the Structure Laboratory of Boğaziçi University. The test results were analyzed and were compared among the specimens to recognize the effects of slab and retrofit configurations.

Three of the specimens had floor slabs in both directions and one specimen did not have the floor slab. Specimens which had floor slabs were named as US3-ES specimens and another specimen was named as US3-E specimen. Specimens which were tested without CFRP application were called as control specimens (US3-E-Control and US3-ES-Control) and those retrofitted CFRP sheets were called as US3-ES-FRP1 and US3-ES-FRP2 (see Figure 3.1). US3 terminology originated from name of 2-D beam-column joint specimens, which have been detailed, constructed and tested as a part of ongoing NSF (grant no: OISE-0535294) and TUBITAK (grant no: ICTAG-I597-NSF103I026) research project. The exact same details as US3 2-D beam-column joint from previously performed experiment are adopted for the beam-column slabs or beam-column with two transverse beams specimens in the present study as continuation of the same NSF and TUBITAK project. The letters “E” and “S” represent exterior and slab, respectively.

Quasi-static cyclic load testing of subassemblies was preferred to simulate the seismic action on the real structure. Loading was controlled by drift ratios and totally 13 different drift ratio levels were applied with three cycles on each drift level. The test setup was designed to hold the specimen from inflection point of columns by pin support and roller support at the inflection point of beam. Details of setup are given on the following parts.

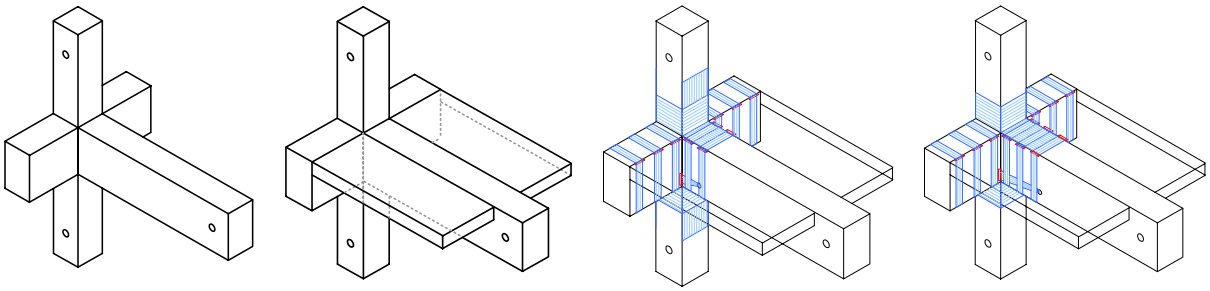

a) US3-E-Control b) US3-ES-Control c) US3-ES-FRP1 d) US3-ES-FRP2

Figure 3.1. Description of test specimens

In the current ACI 352R-02 (Recommendations for Design of Beam-Column Connections in Monolithic Reinforced Concrete Structures), this subassembly was also named as “exterior beam to column connection”. Figure 3.2 illustrates the typical beam-column connections (slabs not shown for clarity) in ACI 352R-02.

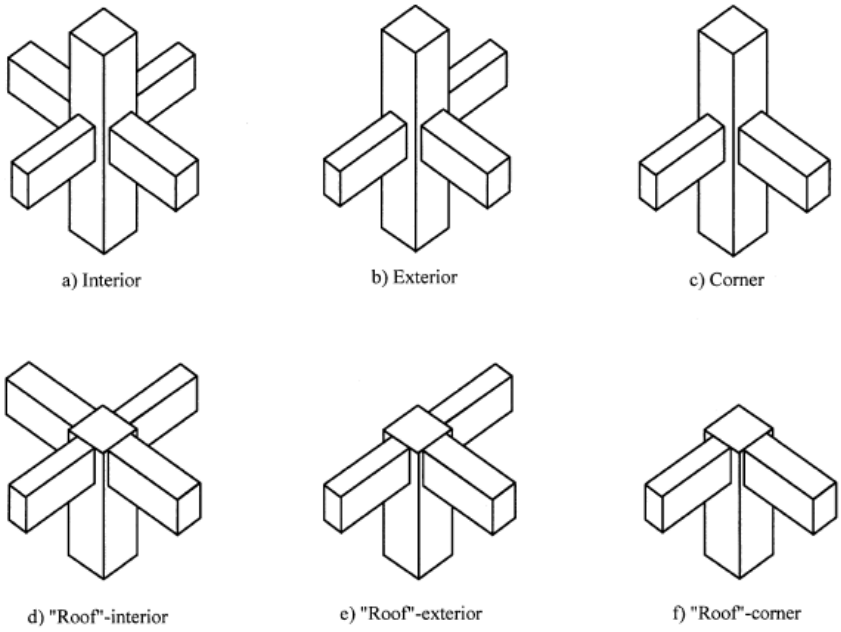

Figure 3.2. Typical beam-column connections.

3.2. Design of Test Specimens

Exterior beam-column joint specimens with transverse beams and with or without floor slabs were designed and constructed by only gravity loads taken into account. Details of reinforcement were constituted according to Pre 1970’s ACI codes (Building Code

Requirements for Structural Concrete and Commentary by American Concrete Institute (ACI)) and the design practices at that time in United States. All the specimens are the same size and reinforcement details, except floor slab details of the US3-E-Control specimen. Figure 3.3 shows the part of the real structure which has been considered as beam-column joint in experimental research.

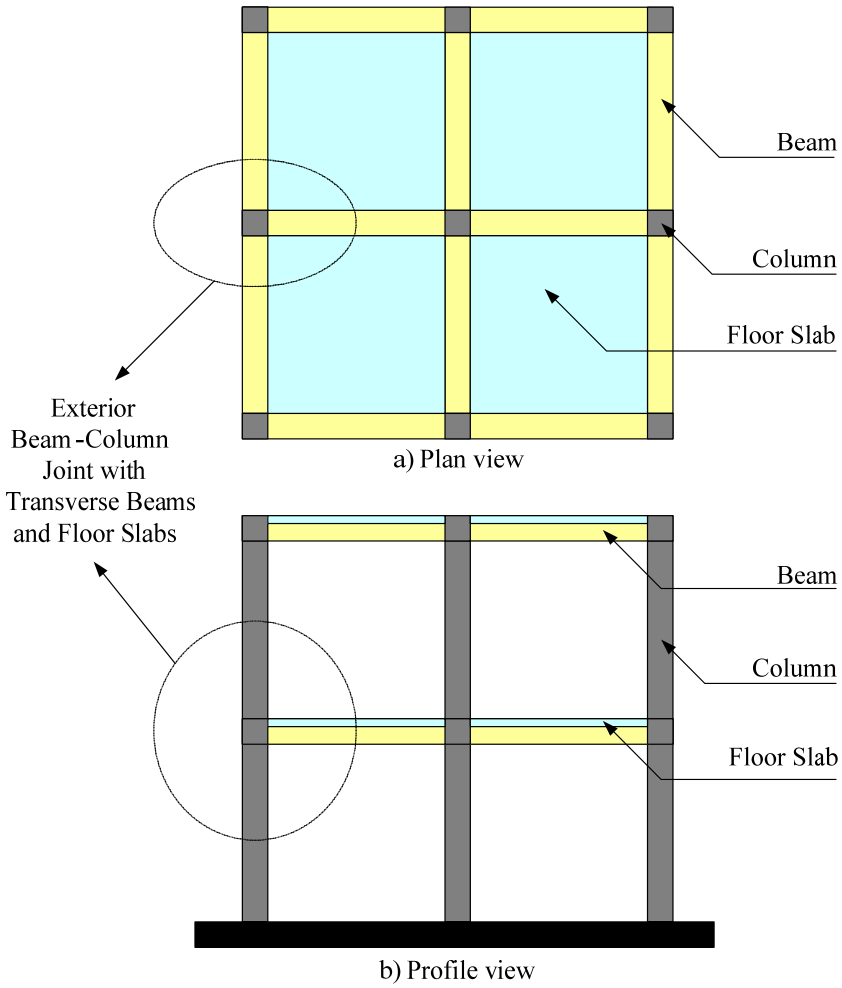

Figure 3.3. Beam-column joint in a real structure

Considering a prototype structure with a story height of approximately 3 meters and column-to-column dimension of roughly 5 meter, the subassemblies represented in this research are approximately 2/3-scale models, with a column pin-to-pin story height of 1.92 m and a longitudinal beam pin-to-pin span length of 3.6 m. In the transverse direction, span length is also assumed as the length of longitudinal beam. However, the length of transverse beams is not as long as longitudinal beams, because the loading is unidirectional and it is applied along the longitudinal direction. In other words, transverse beams cannot

be subjected to forces in their own longitudinal directions. That is to say, they only act in bending under gravity loads and torsional forces which come from the slab. At that point, zero moment point on the transverse beams under gravity loading and effective slab width of the longitudinal beam are taken into account in the determination of length of transverse beams and floor slabs. The length of transverse beam is calculated as 600 mm and details of these calculations are given in the following parts.

Figure 3.4 shows a three-dimensional view of US3-ES specimen. For the US3-E specimen, all the dimensions are the same with the exception of the floor slab. Each specimen consisted of bottom and top columns, one longitudinal beam and two transverse beams in both such directions. For the three US3-ES specimens, floor slab between these longitudinal and transverse beams were designed as two-way slab.

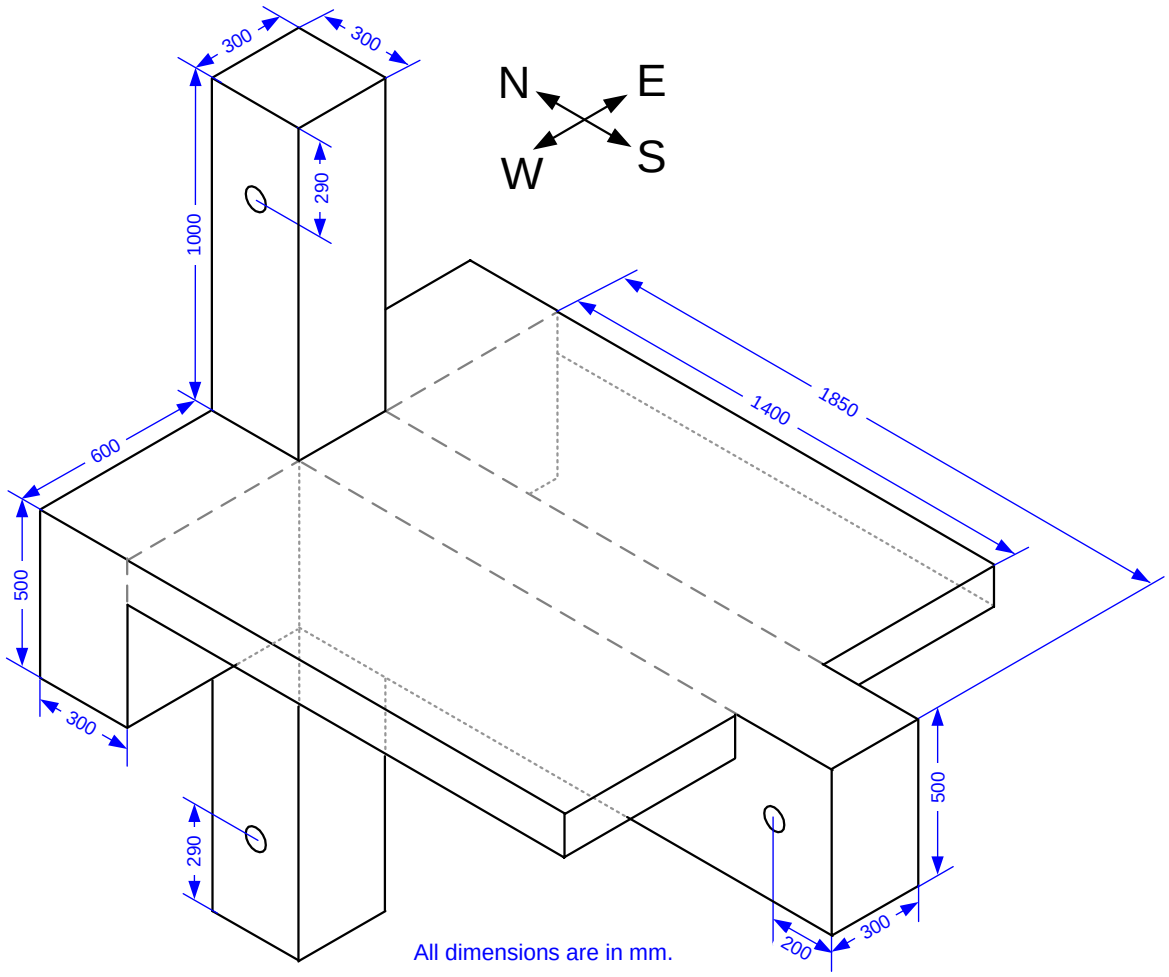

Figure 3.4. Three-dimensional view of the test specimens

3.3. Design Considerations

Widely-used reinforcing details of GLD buildings were investigated in the literature review part. According to these investigations (Beres *et al*. (1992 and 1996), Moehle (2000) etc.), the following details were found typical and judged to be potentially critical to the safety of gravity load designed R/C structures in an earthquake:

- Lapped splices of column reinforcement just above the floor level (maximum moment region),
- Widely spaced column ties,
- Little or no transverse reinforcement within the beam-column joint region,
- Discontinuous positive beam reinforcement with a short embedment length,
- Columns with bending moment capacity close to that of the beams.

Because all members of specimens were designed according to previously described design parameters, reinforcement details of each specimen were not given in the following part separately. There is no different drawing for the specimen without floor slab. For US3-ES-FRP1 and US3-ES-FRP2, details of CFRP orientations and applications were explained individually.

3.4. Details of Specimens

3.4.1. General

According to the design approaches and practices of Pre-1970's, the design of the seismically critical joint was completed in accordance with ACI 318 codes of the time (ACI 318-56 and ACI 318-63), and details of the design can be seen on the following part. In order to make the construction of the specimens easier, all longitudinal rebars for columns and beams were selected as Ø20 and all stirrups and slab reinforcements were selected as Ø10.

The columns had typically 300x300 mm cross-sectional dimensions and 1000 mm length. Six Ø20 deformed reinforcing bars were used as longitudinal reinforcement. No

shear reinforcement in the joint region was supplied and first stirrup was located 180 mm above the beam top level and the second one was located 350 mm above from the first stirrup for the top column. Hence, by the help of the symmetry, shear reinforcements of bottom column were applied. Remaining regions of the column had stirrups with 75 mm intervals because this zone was the support region of the test setup. There was also lap splice region just above the floor level with a length of 500 mm, namely 25 times the diameter of the rebar.

Slab thickness is determined according to minimum requirements of the ACI 318-63. Code defines the minimum thickness by the restriction that in no case shall the slab thickness be 3.5 in. nor less than the perimeter of the slab divided by 180. It was assumed that the span length of prototype structure is 3.5 meter in two directions. Therefore:

$$t_{min} = 3500 \text{ mm x } 4 / 180 = 78 \text{ mm} \quad (1)$$

However, slab thickness has to be at least 3.5 in. and finally slab thickness was determined as 90 mm (3.5 in.). Reinforcement details of the specimen were calculated by making the following assumptions. Live load and dead load on the floor slab were assumed as 125 psf (6 kN/m^2)and 60 psf (2.9 kN/m^2) respectively. Afterwards, floor slab was designed as two-way slab system and its reinforcement was calculated under the provision of related chapter of ACI 318-63 code. The method was based on the design of two-way slabs by strip method as a design of a beam. To compute design moments, empirical formulas and tables, which were provided in the method calculation procedures, were used. These formulas include loading conditions and span lengths. Therefore, loading was assumed as defined above and span length was assumed in accordance with the previously defined dimensions. Finally, 250 mm (9.85 in) interval between two Ø10 rebars in both directions was applied for floor slab.

According to ACI 318-63, in T-beam construction, the effective flange width to be used in the design of symmetrical T-beams shall not exceed one-fourth of the span length of the beam, and its overhanging width on either side of the web shall not exceed eight times the thickness of the slab nor one half of the clear distance to the next beam. So the following calculation was done for flange width.

$b_{f,\,max}$ = 3700 / 4 = 925 mm (2)

$b_{f,\,overhanging}$ = 90 x 8 = 720 mm (3)

$b_{f,max}$ governs the limits and effective flange width is determined 925 mm according to ACI 318-63.

Another important concern on determination of flange length and therefore the length of transverse beam is the torsional behavior of the joint due to slab contribution. According to the test results explained in the Chapter 2.3.6, torsional cracks are diagonal and they reach the distance of the depth of beam. This distance is almost 500 mm from the column face.

Last important concern is the moment diagrams of the beam under gravity loads. Figure 3.5 illustrates the approximate moment diagrams given by ACI 318, Section 8.3.3. The distance *x* is assumed as the point of inflection (zero moment point) of the beam. In this approach, the length of transverse beam was calculated between 265 mm and 700 mm in calculation of moment for positive and negative zones.

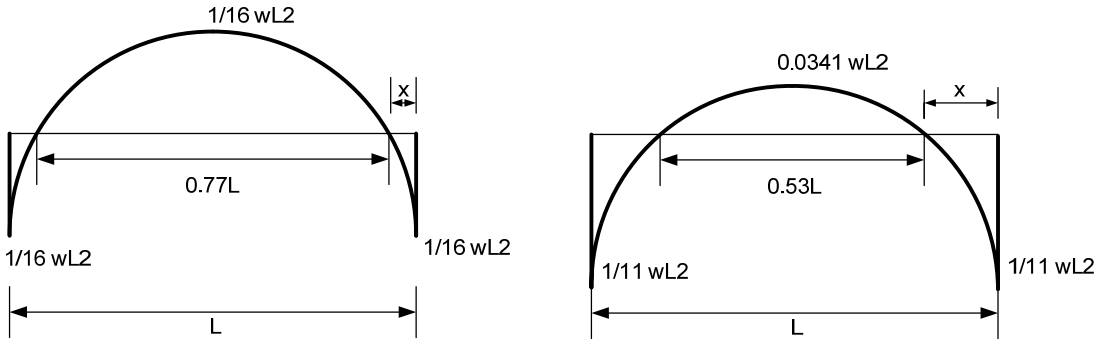

Figure 3.5. ACI approximate moment diagrams

As a result, effective width of the T-beam was assumed to be 600 mm in conformance with all these approaches. By the help of the last approach, the ends of the transverse beams were set free at a distance of 600 mm from the column face.

The length of transverse beams was calculated as 600 mm as explained above and the length of longitudinal beam was taken with respect to following philosophy. The length of the longitudinal beam was determined according to the moment diagram of the moment resisting frame structure under lateral loads. Mid-point of the beam is the zero moment regions under such loading and therefore the length of longitudinal beam was taken as 1850 mm.

The cross-sectional dimensions of both transverse and longitudinal beams are 300x500 mm. Three Ø20 deformed rebars were used as top longitudinal reinforcement and two Ø20 deformed rebars were used as bottom longitudinal reinforcement (see Figure 3.6b and c). For the bottom longitudinal bars of both longitudinal and transverse beams, inadequate embedment length was applied as 150 mm through inside the joint core. First closed stirrup is located at 75 mm away from the beam-column joint surface and the rest is located at 150 mm intervals. In the support region, additional stirrups were supplied to prevent damage outside the test region.

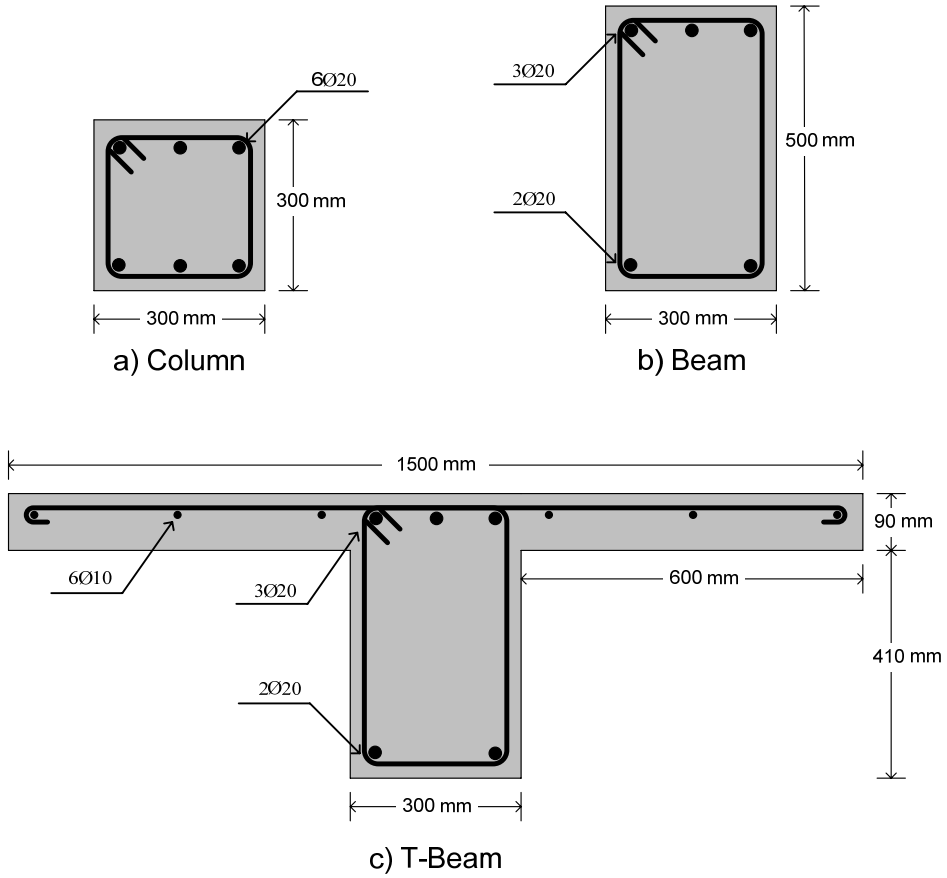

Figure 3.6. Member cross sections

Flexural capacities of the members were calculated in order to compare the test results. Analytical sectional analyses were completed by Response-2000 (version 1.0.5). The ultimate moment capacities of these sections were tabulated in the Table 3.1. For the T-beam analysis, effective flange width was assumed as 1500 mm. For the column, axial load was assumed as 750 kN. Analyses were done in two direction of loading, because of the distribution of the rebars and asymmetric cross-section of T-beams.

Table 3.1. Moment capacities of members

	Member	M_{yield} (kN.m)	$M_{ultimate}$ (kN.m)
Push Direction (Bottom in tension)	Beam	116	131
	Column	159	159
	T-Beam	123	152
Pull Direction (Top in tension)	Beam	171	190
	Column	159	159
	T-Beam	252	270

According to their ultimate moment capacities, column versus beam moment strength ratios were calculated for specimens with or without floor slab as below. Flexural strength ratio was calculated as sum of column capacities divided by sum of beam capacities.

For US3-E-Control Specimen M_r = 159*2 / 131 = **2.43** (Push)

M_r = 159*2 / 190 = **1.67** (Pull)

For US3-ES-Control Specimen M_r = 159*2 / 152 = **2.09** (Push)

M_r = 159*2 / 270 = **1.18** (Pull)

3.4.2. Details of Specimen Geometry and Reinforcement

All four specimens have the same dimensions for columns and beams. Only the difference is the presence of floor slabs in US3-ES-Control, US3-ES-FRP1 and US3-ES-FRP2 specimens, whereas the specimen US3-E-Control does not have floor slabs. In the following figures, details of US3-ES specimens are given. However, it is easy to visualize

the specimen US3-E-Conrtol just without floor slabs. Figure 3.7-3.9 illustrate the reinforcement details of US3-ES specimens by plan and side views.

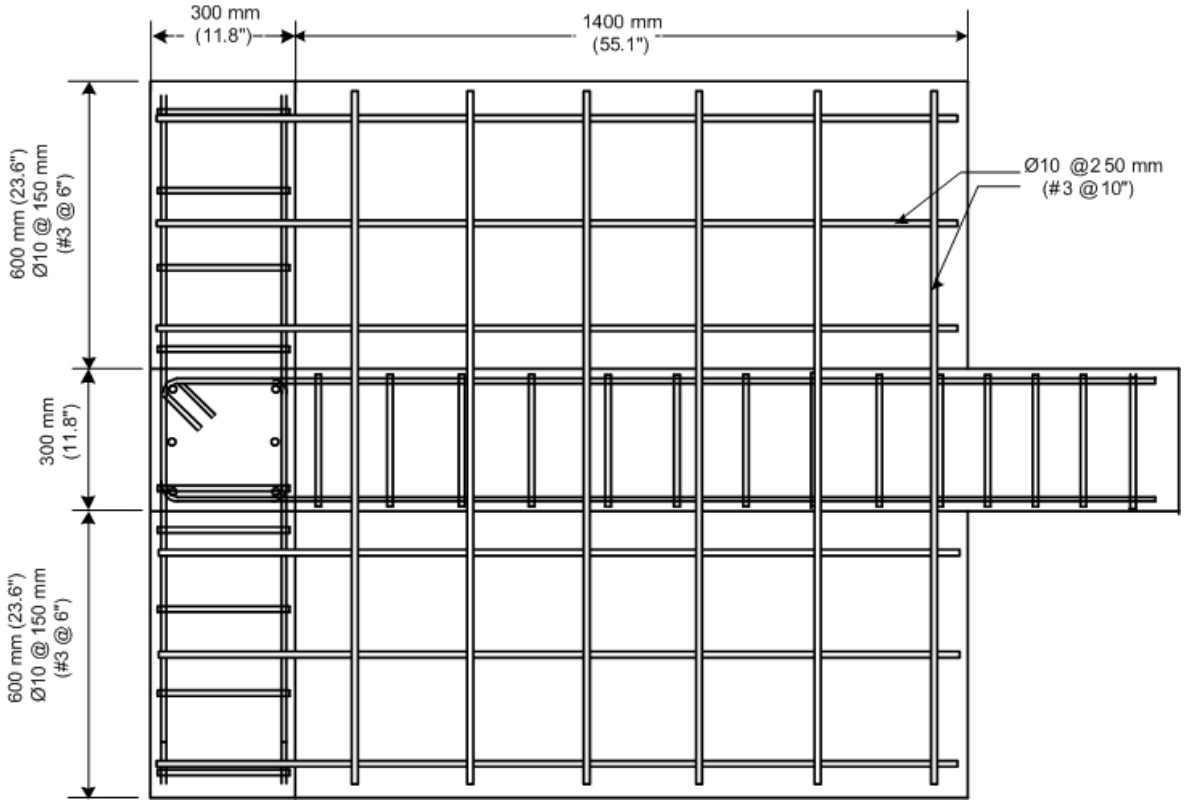

Figure 3.7. Reinforcement details of US3-ES Specimen (Plan view)

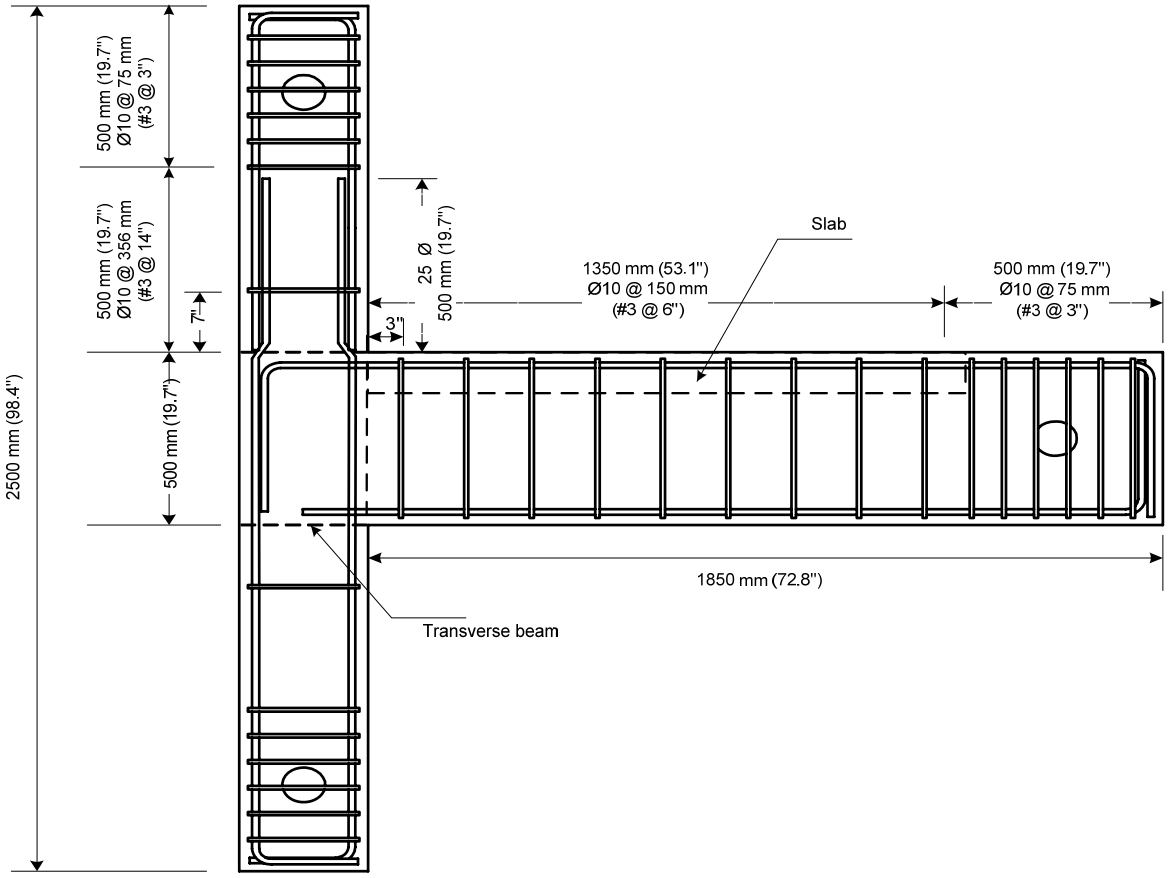

Figure 3.8. Reinforcement details of US3-ES Specimens (Side view)

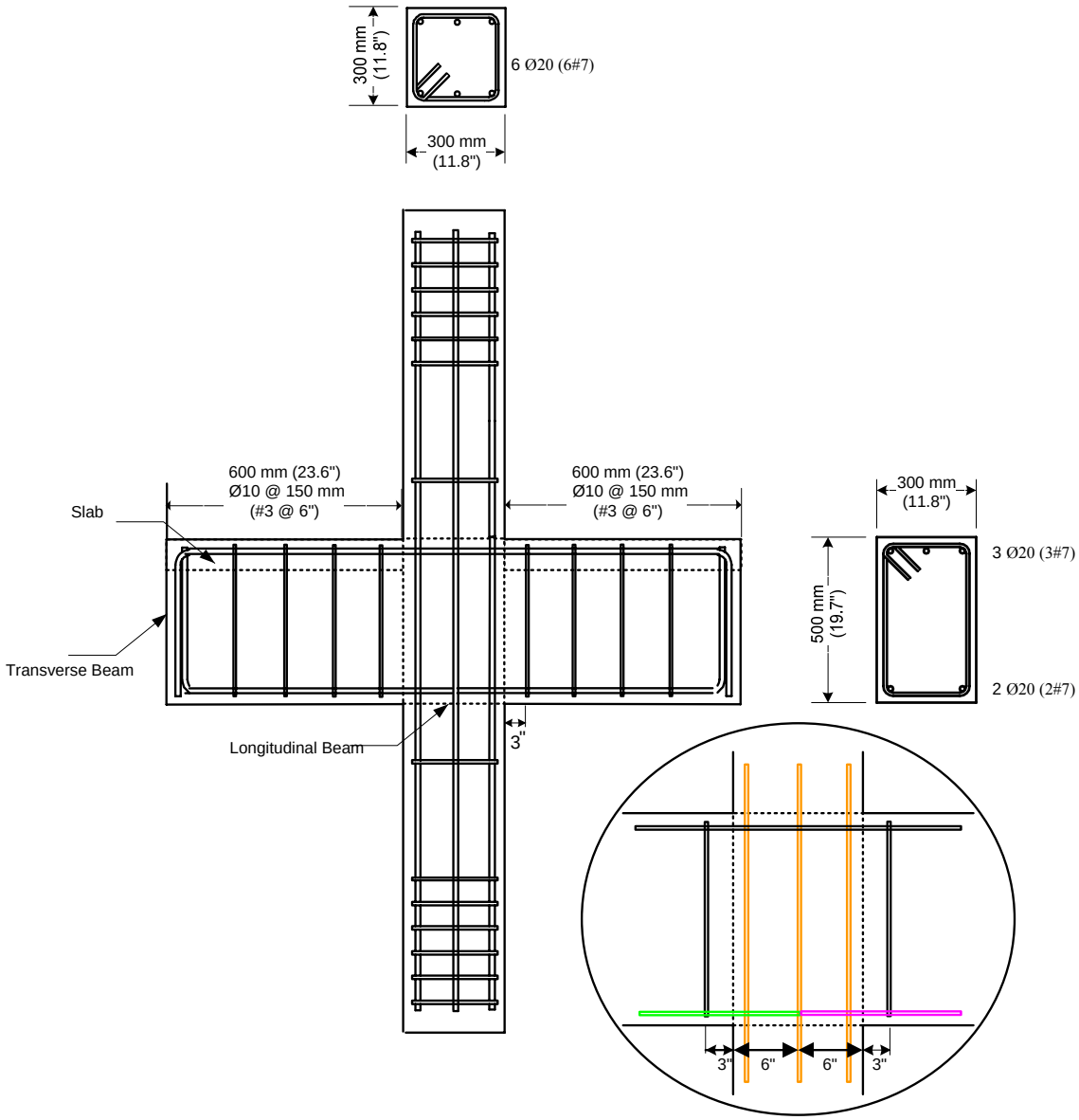

Figure 3.9. Reinforcement details of US3-ES specimens (Side view)

3.4.3. Details of CFRP Applications

3.4.3.1. US3-ES-FRP1

Design philosophy of the retrofitting methods should be explained briefly before the description of FRP application details. First of all, retrofitting strategy was constituted according to deficiencies in the joint, and the failure behavior and results of US3-ES-Control specimen. Deficiencies of the joint and members had been known; however, contribution of these deficiencies on failure of the specimen was not known well. Therefore, these outcomes were evaluated carefully before determination of retrofitting strategy and configurations of CFRP retrofitted beam-column-slab joints were developed as a result of collaborative research by Dr. Parvin, Dr. Yalcin and the author.

First of all, slippage of the bottom rebars of longitudinal beam seemed the most important problem in the push direction of loading. In order to solve this problem, using CFRP sheets through beam to end of the joint was selected as a reasonable solution. This application was named as belt application. In order to apply belts, transverse beams should be drilled in the way of slots, in spite of holes, at the location close to the level of rebars, inadequately embedded. Afterwards, these belt layers should be anchored to the longitudinal beam by application of hole. This was the main provision against slippage problem in the push direction of loading.

Secondly, spalling of concrete at the exterior (north) side of the joint core due to bending of top rebars of longitudinal beam seemed the most important problem in the pull direction of loading. Besides, shear and torsional deformations were also effective in terms of strength degradation of the specimen in this loading direction. In order to solve these problems, a few different methods were combined. Initially, FRP sheets were applied both vertical and horizontal directions. These layers extended through the end of the transverse beams in the horizontal direction, and through support regions of columns vertically. In order to fix these layers, column confinement layers in vertical FRP application and strips on transverse beams in horizontal direction were used.

The flexural capacities of the columns and longitudinal beam were enhanced by application of FRP sheets from top column face to top of the beam and from bottom column face to bottom of the beam. Another FRP layers were used at the north side to prevent spalling of concrete.

In order to prevent shear cracks on longitudinal beam, strips as a closed stirrup were used. These strips also worked for confinement. Other strips on the transverse beams were aimed also to reduce effect of the torsional cracks as well as shear cracks. Moreover, they confined the joint and beams.

The specimen US3-ES-FRP1 was strengthened using CFRP sheets by taking considerations given above into account. Strengthening details, namely, CFRP orientations and their application were explained step by step and also illustrated by the related figures.

At the first stage, slots were opened on floor slab in order to apply the FRP strips around both transverse and longitudinal beams. There were other slots which were opened for belt to prevent the slippage of the embedded bottom reinforcement. This belt would also be anchored to the longitudinal beam with 20 mm diameter hole. Totally, 10 slots for beam strips, two slots and one hole for belt were drilled and their details and orientations were given in the Figure 3.10. All the slots were 100 mm length and 20 mm width.

Secondly, application zones of FRP sheets were prepared. All the sharp corners of the members were beveled as well as sharp edges of drilled slots and holes. Application surfaces were also smoothened and prepared for FRP application. Afterwards, surface was cleaned with using FRP manufacturer's suggested equipment. Subsequently, epoxy primer coating was applied before wrapping FRP sheets.

First FRP practice of the specimen was performed by application of belts in order to prevent the slippage. 6 layers of belts were applied passing from transverse beams via slots and longitudinal beam via hole. Details of application are demonstrated in Figure 3.11.

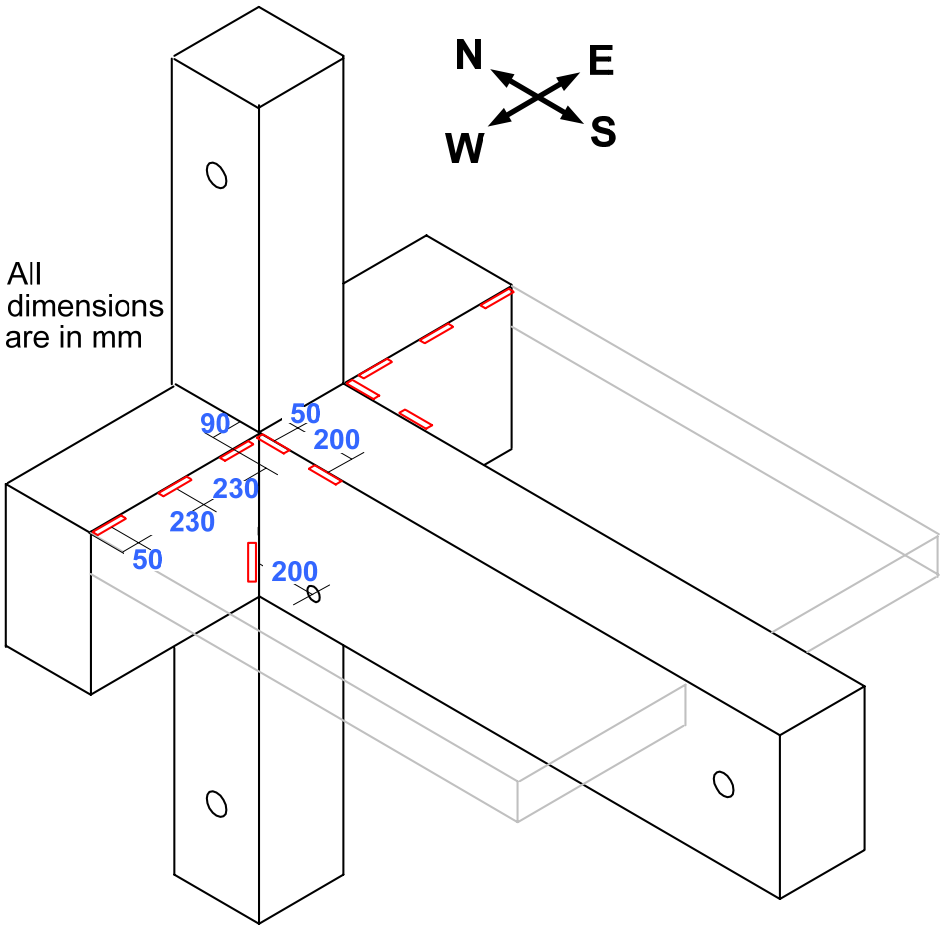

Figure 3.10. Drilling of anchorage holes

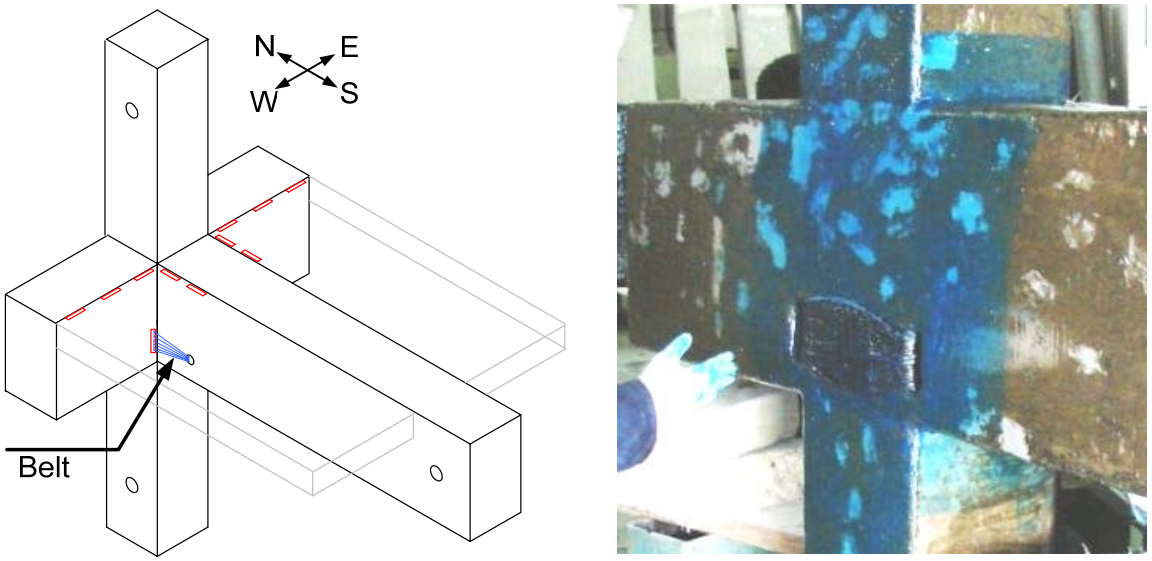

Figure 3.11. Application of belts

In the 4th step, three layers of 300 mm width CFRP sheets were applied at north and south side of the columns in order to increase flexural capacity of the columns. These layers covered the 600 mm part of the column in both sides. Due to the longitudinal beam, these layers in the south side were applied as L-shape and extended top and bottom of the longitudinal beam with a length of 300 mm. Figure 3.12 illustrates the details of application.

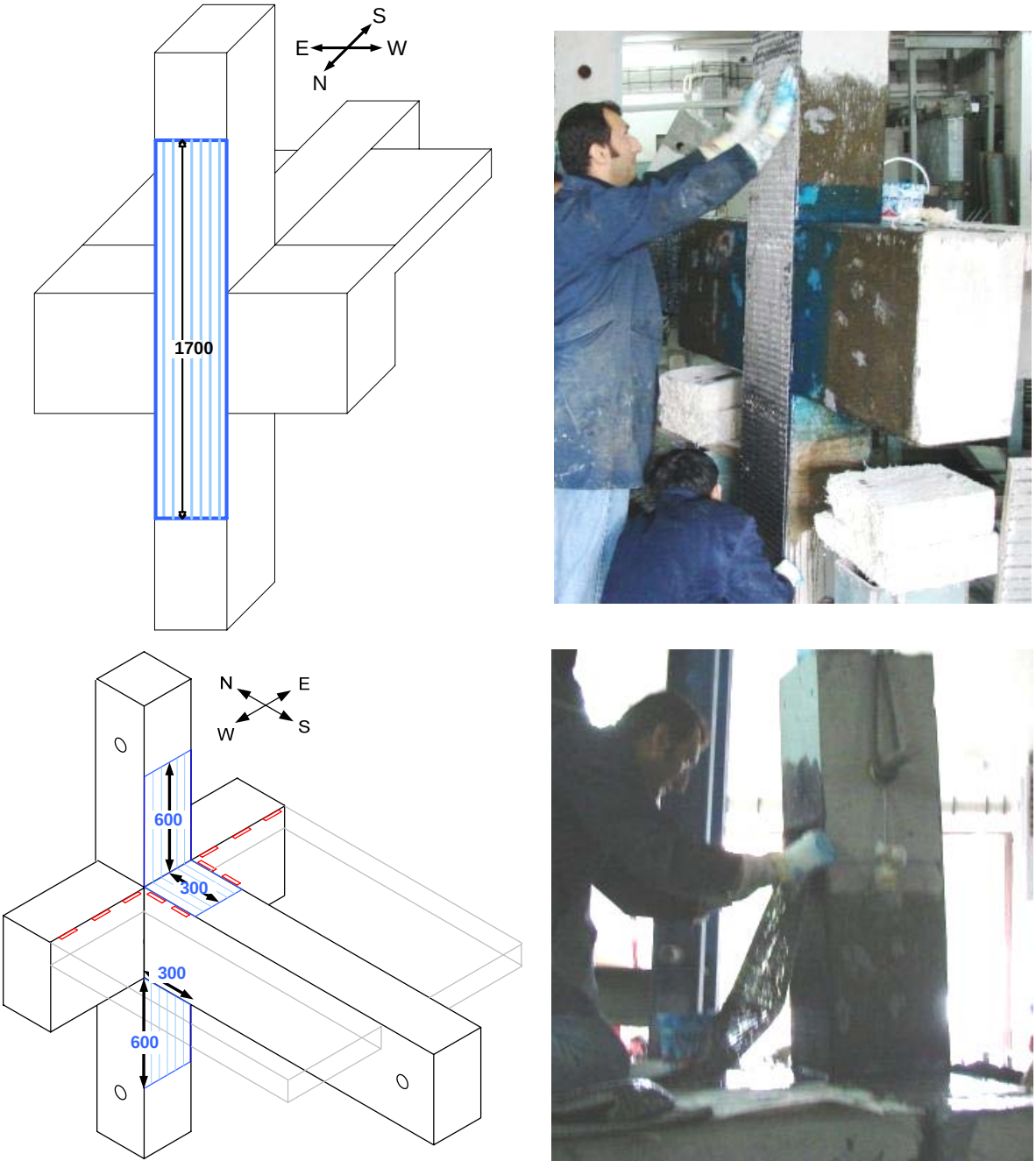

Figure 3.12. Application of column flexure sheets

After application of column flexure sheets, 6 layers of 500 mm width CFRP sheets were applied to the north side of the transverse beams and joint core in order to increase the shear and torsion capacity of the transverse beam and to prevent the spalling of joint core (see Figure 3.13).

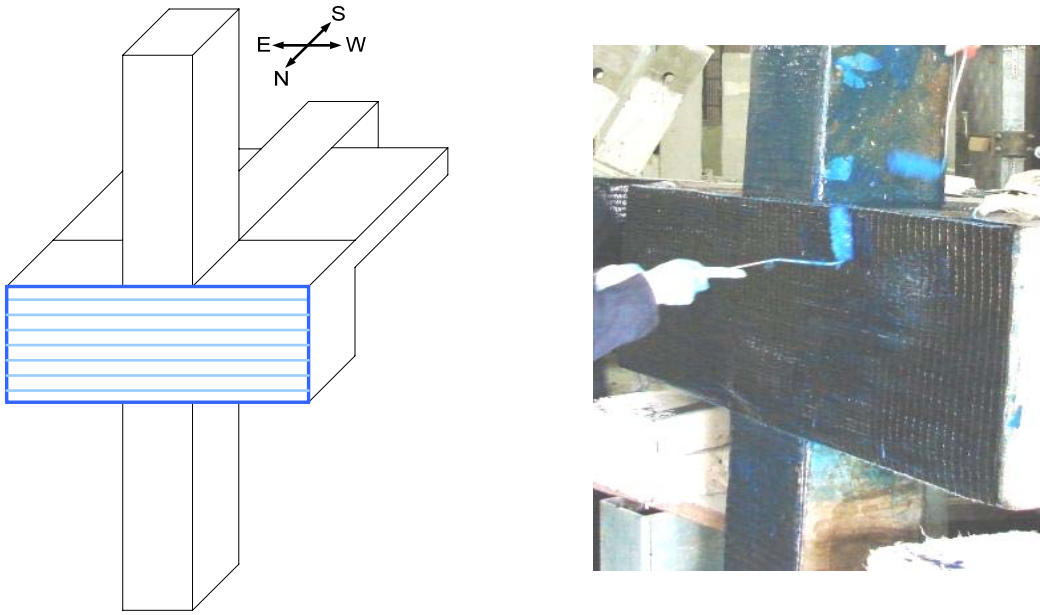

Figure 3.13. Application of CFRP on backside of the specimen

At the 6th step, column wraps were applied to increase the confinement effect in the columns. 300 mm part of the column from the joint was wrapped with 3 layers of CFRP sheets at the top and bottom column (see Figure 3.14).

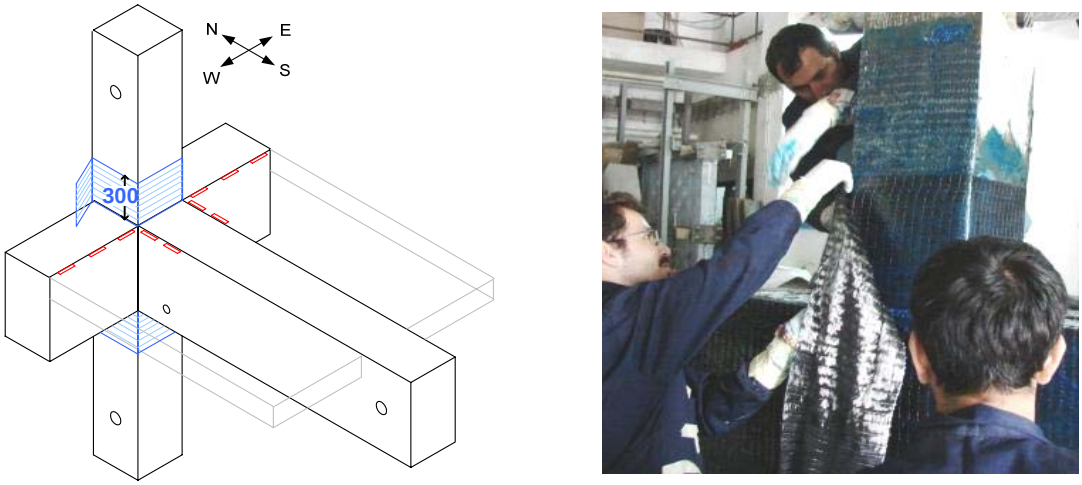

Figure 3.14. Application of column wraps

At the final step, 100 mm width 6 strips were applied around the beams in order to prevent debonding and increase shear capacity of the corresponding members and joint (see Figure 3.15).

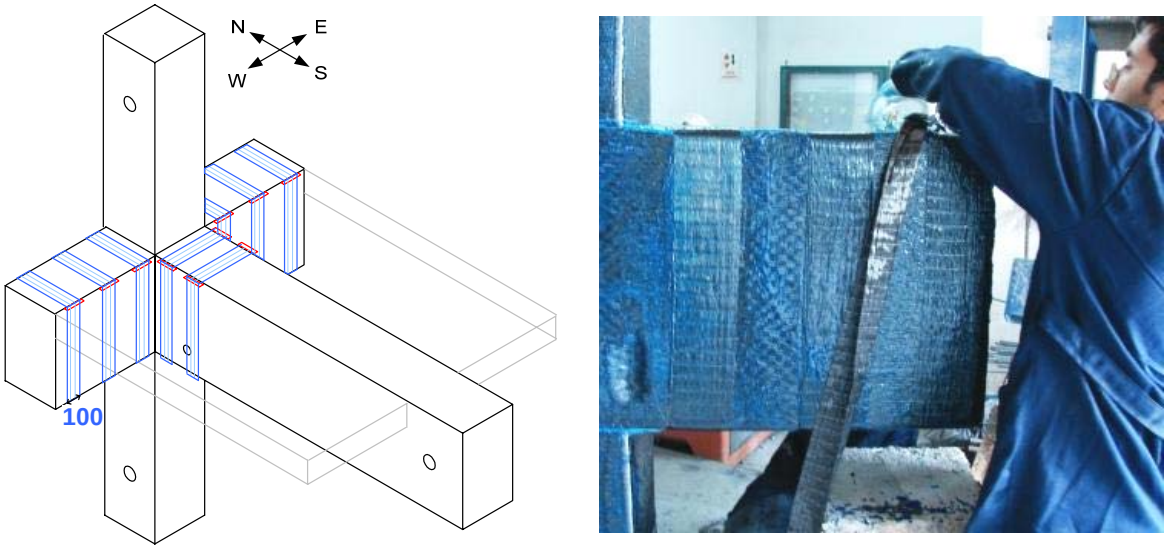

Figure 3.15. Application of CFRP strips

3.4.3.2. US3-ES-FRP2

For the second FRP retrofitted specimen, retrofitting strategy was determined according to the test observations and results of US3-ES-FRP1 specimen. Whereas the deficiencies of specimen were known well, effects of FRP retrofitting could also be evaluated with the help of comparison of the test results. After such detailed evaluation, modifications on FRP orientation and application of the 2nd FRP retrofitted specimen were determined.

In the push direction of loading, performance of the FRP retrofitted specimen was highly desirable up to the drift level 3.50%. Slippage of bottom re-bars of longitudinal beam was prevented up to this drift level. Afterwards, slippage occurred at the zone after the FRP belts. Therefore, the length of belt was extended 300 mm more from the column surface.

In the pull direction of loading, the performance was adequate and therefore other FRP orientation was not changed except column flexural sheets. Strain on column flexural sheets were so small after 300 mm from the floor level and therefore these FRP sheets both in north and south sides were shortened 200 mm.

Details of FRP orientation, actually the modifications on FRP orientation of US3-ES-FRP2 specimen were given on the following paragraphs with corresponding figures and applications photos. Considerations explained above were also legitimate for this application.

Initially, slots and holes were drilled as done in US3-ES-FRP1 specimen except the locations of holes on the longitudinal beam. And also one more additional strip would be applied; therefore two more slots were opened on the slab. Dimensions of the slots and holes were the same with the previous specimen. Details were given in the Figure 3.16. Afterwards, application surfaces of FRP were prepared as defined before and epoxy primer was applied to these surfaces. Then, 6 layers of 150 mm width FRP belts were also applied first. Figure 3.17 illustrate this application by corresponding drawing and application photo.

Three layers of 300 mm width FRP sheets were applied north and south sides of the columns as well as 500 mm length of beams. The aim of these layers was to increase flexural capacity of the columns and beams. Figures 3.18 and 3.19 illustrate the details of application.

Afterwards, six layers of 500 mm width FRP sheets were applied to the north side of the transverse beams and joint core in order to increase the shear and torsion capacity of the transverse beam and to prevent the spalling of joint core (see Figure 3.20).

Figure 3.21 illustrates the application of column wraps which were used for confinement of the columns. 300 mm part of the column from the joint was wrapped with three layer FRP sheets at the top and bottom column.

Finally, six layers of strips with 100 mm width were applied around the beams in order to prevent debonding and increase shear capacity of the corresponding members and also joint. Figure 3.22 illustrates the application.

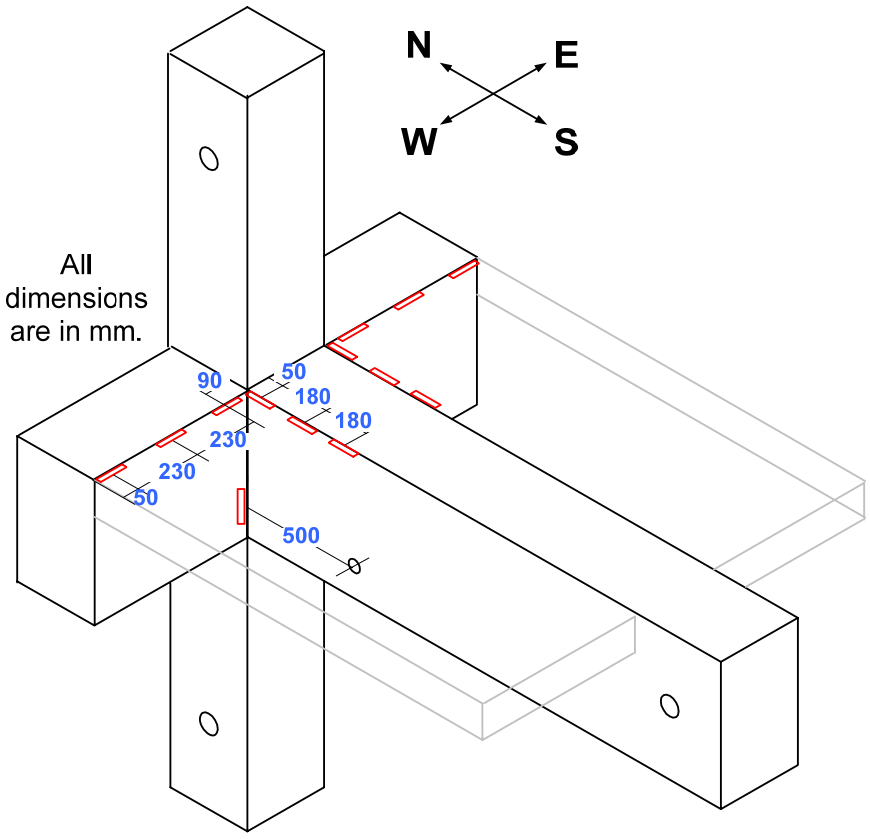

Figure 3.16. Drilling of anchorage holes

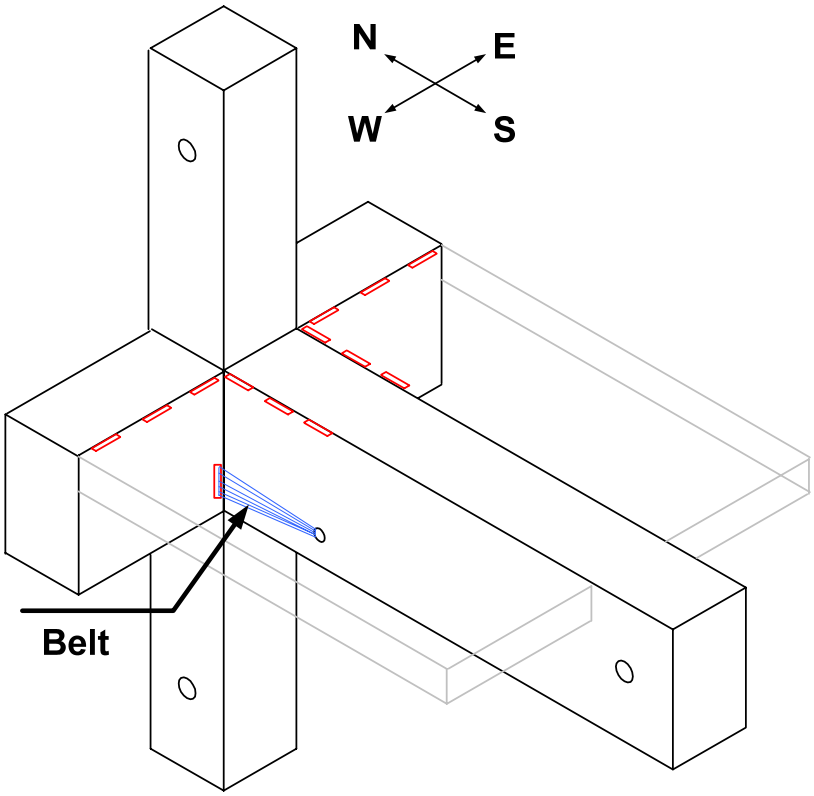

Figure 3.17. Application scheme of belts

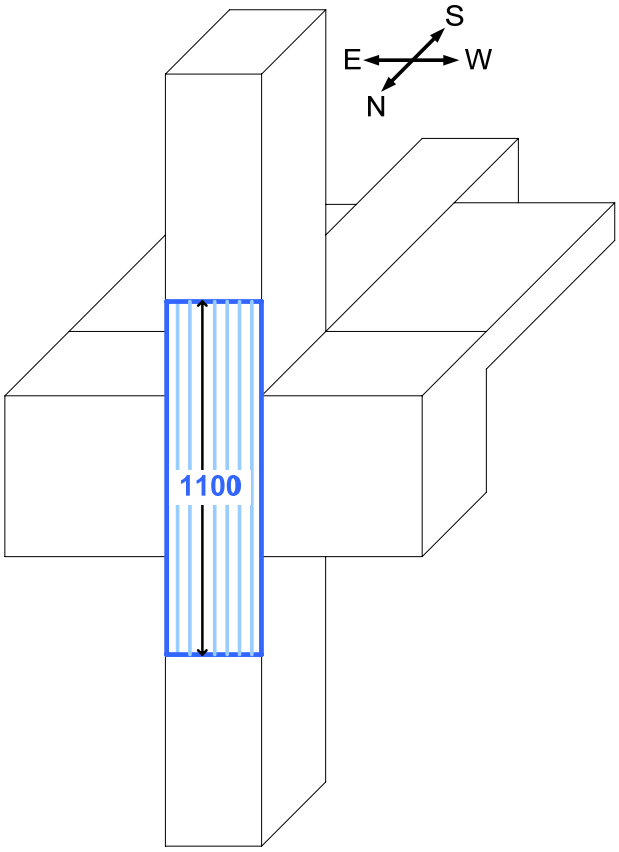

Figure 3.18. Application of column flexure sheets

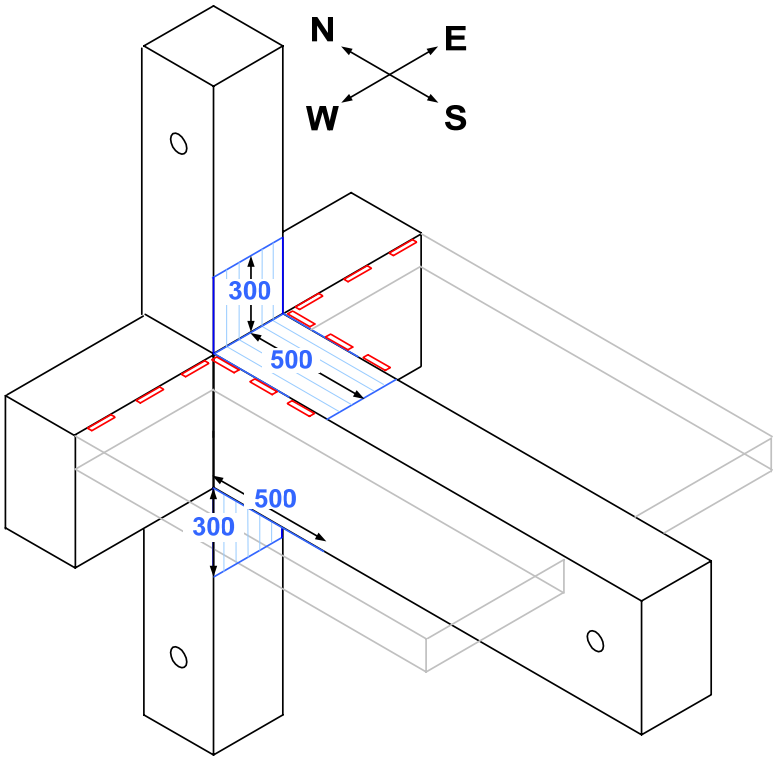

Figure 3.19. Application of column flexure sheets

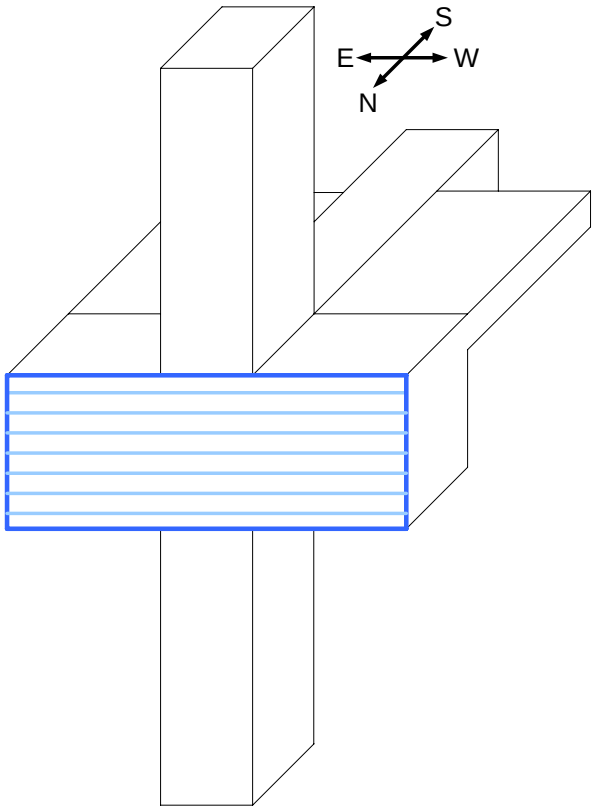

Figure 3.20. Application of CFRP on backside of the specimen

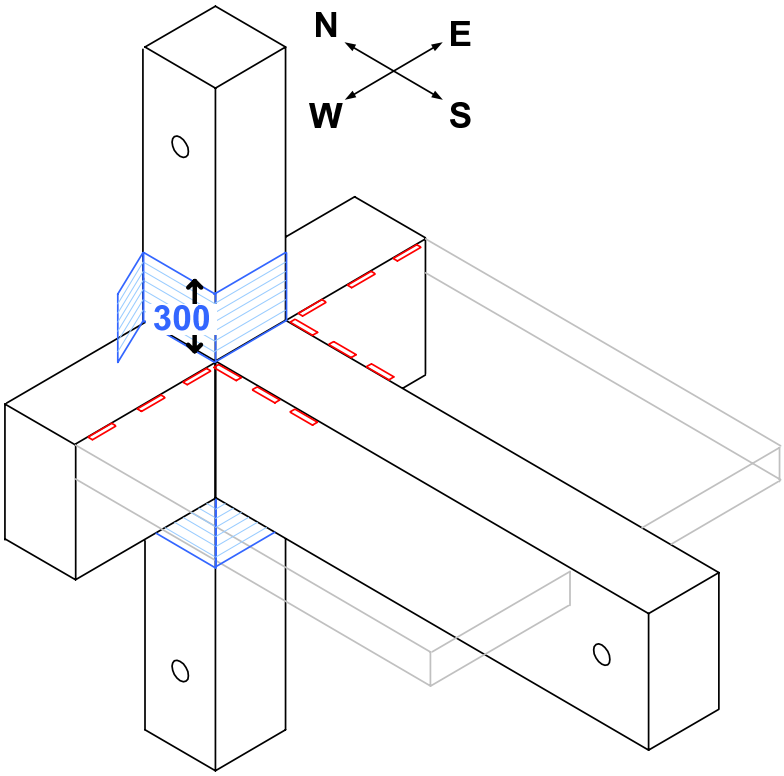

Figure 3.21. Application of column wraps

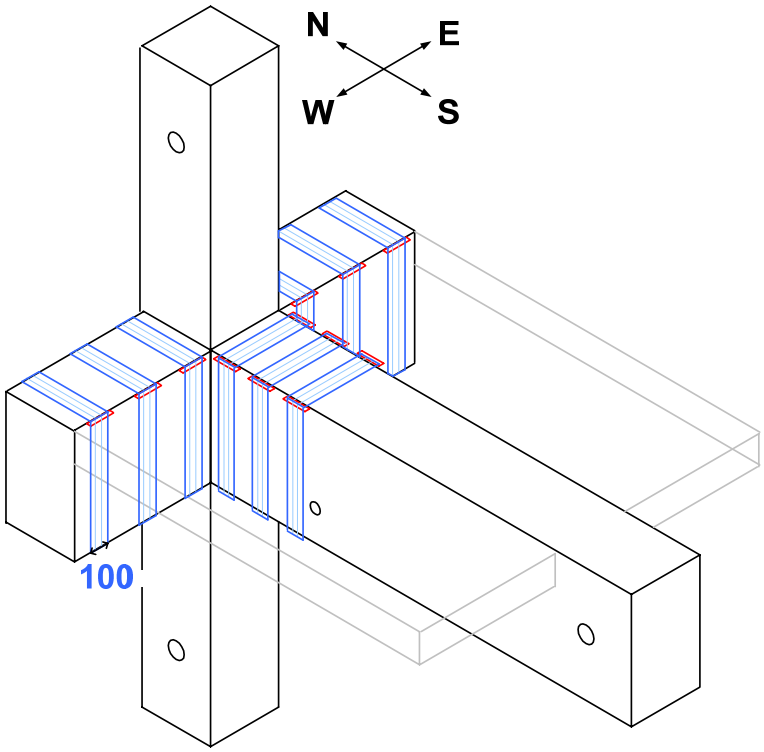

Figure 3.22. Application of CFRP strips

3.5. Material Properties

According to typical concrete strength of the buildings, which were built pre 1970's, C25 type concrete, the design compressive strength of 25 MPa (3626 psi), was used. While pouring the concrete, cylindrical test specimens with 150x300 mm dimensions were taken. After 28 days period, compressive strength tests were conducted on five cylinder test specimens. The modulus of elasticity of the concrete was computed according to the test data. Slope of the strain versus stress curve of the concrete was assumed as modulus of elasticity. All the compressive test results are given in table 3.2.

Table 3.2. Concrete compressive test results after 28 days

Test Specimen	Compressive Strength	Modulus of Elasticity
SP1	31,17 MPa	21,50 GPa
SP2	27,15 MPa	22,68 GPa
SP3	29,23 MPa	20,65 GPa
SP4	29,00 MPa	19,40 GPa
SP5	29,14 MPa	23,43 GPa
Average	**29,14 MPa (4226 psi)**	**21,53 GPa (3123 ksi)**

For the columns, 6Ø20 deformed rebars were used as longitudinal reinforcement, corresponding to 2.09% reinforcement ratio, representing the old practice of approximately 2% of the total area of column cross-section. For transverse reinforcement, Ø10 deformed rebars were used and spaced at 180 mm just above and below the joint region in order to produce typical unconfined columns. Transverse and longitudinal beams were reinforced with 3Ø20 deformed rebars at top and 2Ø20 deformed rebars at bottom as longitudinal reinforcement. Ø10 deformed rebars were used as stirrup with a space of 150 mm in transverse and longitudinal directions. Shear reinforcement was not used in the joint region in also both directions. These all reinforcement details represent the code requirements and construction practice of the pre 1970's.

Tensile tests were conducted for the rebars with each diameter, namely, Ø10 and Ø20, and their strength properties were determined exactly. For each diameter, three tests were done and average value of the test results was taken. Load and deformation data was

collected and their stress-strain relationships were determined. Mechanical properties of Ø10 and Ø20 reinforcements were given in Table 3.3 and 3.4.

Table 3.3. Mechanical properties of deformed rebars (Ø20)

Test Specimen	**Yield Strength**	**Ultimate Strength**	**Rupture Strain**
SP1	440.5 MPa	512.4 MPa	0.23
SP2	434.3 MPa	515.5 MPa	0.20
SP3	445.2 MPa	512.4 MPa	0.22
Average	440.0 MPa (63.8 ksi)	513.4 MPa (74.5 ksi)	0.22

Table 3.4. Mechanical properties of deformed rebars (Ø10)

Test Specimen	**Yield Strength**	**Ultimate Strength**	**Rupture Strain**
SP4	397.3 MPa	621.3 MPa	0.18
SP5	397.3 MPa	628.5 MPa	0.21
SP6	397.3 MPa	624.9 MPa	0.24
Average	397.3 MPa (57.6 ksi)	624.9 MPa (90.6 ksi)	0.21

FRP materials are widely used in different areas due to their excellent properties. In this research CFRP material, MBrace CF 130, produced by BASF was used. In strengthened specimens, Properties of CFRP are given in Table 3.5 and stress strain curve is given in Figure 3.23. These values and graph were taken from the manufacturer product data sheet.

Table 3.5. Properties of CFRP as per BASF catalogue

Nominal Thickness	0.176 mm/ply
Ultimate Tensile Strength (0°)	3800 MPa
Tensile Modulus (0°)	240 GPa
Ultimate Rupture Strain (0°)	1.55 %

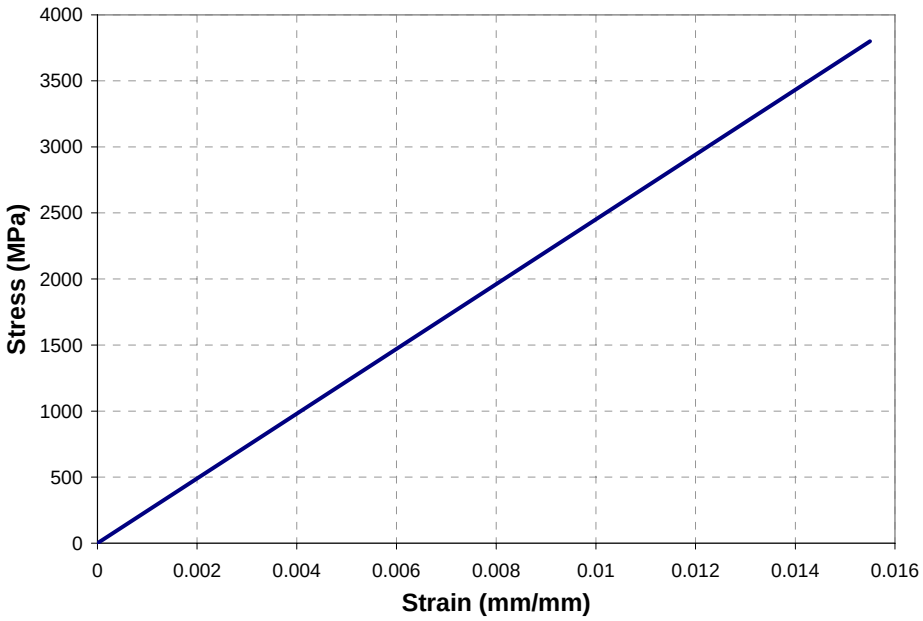

Figure 3.23. Stress-Strain Relations of CFRP

In order to apply the CFRP sheets, MBrace Primer is applied onto the cleaned surface. After the required time of curing of this primer, CFRP is wrapped with MBrace Saturant Adesivo, an epoxy-based chemical adhesive, to the concrete surface. Properties of these chemicals produced by BASF are given in the Table 3.6 and Table 3.7.

Table 3.6. Properties of MBrace Primer

Tensile strength	> 12 MPa
Bending strength	> 24 MPa
Tensile Modulus	> 700 MPa

Table 3.7. Properties of MBrace Saturant Adesivo

Tensile strength	> 50 MPa
Bending strength	> 120 MPa
Compressive strength	> 80 MPa
Tensile Modulus	> 3000 MPa
Bending Modulus	> 3500 MPa

3.6. Construction of Test Specimens

Test specimens were constructed in the Structure Laboratory of Boğaziçi University. Steel and wooden formworks were used to cast the subassemblies and all formworks were produced at once, and therefore all specimens were constructed at the same time. The forms were greased prior to concrete casting, to prevent concrete moisture loss and to help in the process of formwork removal. All longitudinal and transverse reinforcement steel bars of beam, column and floor slab were prepared in the laboratory according to shop drawings. The strain gauges were installed at key positions on the reinforcing bars after the bars assembled into steel cages and before placing into the formwork. Strain gauge wires were carefully arranged and protected during concrete pouring. 70 mm diameter steel pipes were installed on specified locations of the formwork to maintain proper support conditions on the test setup. The concrete was placed in the upright position of the form, as in field construction. The concrete was carefully vibrated with electric vibrators for proper consolidation. For each subassembly, all members were cast at once, using concrete from a local ready-mix concrete supplier. Figure 3.24 illustrates the pictures taken during production of the test specimens.

Figure 3.24. Construction of specimens

3.7. Test Setup

The loading set up is shown in Figure 3.25. The specimens were positioned in such a way that beam placed horizontally and hinged at the far end simulation a roller support. The column was in the vertical position and supported by a universal pin at the bottom end. For the transverse beams, there was no support applied and therefore they were left free. Constant axial load was applied with a vertical 1000 kN capacity hydraulic cylinder, while statically horizontal load was applied by displacement control with the horizontal actuator that had a capacity of 250 kN. Three cycles of the same amplitude in story drift were repeated before displacement amplitude was increased. The amount of the axial force applied was 30% of $f_c' A_g$, where f_c' is the characteristic strength of concrete and A_g is the cross-sectional area of column.

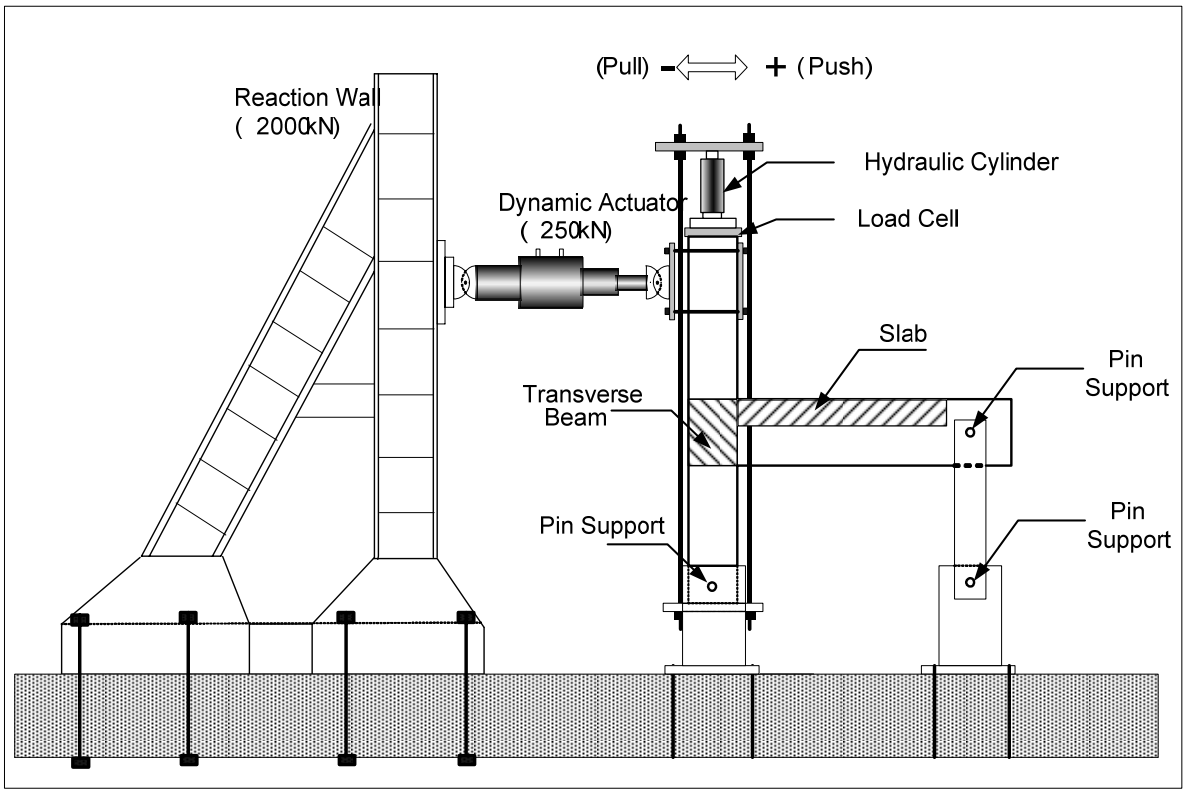

Figure 3.25. Test setup

3.8. Loading Pattern

Quasi-static cyclic loading in terms of interstorey drift was selected as experimental method of seismic action simulation. Details of this preference and basis of this loading philosophy were explained in the related part of the literature survey (Chapter 2.3.7). Therefore, the lateral load was applied based on the displacement control criteria. Displacements of the each drift level were calculated by the drift ratios. 39 reversed cycles were applied throughout the test and the details of the loading cycles can be seen in figure 3.26.

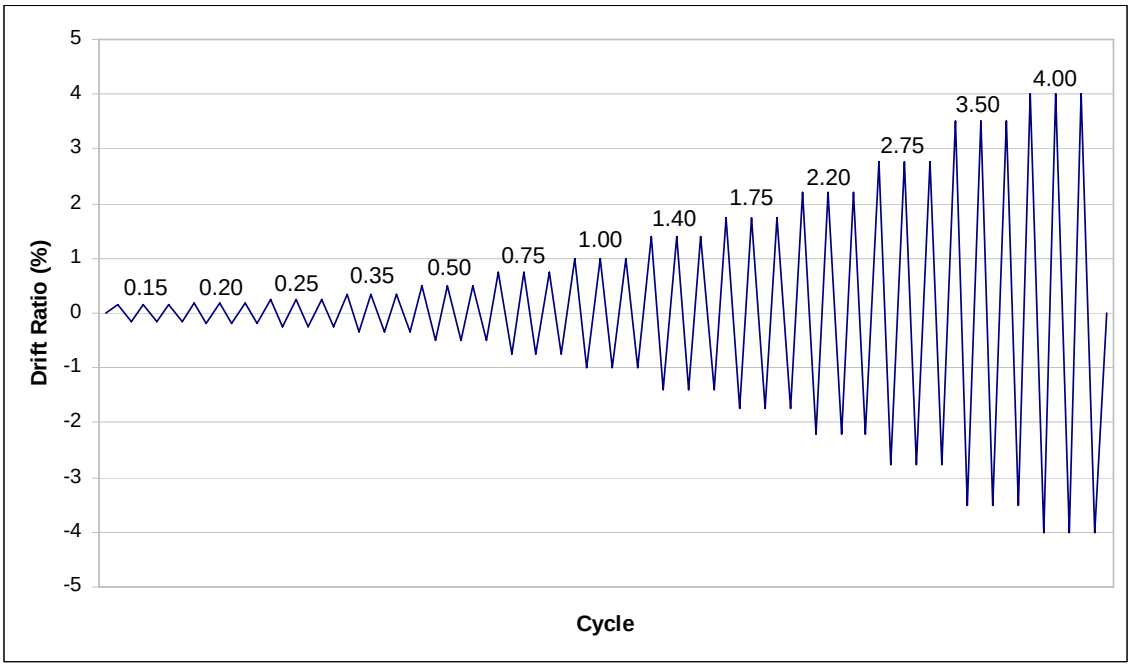

Figure 3.26. Loading pattern

3.9. Test Procedure and Data Collection

Test will be performed according to ACI T1.01 recommendations. Minimum requirements of the test procedure can be summarized as follows:

- Test modules shall be subjected to a sequence of displacement–controlled cycles representative of the drifts expected under earthquake motions for that portion of the frame represented by the test module. Cycles shall be predetermined drift ratios.

- Three fully reversed cycles shall be applied at each drift ratio.
- The initial drift ratio shall be within the essentially linear elastic response range for the module. Subsequent drift ratios shall be values not less than one and one-quarter times, and not more than one and one-half times the previous drift ratio.
- Testing shall continue with gradually increasing drift ratios until drift ratio equals or exceeds 0.035.
- Data shall be recorded from the test such that a quantitative, as opposed to qualitative, interpretation can be made of the performance of the module. As continuous recording shall be made of the test module, drift ratio versus column shear force, and photographs shall be taken that show the condition of the test module at the completion of testing for each sequence of three cycles.

3.10. Instrumentation

Mainly, two types of instrumentation were applied to specimens in order to make required analysis of the sections, member responses and system behavior. All the movement of members and sections on the critical locations were measured with linear variable differential transformers (LVDTs). Possible critical sections of the members were analyzed and strain values of the rebars were measured using strain gauges. After the application of CFRP sheets, strain values on possible failure zones were also measured by the strain gauges.

a) LVDT b) Strain gauge

Figure 3.27. LVDT and strain gauge

In placement of LVDTs, supports of LVDTs have to be fixed very well in order to take proper readings. Therefore, they were fixed to the members by drilling holes and nailing. However, this application used for the control specimens could not be appropriate

due to presence of CFRP sheets. Consequently, they were fixed on CFRP sheets by epoxy-based adhesives.

Strain gauges were mounted on rebars by the method, which consisted of numerous application steps. First of all, the surface of the rebars was smoothened by proper equipment until polished surface was obtained. Then, the strain gauges were glued by using a particular adhesive substance after the surface was cleaned by alcohol. After checking of the proper bonding between strain gauge and steel surface, cables were installed with soldering equipment. Strain gauges were then checked by measuring their resistances. Afterwards, the strain gauges were coated by silicone to avoid moisture and impact during the casting period of concrete. Figure 3.28 illustrates steps of application.

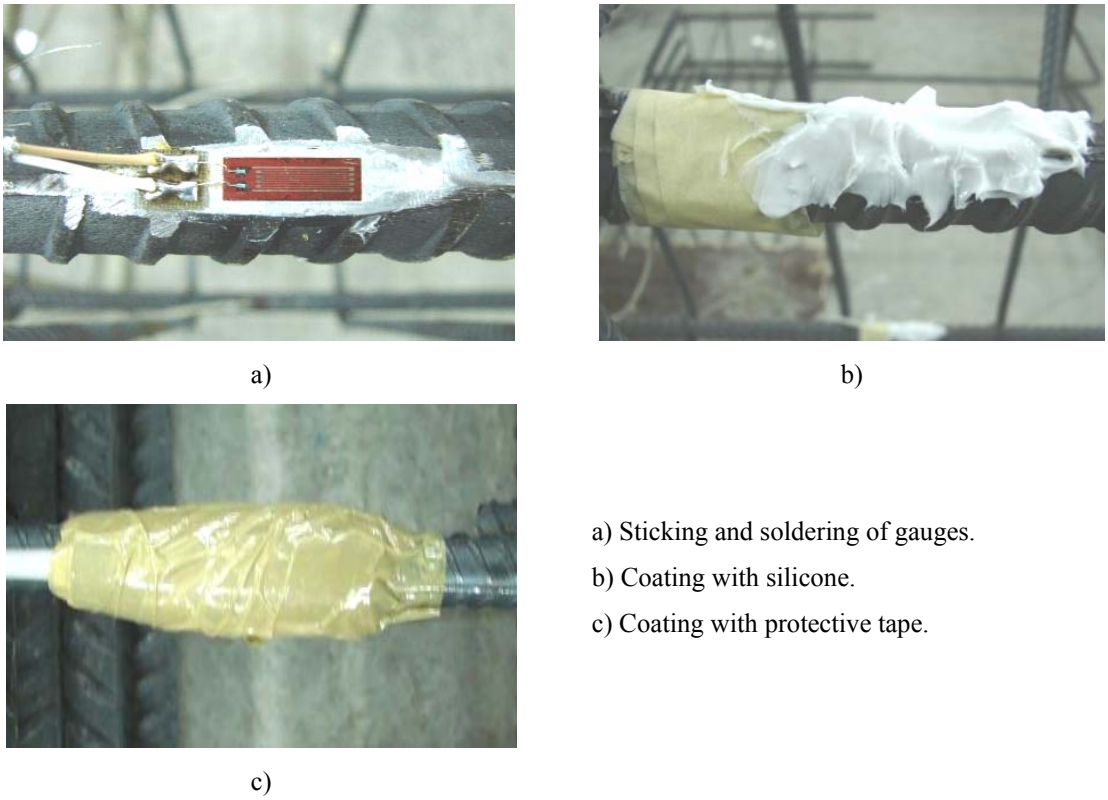

a) Sticking and soldering of gauges.
b) Coating with silicone.
c) Coating with protective tape.

Figure 3.28. Application of strain gauges

For the strain gauges on CFRP sheets, similar procedure was applied. First of all, a proper surface as smooth as possible was selected and cleaned by using alcohol. And then strain gauges were mounted carefully and the same procedures mentioned above were repeated except the coating.

3.10.1. Locations of Strain Gauges

As it was mentioned above, strain gauges were located on the critical sections. Details of strain gauge locations are the same for all of the specimens, except the locations of strain gauges on slab reinforcements. US3-E-Control specimen does not have floor slab and therefore such application cannot be mentioned. Amongst the US3-ES specimens, US3-ES-Control specimen has 11 extra strain gauges on the floor slab rebars with respect to other US3-ES specimens. The aim of application of extra strain gauges is to define the strain contours on floor slab and see the contribution of the slab on behavior of joint and longitudinal beam. Figure 3.29 illustrates the location of strain gauge instrumentation on column and beam rebars. Details of strain gauges on slab rebars are given in Figure 3.30.

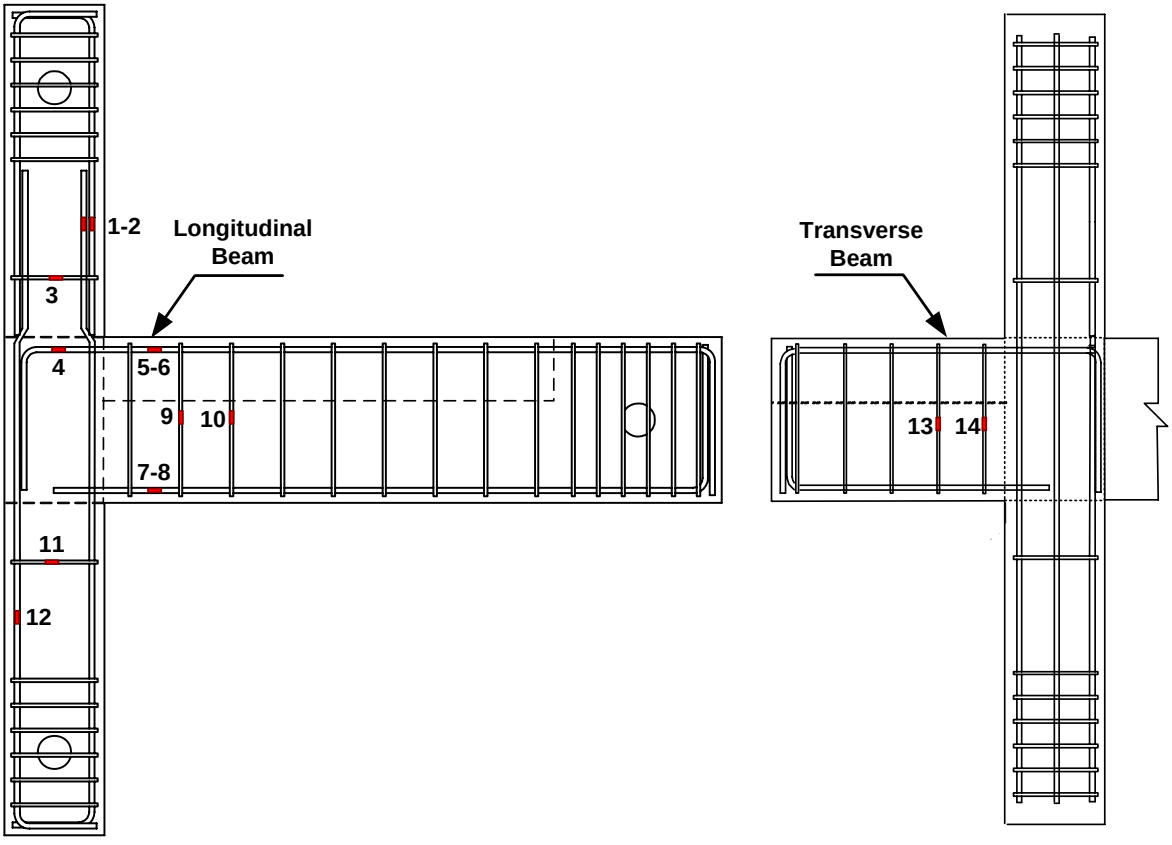

Figure 3.29. Location of strain gauges on rebars of beams and columns

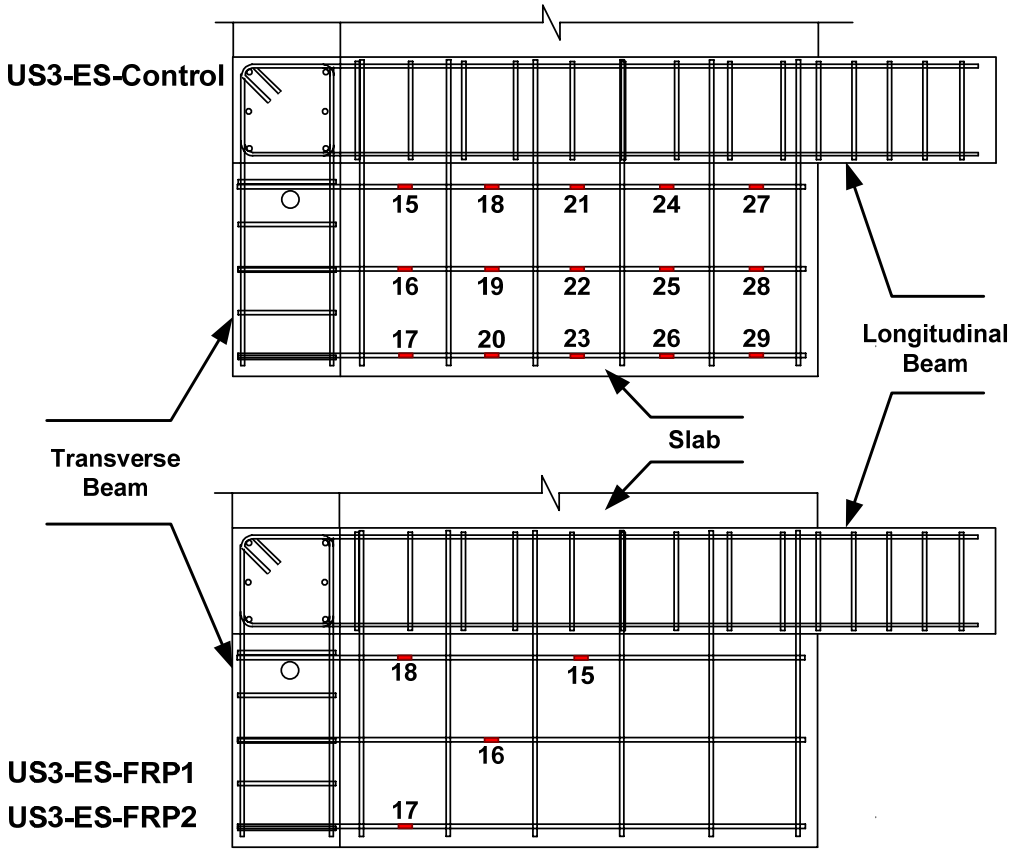

Figure 3.30. Location of strain gauges on rebars of floor slab

Strain gauges were also applied on CFRP sheets to measure strains on CFRP sheets. For US3-ES-FRP1 and US3-ES-FRP2, locations of strain gauges are shown in Figure 3.31 and Figure 3.32.

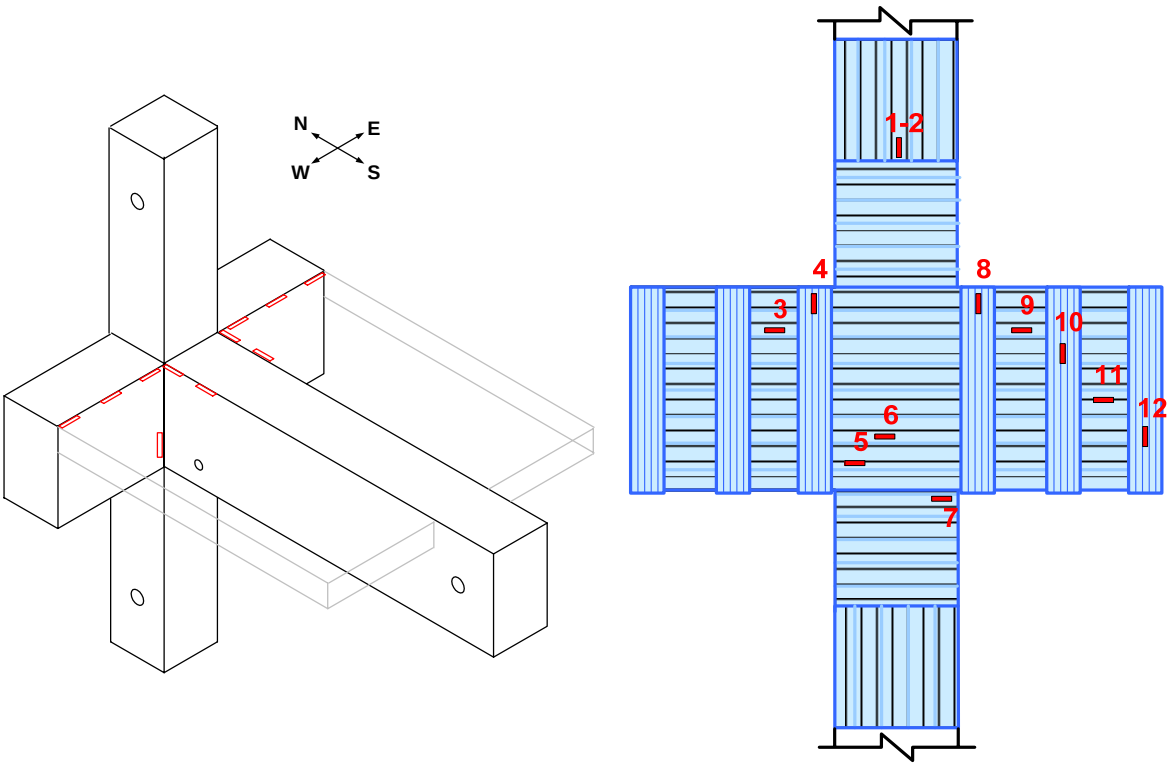

a) 3-D View

b) North View

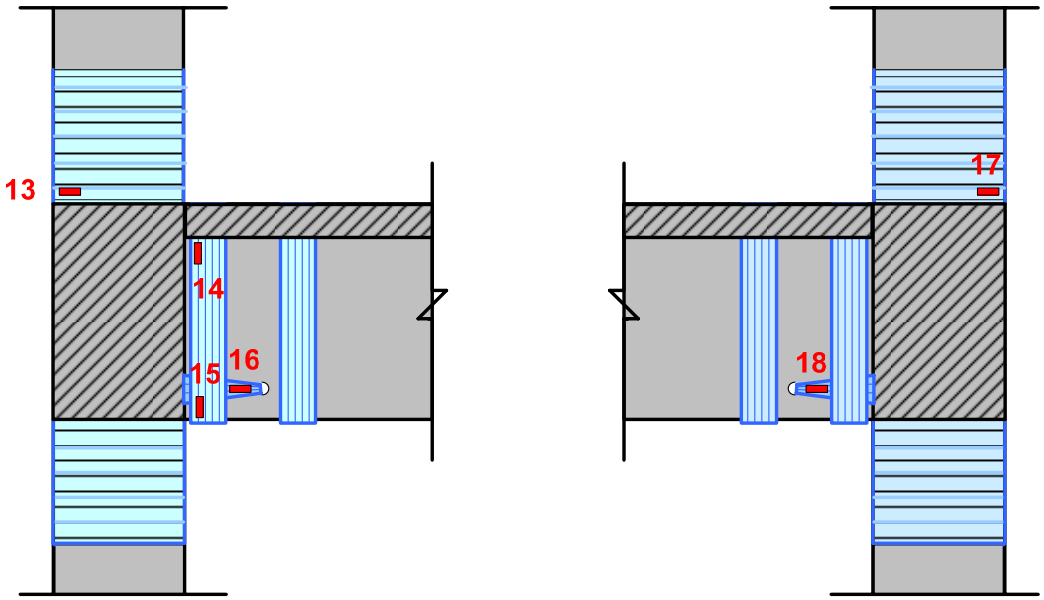

c) West View

d) East View

Figure 3.31. Locations of strain gauges on CFRP sheets for US3-ES-FRP1

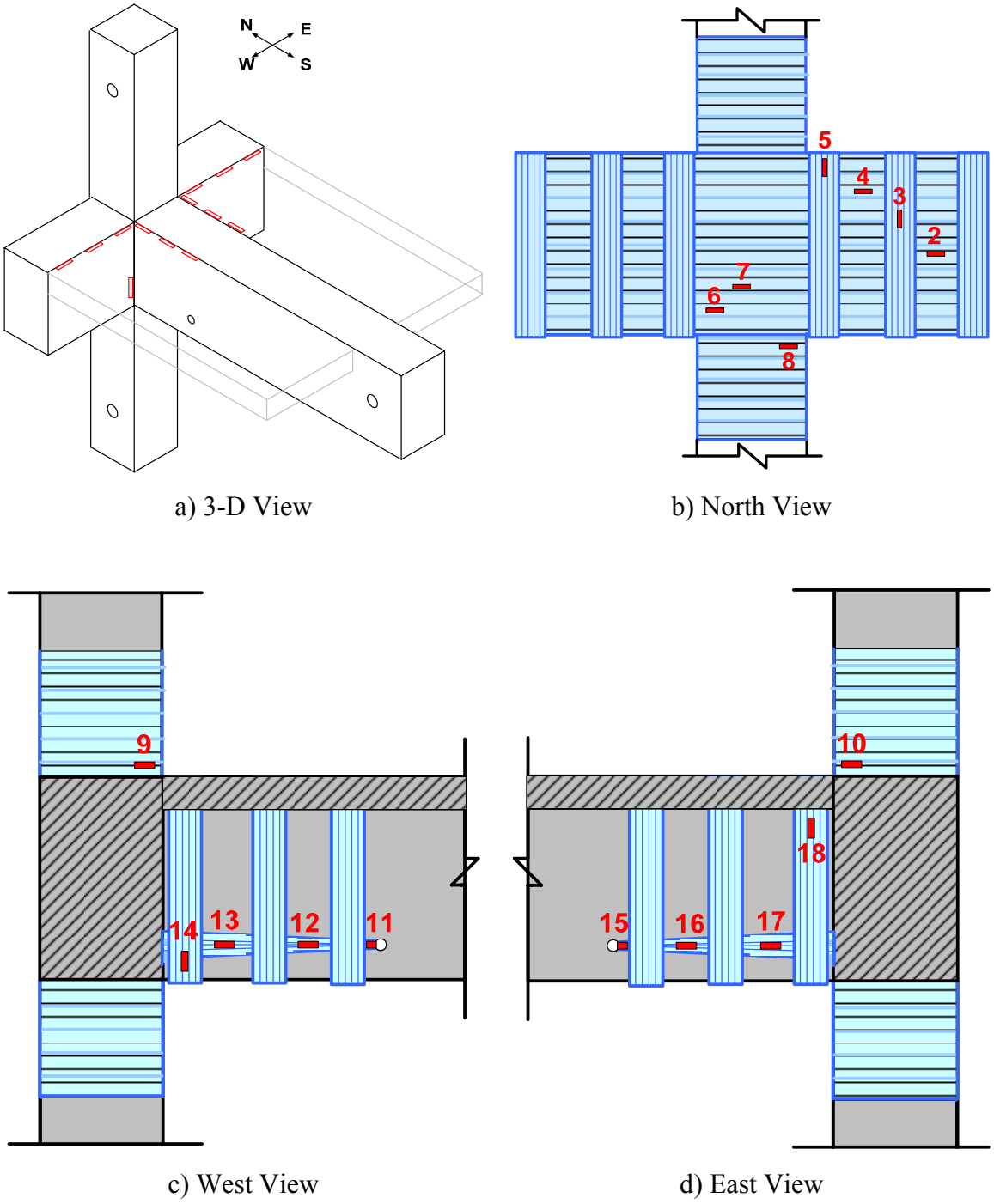

a) 3-D View

b) North View

c) West View

d) East View

Figure 3.32. Locations of strain gauges on CFRP sheets for US3-ES-FRP2

3.10.2. Locations of LVDTs

Locations of LVDTs were defined in order to measure curvature values at some critical sections, namely maximum moment regions, average top displacement of the specimen and slip of the bottom rebar of longitudinal beam. For all of the specimens, the same locations LVDTs were used as possible as it could be. Figure 3.33 shows the details of this application.

LVDT 1&2 were used for top displacement measurements. The average of these readings is assumed as top displacement. LVDT 16 quantified the support movement. LVDT 3&4 and 5&6 measured the shear deformation in vertical and horizontal directions respectively. LVDT 7 measured the crack opening for control specimens. LVDT 8&9, 10&11, 12&13 and 14&15 were used for curvature at top and bottom columns, and beams respectively. LVDT 17 was used for deflection at the support behind the longitudinal beam.

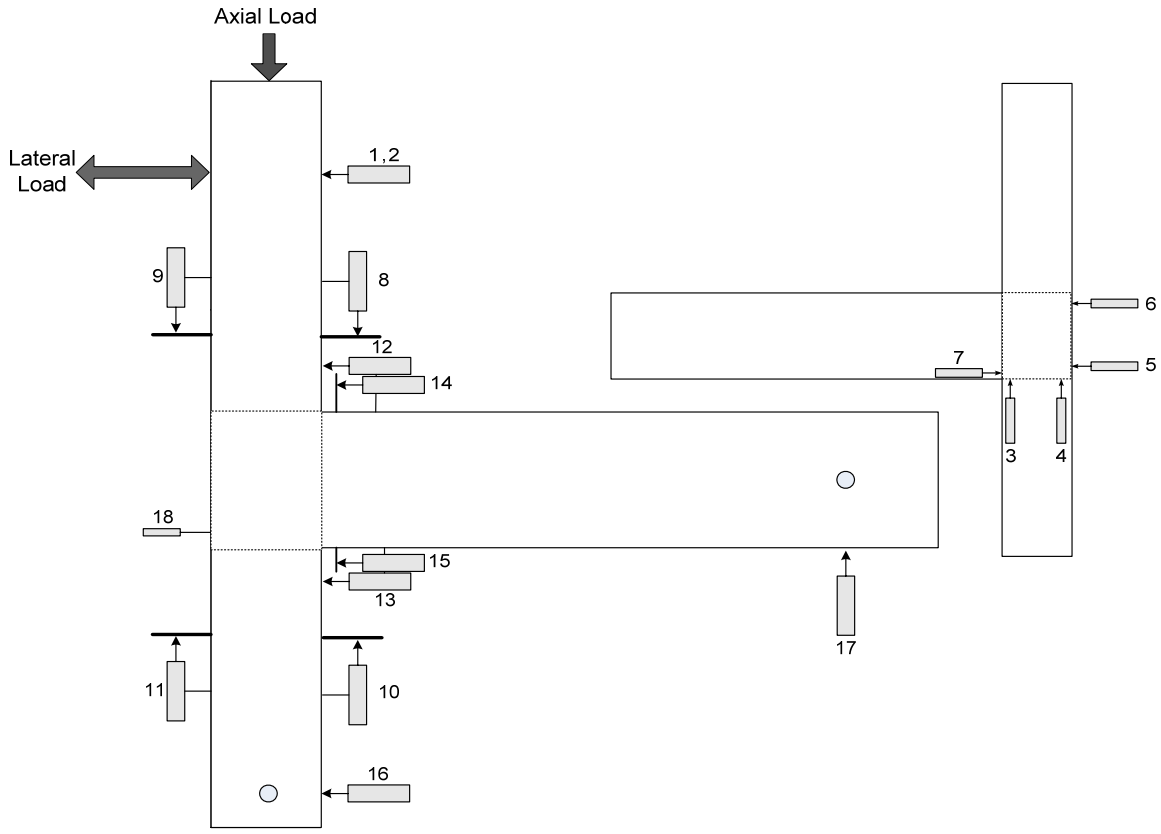

Figure 3.33. LVDT instrumentation

4. EXPERIMENTAL RESULTS AND DISCUSSIONS

4.1. General

The experimental results for two R/C beam-column joint specimens with and without floor slab as control specimens and two CFRP retrofitted beam-column joint with transverse beams and floor slab subjected to reversed-cyclic unidirectional loading are presented in this chapter. In order to investigate the overall behavior of the specimens, the load versus story drift response and the cracking pattern are discussed in the first stage. Stiffness degradation is also explored in order to compare the performance of joints. The behavior of the connection region is then presented in terms of joint shear deformations and slippage of beam reinforcement. Energy dissipation capacities of the specimens are discussed and the story drift components are presented to indicate the contribution from the deformations in each member to the story drift. The strain gauge readings are given to study the spread of yielding and the anchorage conditions for the reinforcements.

Before the discussion of the experimental results, repeating the names of the specimens is very helpful in understanding of the test outcomes properly. Figure 4.1 illustrates the specimens which were tested through this study.

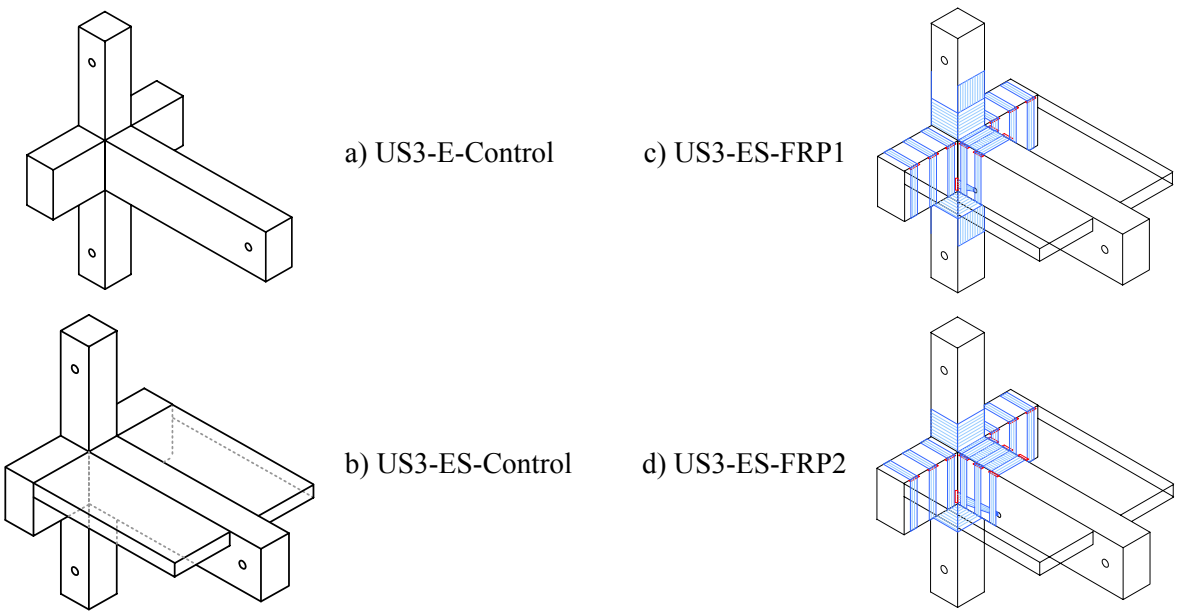

Figure 4.1. Description of test specimens

4.2. Overall Load versus Drift Response

It is very effective to discuss the overall load versus drift response of unidirectional subassemblages' tests in two main loading directions, namely, pull and push directions. Figure 4.2 to 4.5 illustrate the lateral load versus story drift response of the specimens, namely, US3-E-Control, US3-ES-Control, US3-ES-FRP1 and US3-ES-FRP2 respectively.

4.2.1. Push Direction

For the US3-E-Control specimen; the load versus drift graph in push direction shows an undesired behavior due to bond slippage of the bottom reinforcement of the longitudinal beam. It is also possible to say that the decrease of the lateral load in the push direction of loading merely stems from the slippage of the rebars of the longitudinal beam. For the US3-ES-Control specimen, the same slippage problem could be observed apparently. The reason of the slippage is inadequate anchorage length of reinforcement.

For the US3-ES-FRP1 specimen, the retrofitting methodology seems successful in solving the slippage problem. As it was explained in the experimental study chapter, CFRP sheets, named as belt, were applied in the region of inadequate embedment length. Besides of these CFRP sheets, L-shaped CFRP sheets were also applied from top of the bottom column through bottom of the longitudinal beam to prevent the possible slippage problem as well as increase the flexural capacity of the column. These retrofitting methods worked very effectively and delayed the failure up to drift level of 3.5%. In this drift level, crack which was occurred at the location of anchorage hole was opened extremely due to slippage. Finally, load decreased suddenly.

Retrofitting methodology of second CFRP retrofitted specimen (US3-ES-FRP2) was quite similar to previous one. The distance of belt's anchorage hole was extended to 500 mm from the column surface to the longitudinal beam. However, such modification did not enhance the slippage problem and the specimen showed almost the same behavior with the first CFRP retrofitted specimen.

4.2.2. Pull Direction

In the pull direction of the loading, the behavior of beam-column connection seems more complicated than those of in the push direction. Shear forces acted on the joint, torsional effect of floor slab, slab contribution on flexural capacity of the longitudinal beams and combined action of all these factors determine the behavior of joint.

For US3-E-Control specimen, longitudinal beam reached its yielding capacity at 1.40% drift level. On the following drift levels, a wide yield plateau could be observed clearly. Whereas the load diminished at the drift level of 4.00%, such load reduction was not adequate for failure criteria of 20% load decrease. Besides of this, due to limitation of the actuator stroke, the target displacement could not be exactly reached for this specimen. If the target displacement was reached exactly, the load would increase rather. Therefore, the performance of the US3-E-Control specimen in the pull direction of loading is quite excellent.

Effect of slab reinforcements of US3-ES-Control specimen in pull direction of loading could be observed as an increase in the load capacity of the beam. Although longitudinal beam could carry 40% higher flexural forces than the beam without slab, the failure of US3-ES-Control specimen was observed according to failure criteria described above. The mode of failure is highly complicated. First of all, the section is almost reached its flexural capacity. According to strain gauge readings, observation of yielding on some of reinforcement bars confirmed this action. Section analysis also verified that the section reached its moment capacity. Secondly, shear forces acted on the joint could cause cracks from joint core towards both upper side of the top column and through the end of transverse beams. Whereas the joint core could not be seen obviously, these cracks expressed that the shear failure occurred in the beam-column joint region. Finally, top rebars, inside the joint core, of longitudinal beam were bended and caused the spalling of the concrete at the exterior (north) side of the joint region. Such bending action might stem from the joint deterioration due to shear forces.

FRP retrofitting technique appears very effective on behavior of US3-ES-FRP1 specimen in pull direction of loading. Load carrying capacity increased 20% with respect

to capacity of US3-ES-Control specimen. Furthermore, failure criterion which had been mentioned above was not achieved. The gradual decrease of 5% in lateral load capacity was observed. Therefore, the performance of the specimen could be accepted as sufficient.

For US3-ES-FRP2 specimen, it is possible to express that the specimen behaved similar to the previous CFRP retrofitted specimen in pull direction of loading. Load carrying capacities of these specimens were almost the same. Due to no significant changes on CFRP retrofitting schemes of these specimens, the results were obtained as expected.

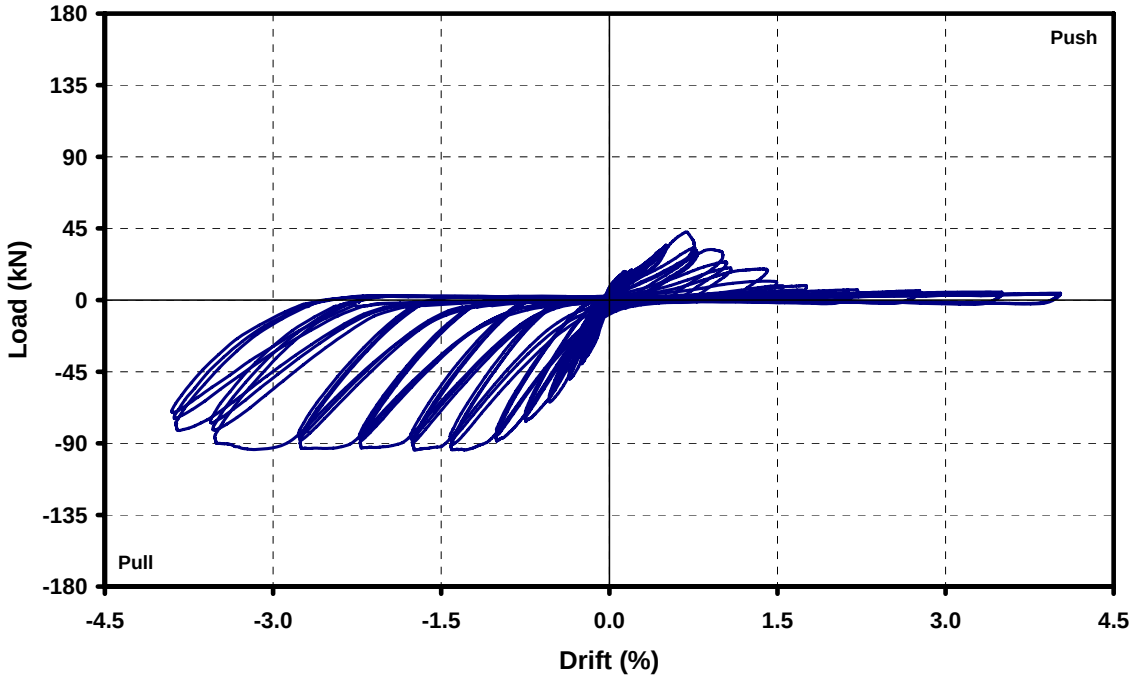

Figure 4.2. Lateral load versus story drift graph for US3-E-Control specimen

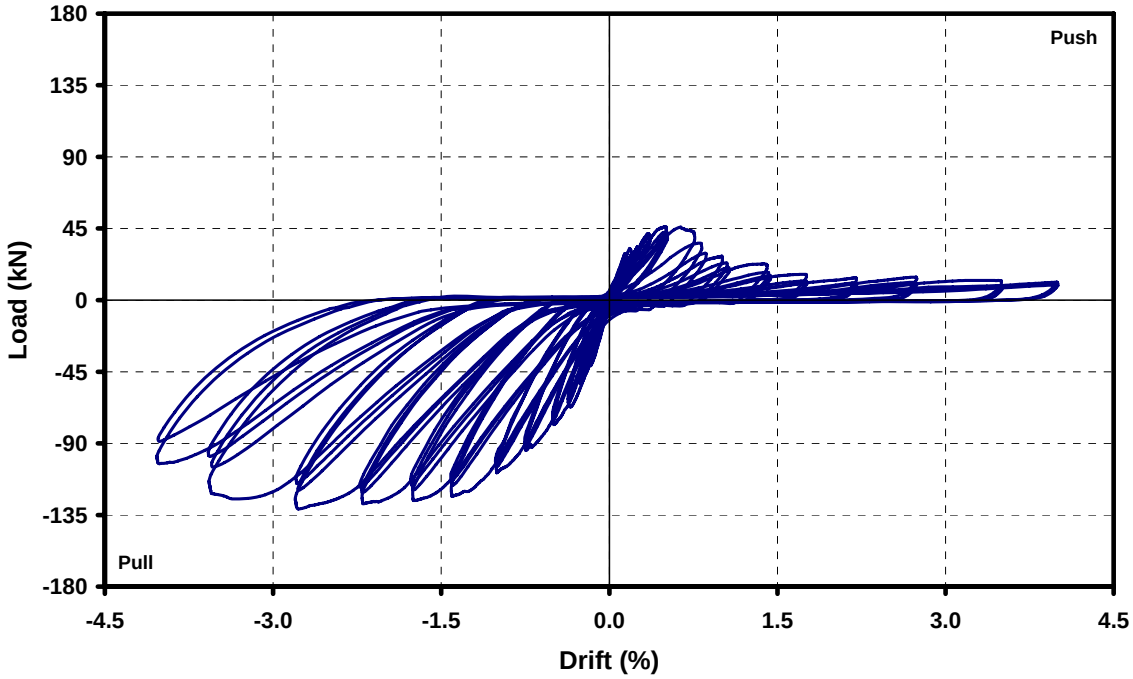

Figure 4.3. Lateral load versus story drift graph for US3-ES-Control specimen

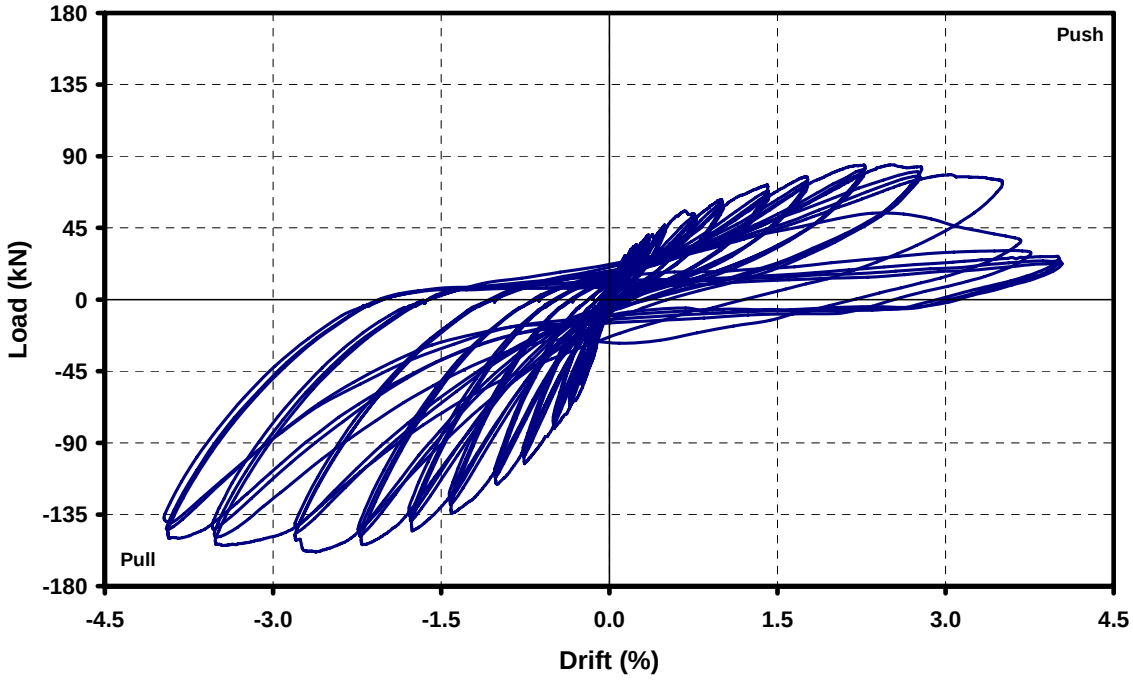

Figure 4.4. Lateral load versus story drift graph for US3-ES-FRP1 specimen

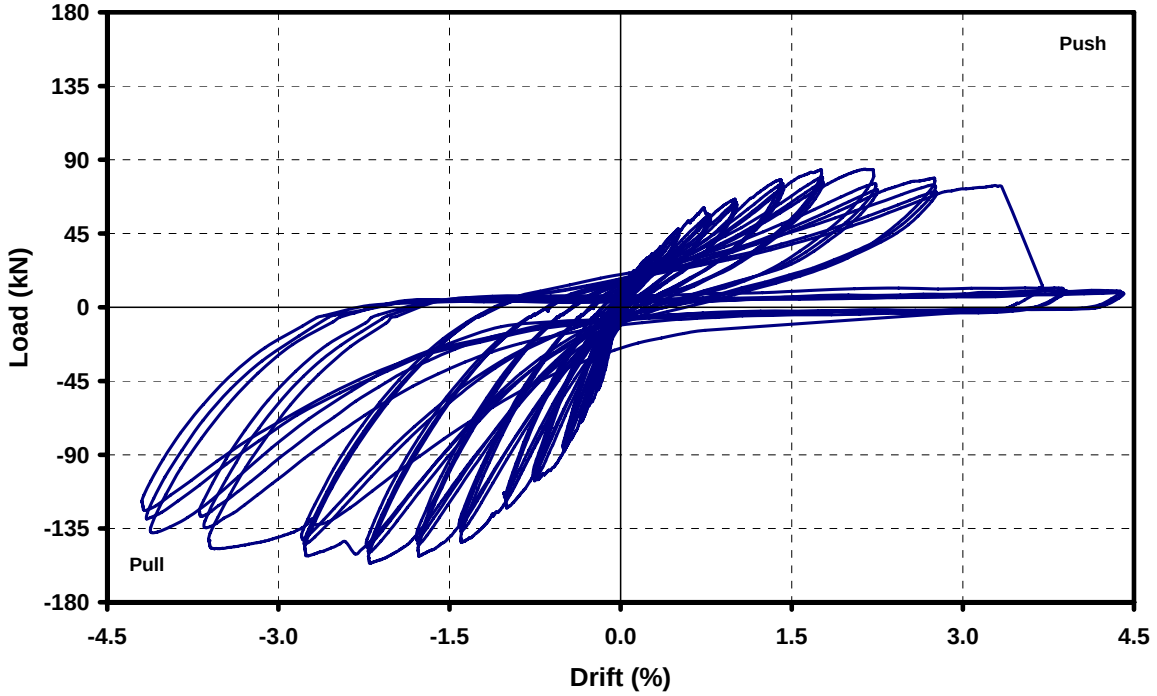

Figure 4.5. Lateral load versus story drift graph for US3-ES-FRP2 specimen

Figure 4.6 compares all four specimens using envelope curves of lateral load versus story drift responses. US3-E-Control specimen presented the worst performance among the specimens. US3-ES-Control behaved better due to the contribution of floor slab. Lateral load capacity was increased distinctly.

Envelope curves of specimens obviously demonstrate the enhanced behavior of beam-column joints after strengthened with CFRP sheets. On the following parts, such enhancement would be discussed in terms of other important parameters, like energy dissipation and deformation capacities. The behaviors of retrofitted specimens are so similar under cyclic loading and they present a great improvement especially in the push direction of loading.

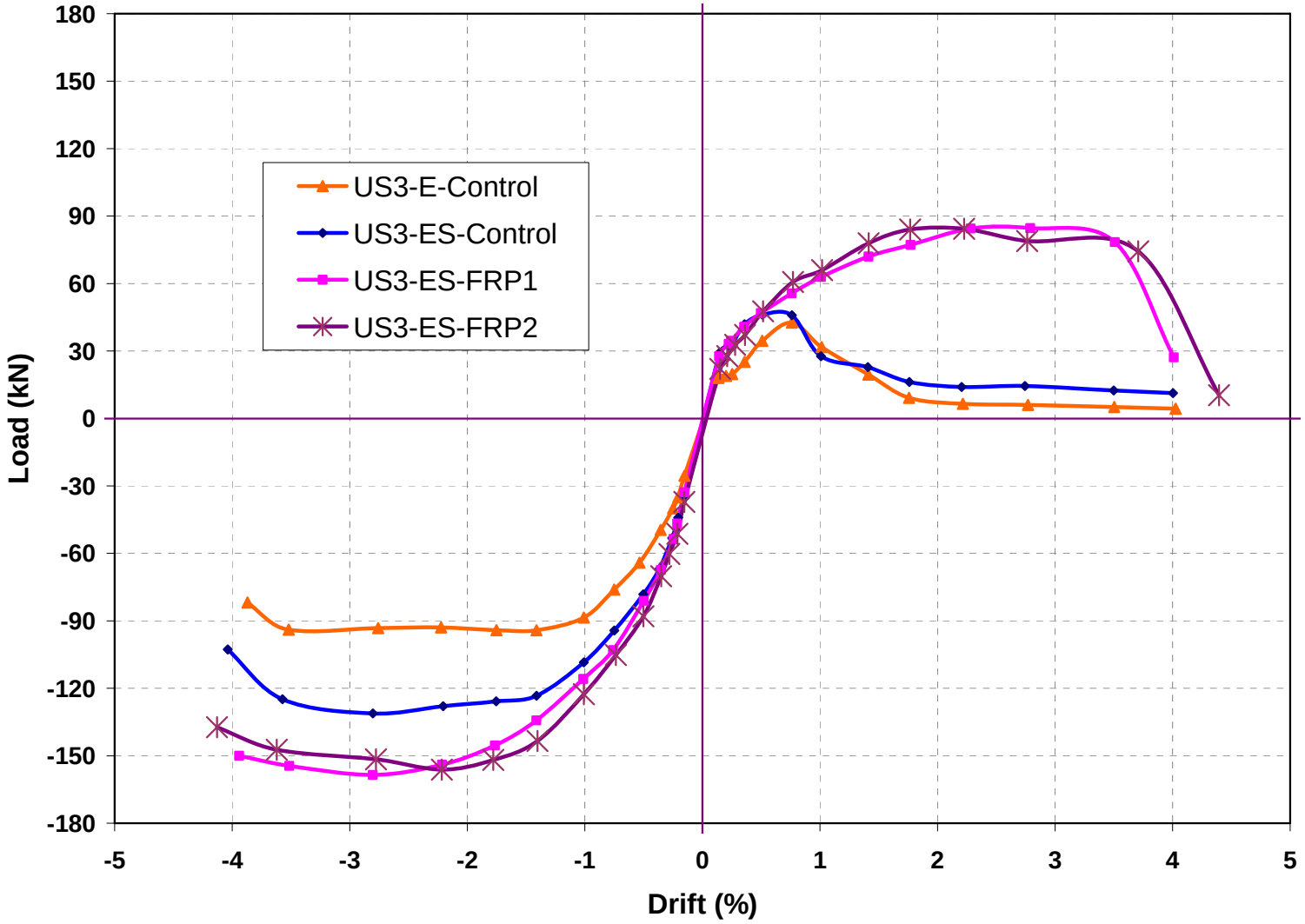

Figure 4.6. Comparison of lateral load versus story drift response of specimens

4.3. Stiffness Degradation

Stiffness of the beam-column joint specimen was investigated in both push and pull directions of loading individually due to different behavior of joint and discussed in the following paragraphs. In calculations, maximum story shear force (the lateral load) was divided by the corresponding displacement of each cycle in order to define the stiffness term.

4.3.1. Push Direction

Stiffness degradation of the US3-E-Control specimen was illustrated in Figure 4.7. Stiffness of the specimen was decreased gradually due to some small flexural and shear cracks up to the drift level of 0.75%. Afterwards, slippage of the longitudinal beam rebars occurred and the stiffness of the joint declined rapidly. After 1.5% drift ratio, stiffness term reached almost zero. For the US3-ES-Control specimen, almost the same manner of the stiffness degradation could be observed after the slippage occurred. However, before the slippage, the stiffness values of US3-ES-Control specimen were higher than those of US3-E-Control. Such difference is due to slab contribution. Figure 4.8 shows the behavior of US3-ES-Control specimen in terms of stiffness degradation.

For the US3-ES-FRP1 specimen, trend line of the stiffness degradation expressed an enhanced behavior with respect to control specimen (see Figure 4.9). Affirmative effect of CFRP retrofitting on slippage trouble could also be observed obviously. From the 0.75% drift level, the stiffness of the specimen did not decrease sharply unlike control specimens; besides, it decreased gradually due to flexural and shear cracks.

It is possible to say the same algorithm on stiffness degradation behavior for the US3-ES-FRP2 specimen could be observed. Figure 4.10 illustrates the behavior of the specimen.

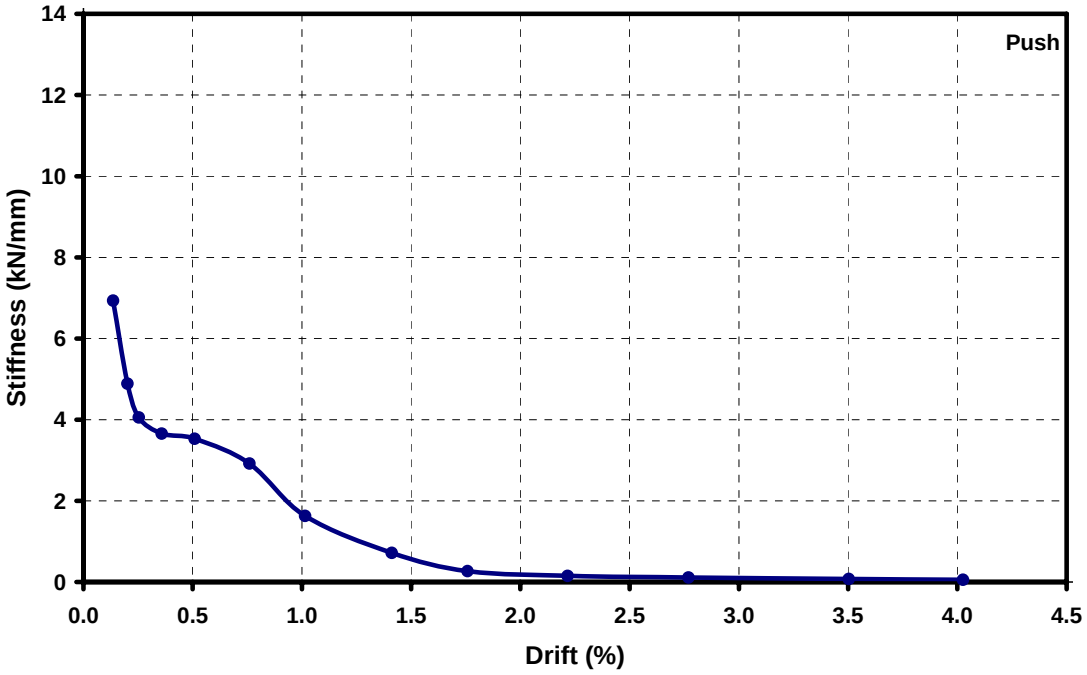

Figure 4.7. Stiffness degradation of US3-E-Control specimen

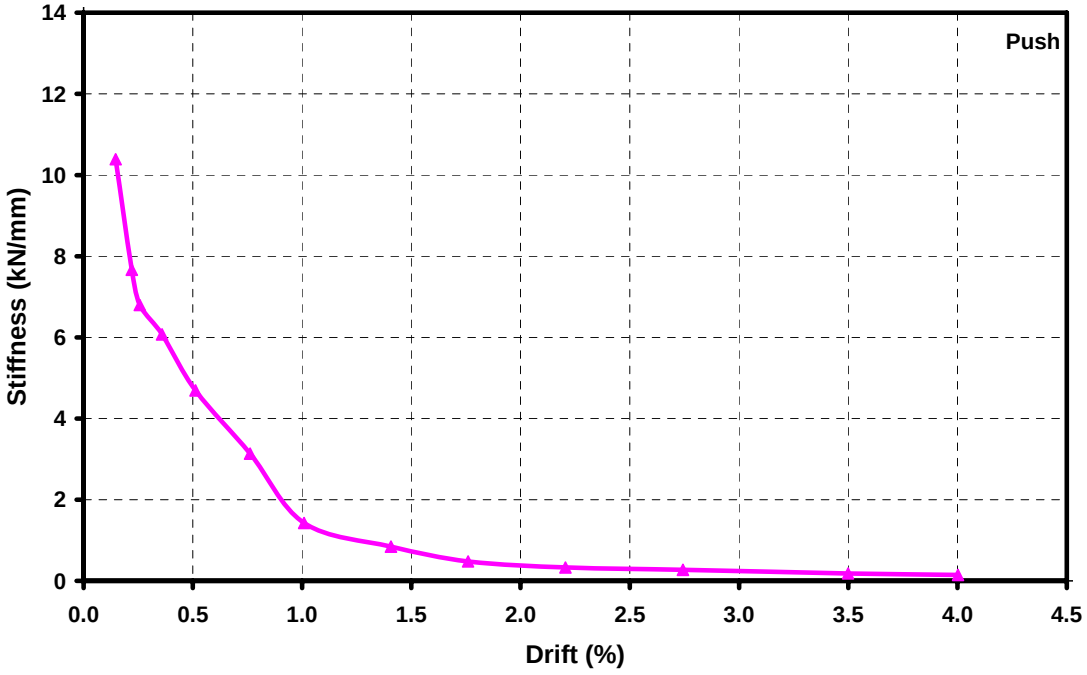

Figure 4.8. Stiffness degradation of US3-ES-Control specimen

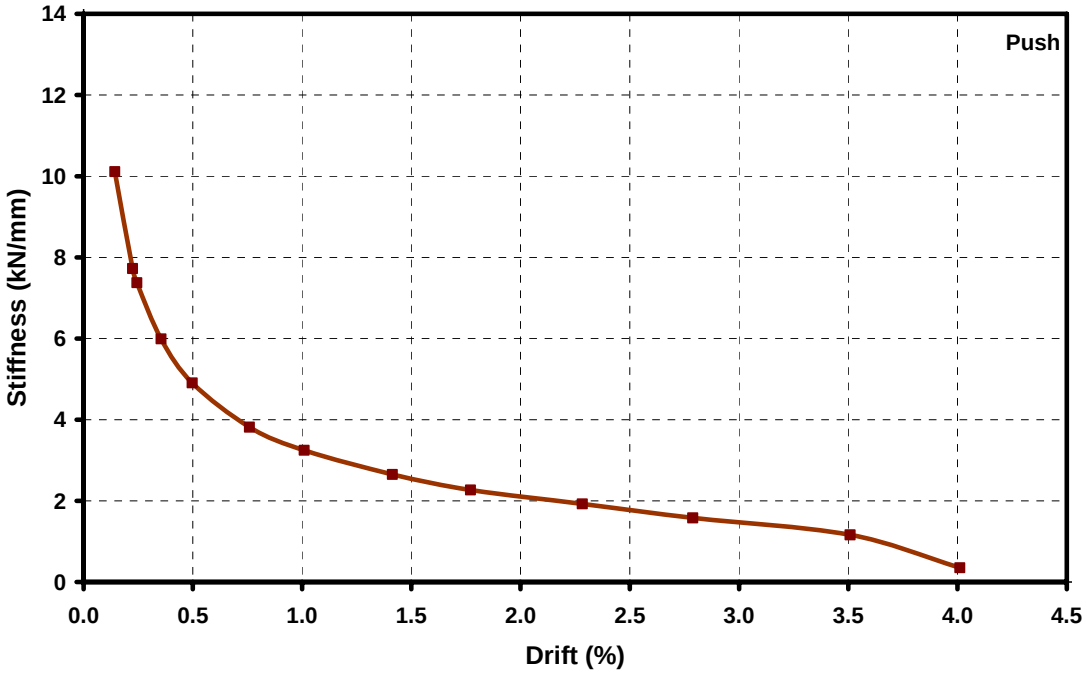

Figure 4.9. Stiffness degradation of US3-ES-FRP1 specimen

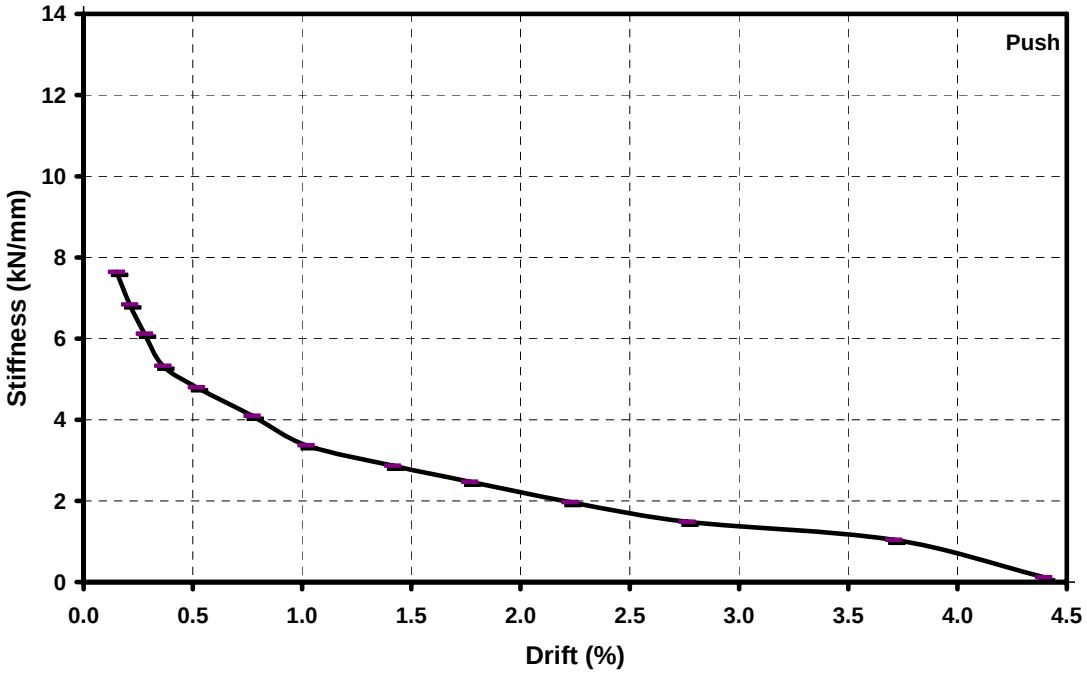

Figure 4.10. Stiffness degradation of US3-ES-FRP2 specimen

4.3.2. Pull Direction

In the pull direction of the loading, longitudinal beam of the US3-E-Control specimen reached its yielding capacity at 1.40% drift level. Therefore, the yielding plateau was observed in the load versus displacement graph and stiffness degradation could be defined as an almost desired behavior. As it was explained in the previous part, stiffness decreased due to flexural cracks in the initial drift levels (up to 0.75%), and due to the combined shear and flexural cracks in the later drift ratios. Figure 4.11 illustrates the stiffness degradation of the US3-E-Control specimen.

Slab contribution was also observed in the pull direction of loading for US3-ES-Control specimen. Due to involvement of the reinforcement bars of slab, lateral load capacity of the specimen increased and therefore stiffness increased at the initial drift levels with respect to US3-E-Control specimen. On the following drift levels, stiffness decreased due to shear and flexural cracks, but it did not decrease as much as stiffness of US3-E-Control specimen. The stiffness degradation pattern can be seen in Figure 4.12.

Figure 4.13 indicates the enhanced behavior of the first CFRP retrofitted specimen (US3-ES-FRP1). Although, in the early drift levels, the stiffness did not appreciably improve, but at the later drift levels, it demonstrates an excellent progress. It should be reminded that any apparent failure in the pull direction of loading could not be observed for this specimen. For the US3-ES-FRP2 specimen, similar stiffness degradation behavior was also observed (See Figure 4.14). Besides, FRP orientation of the specimen did not change much as it was explained in section 3.4.

Table 4.1 summarizes the stiffness data of all specimens. By the help of this table, it is possible to see the differences in stiffness terms at a certain drift level. It is also achievable to compare the strength degradation of these specimens in push and pull directions, separately.

Figures 4.15 and 4.16 also compare the stiffness degradation behavior of all specimens with respect to drift ratios in push and pull directions respectively. For the

initial drift ratios (0.15% and 0.20%), stiffness terms might not be so reasonable due to the fact that the lateral displacements are so small in these drift levels.

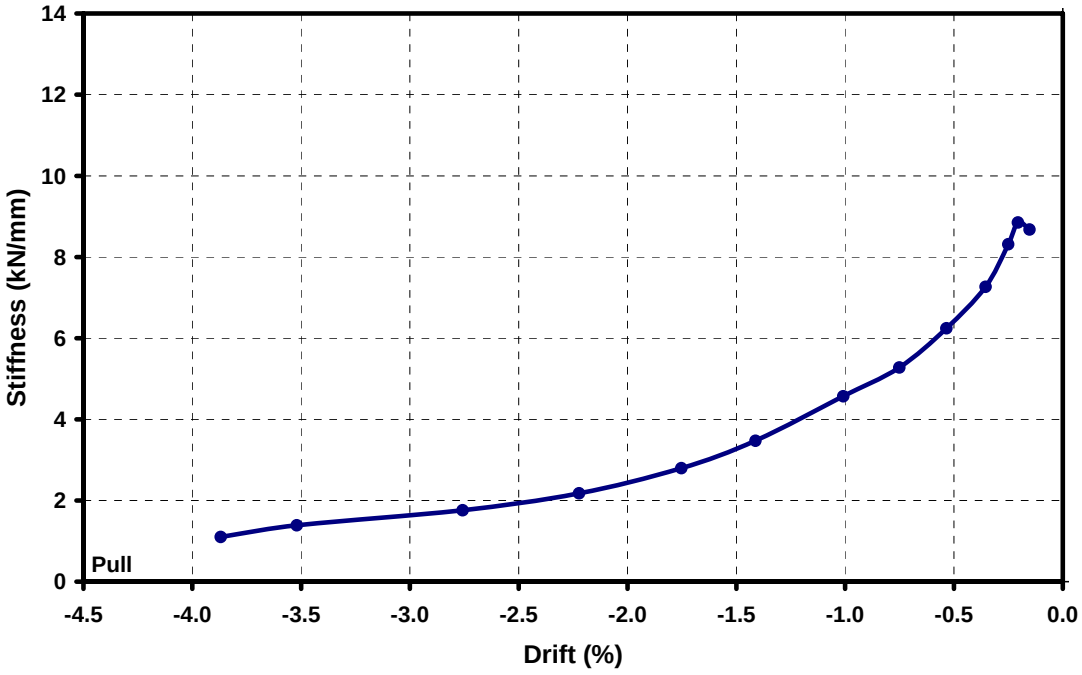

Figure 4.11. Stiffness degradation of US3-E-Control specimen

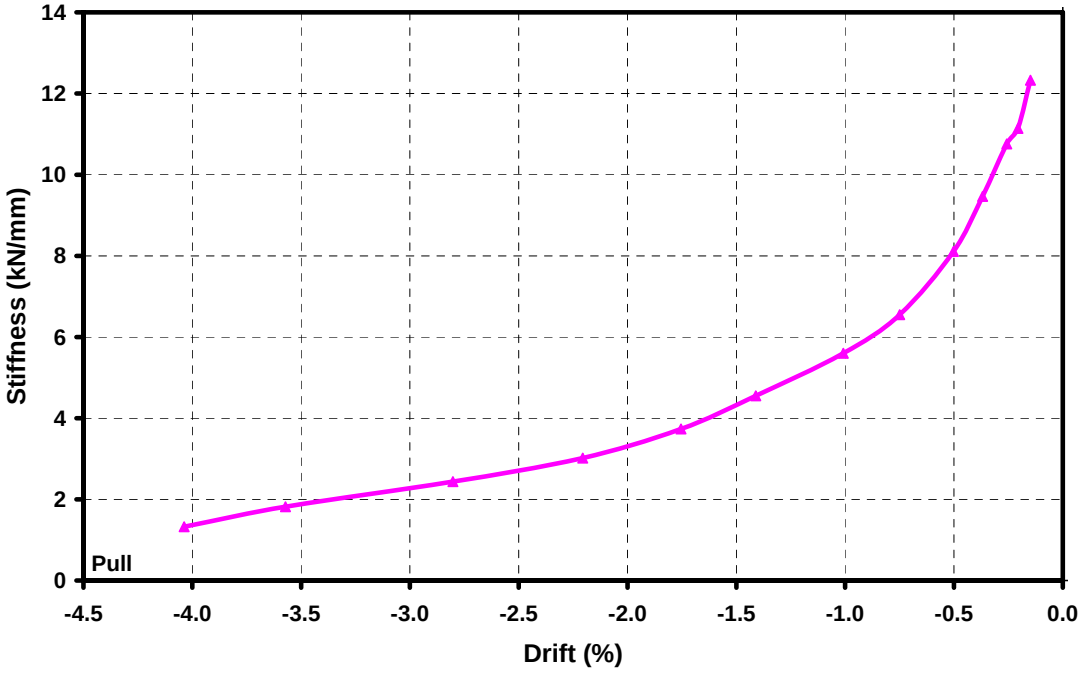

Figure 4.12. Stiffness degradation of US3-ES-Control specimen

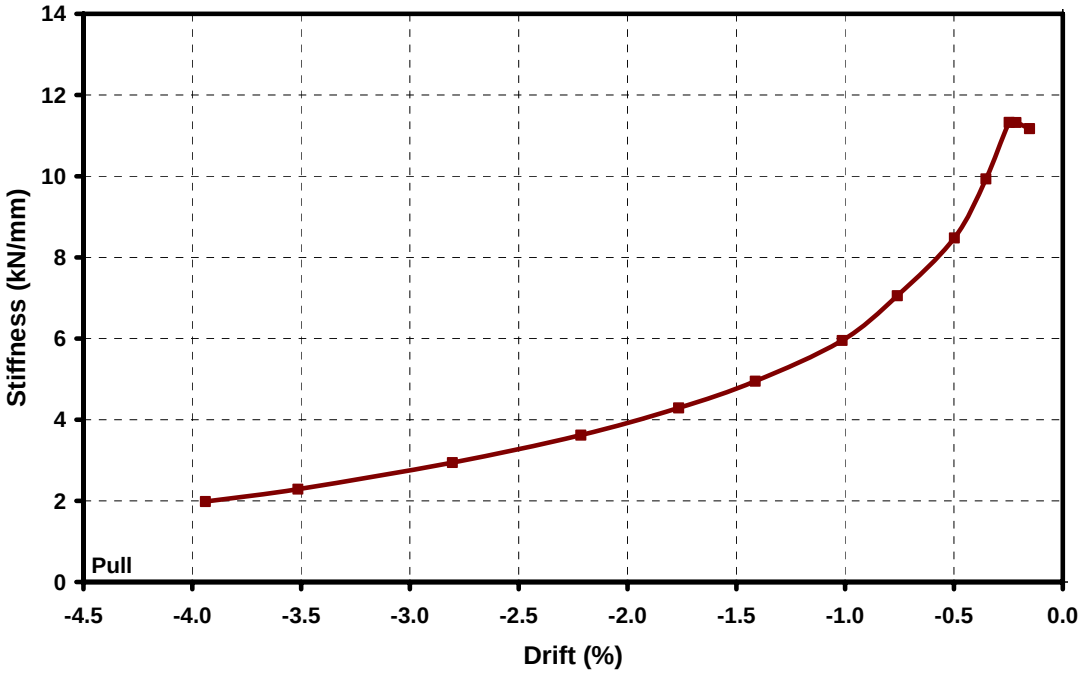

Figure 4.13. Stiffness degradation of US3-ES-FRP1 specimen

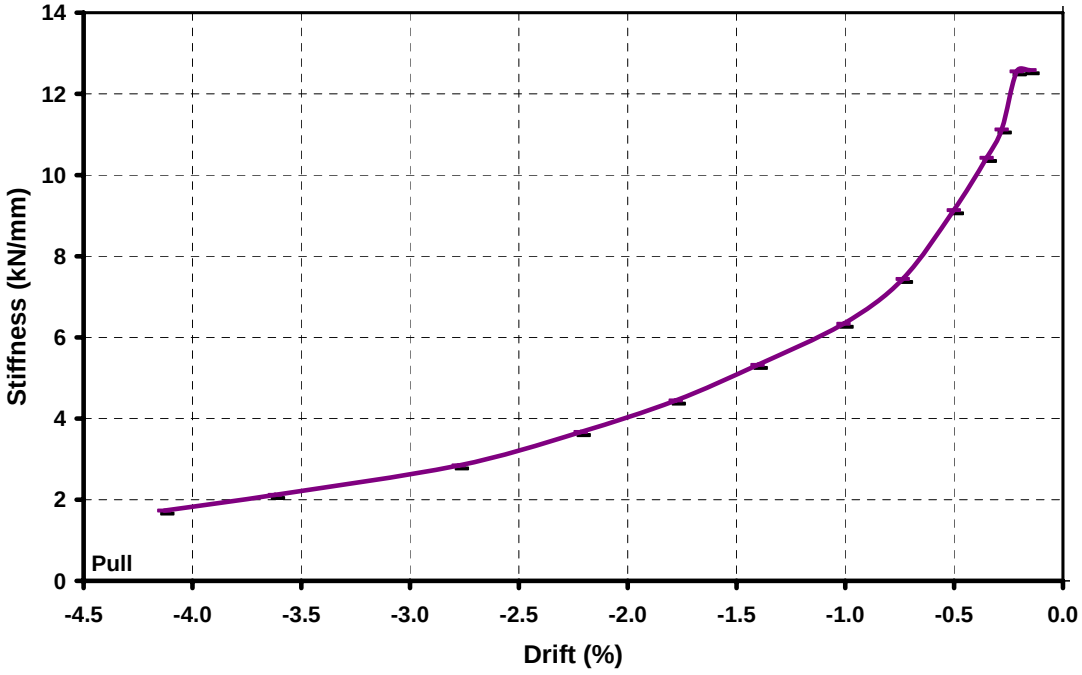

Figure 4.14. Stiffness degradation of US3-ES-FRP2 specimen

Table 4.1. Comparison of stiffness degradation

		Stiffness (kN/mm)												
	Story Drift (%)	**0.15**	**0.20**	**0.25**	**0.35**	**0.50**	**0.75**	**1.00**	**1.40**	**1.75**	**2.20**	**2.75**	**3.50**	**4.00**
Push Direction	**US3-E-Control**	6.9	4.9	4.1	3.7	3.5	2.9	1.6	0.7	0.3	0.2	0.1	0.1	0.1
	US3-ES-Control	10.4	7.7	6.8	6.1	4.7	3.1	1.4	0.8	0.5	0.3	0.3	0.2	0.1
	US3-ES-FRP1	10.1	7.7	7.4	6.0	4.9	3.8	3.2	2.7	2.3	1.9	1.6	1.2	0.4
	US3-ES-FRP2	7.5	6.8	6.1	5.3	4.8	4.1	3.4	2.9	2.5	2.0	1.5	1.0	0.1
Pull Direction	**US3-E-Control**	8.7	8.8	8.3	7.3	6.2	5.3	4.6	3.5	2.8	2.2	1.8	1.4	1.1
	US3-ES-Control	12.3	11.1	10.8	9.5	8.1	6.6	5.6	4.6	3.7	3.0	2.4	1.8	1.3
	US3-ES-FRP1	11.2	11.3	11.3	9.9	8.5	7.1	6.0	4.9	4.3	3.6	2.9	2.3	2.0
	US3-ES-FRP2	12.6	12.6	11.1	10.4	9.1	7.4	6.3	5.3	4.4	3.7	2.8	2.1	1.7

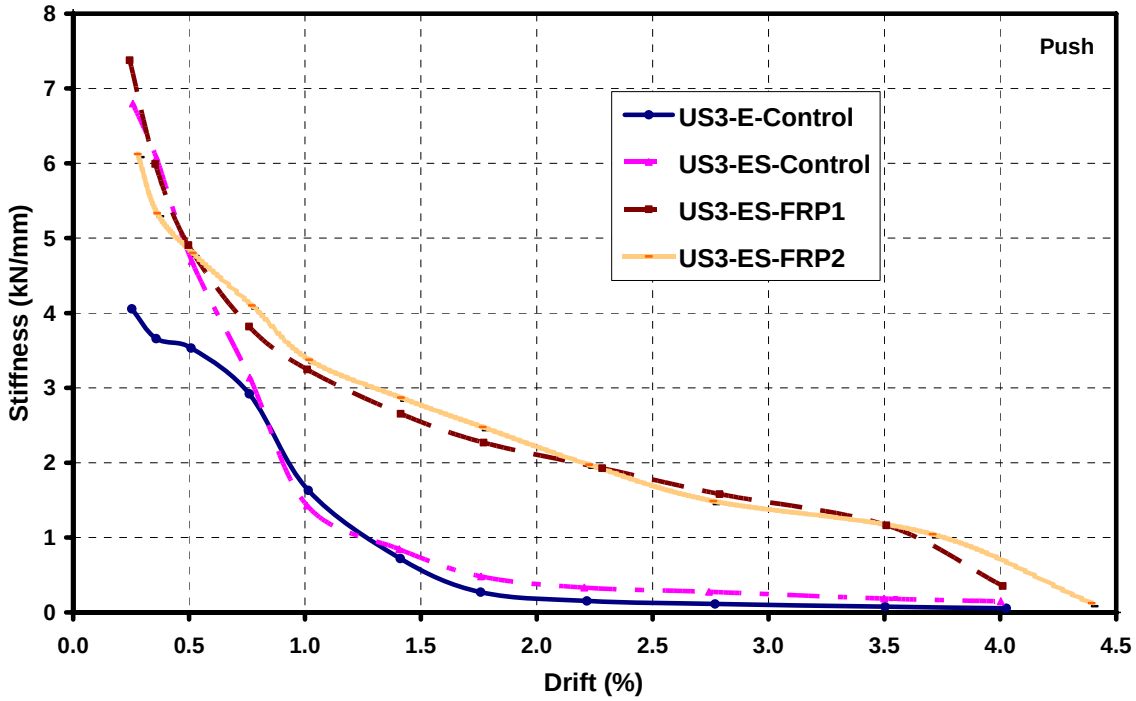

Figure 4.15. Comparison of stiffness degradation in push direction

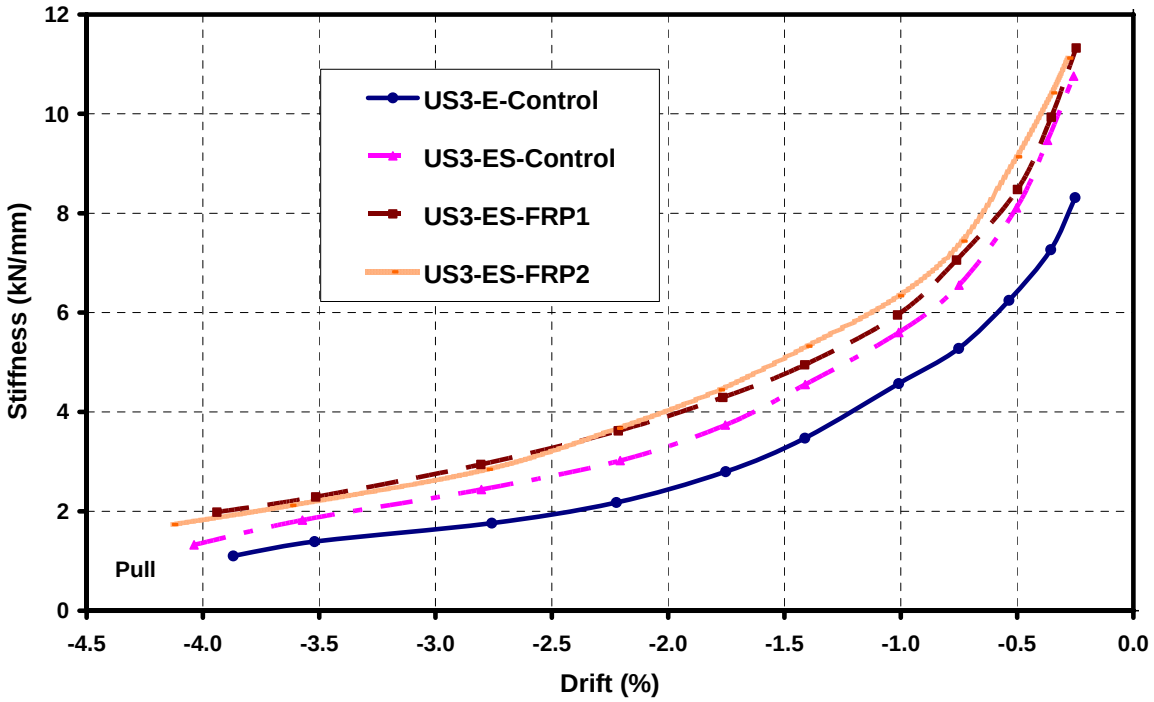

Figure 4.16. Comparison of stiffness degradation in pull direction

4.4. Energy Dissipation

In the calculation of energy dissipation, the area enclosed by the corresponding load versus displacement hysteretic loop during a loading cycle was assumed as dissipated energy. Energy dissipation in each cycle of loading was calculated, separately. Cumulative energy dissipation was then calculated by summing up energy dissipated per cycle throughout the test. Normalization was computed as the dissipated energy divided by maximum energy levels of corresponding specimen. In order to compare the dissipated energy levels of each specimen at various drift ratios and at each cycle, normalized cumulative and cyclic energy dissipation graphs were also given for each specimen, independently.

US3-E-Control specimen had a rather poor energy dissipation capacity among all the specimens. In the push direction of loading, lateral load capacity decreased due to slippage of bottom rebars of longitudinal beam. In the other loading direction, longitudinal beam reached its yielding capacity and this caused to dissipate more energy than in the push direction. However, due to lower lateral load capacity and slippage, energy dissipation capacity was limited to approximately 19 kN.m. Figures 4.17 and 4.18 illustrate the energy dissipation behaviors of US3-E-Control specimen in normalized cumulative and normalized cyclic forms. In Figure 4.18, cyclic energy absorbed in 0.50% drift ratio was smaller than those of in the 0.75%. Such decrease in energy stemmed from the slippage failure in the push direction of loading. Otherwise, another decrease in energy could be observed in 4.00% drift ratio. This originated from the failure of the joint in the pull direction of loading.

A similar behavior was observed in US3-ES-Control specimen as compared to US3-E-Control specimen. Whereas the slippage problem in the push direction of loading remained, load capacity in the pull direction increased due to slab contribution and therefore, amount of dissipated energy was increased. It should be reminded that, failure in the joint due to torsion and shear forces could eventuate in rather less energy dissipation than the ductile failure of the beam-column joint. As a result of these effects, 28 kN.m energy dissipation was calculated at the end of the experiment. In Figure 4.19, cumulative energy dissipation could be observed. Cyclic energy behavior was also affected from the

same failure modes. However, decrease in load capacity in push direction did not eventuate in any decrease of the cyclic energy due to increased load capacity in the pull direction (see Figure 4.20). After 3.50% drift level, the specimen could not dissipate any significant energy due to failure of the joint in pull direction.

FRP retrofitting strategies also focused on higher energy dissipation capacity during the seismic action. That is to say, higher energy dissipation capacity is highly preferable in terms of seismic resistance of reinforced concrete structures. It seems that this goal was achieved according to results of US3-ES-FRP1 and US3-ES-FRP2 specimens. Both in pull and push directions of loading, lateral load capacity increased. Slippage problem in the push direction of loading, and torsional and shear failures in the pull direction were limited. Due to such improvements, energy dissipation capacity reached desired levels, namely, 58 kN.m. and 54 kN.m. for US3-ES-FRP1 and US3-ES-FRP2 specimens, respectively (see Table 4.2 and 4.3). Figures 4.21 and 4.22 illustrate the energy dissipation behaviors of US3-ES-FRP1 specimen in normalized cumulative and normalized cyclic forms. Energy dissipation behaviors of US3-ES-FRP2 specimen were summarized in Figure 4.23 and 4.24. Cyclic energy absorbed was decreased at the last drift ratio, namely, 4.00%, due to slippage in the push direction and combined shear and torsional failure in the pull direction (see Figures 4.22 and 4.24).

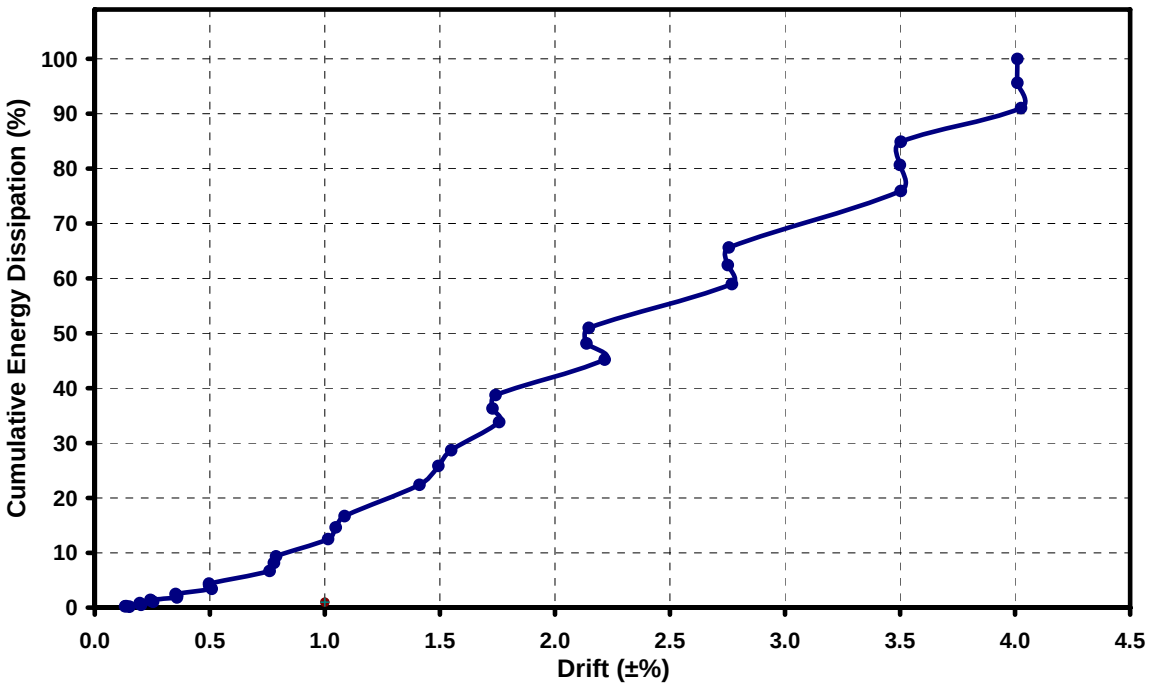

Figure 4.17. Normalized cumulative energy dissipation of US3-E-Control specimen

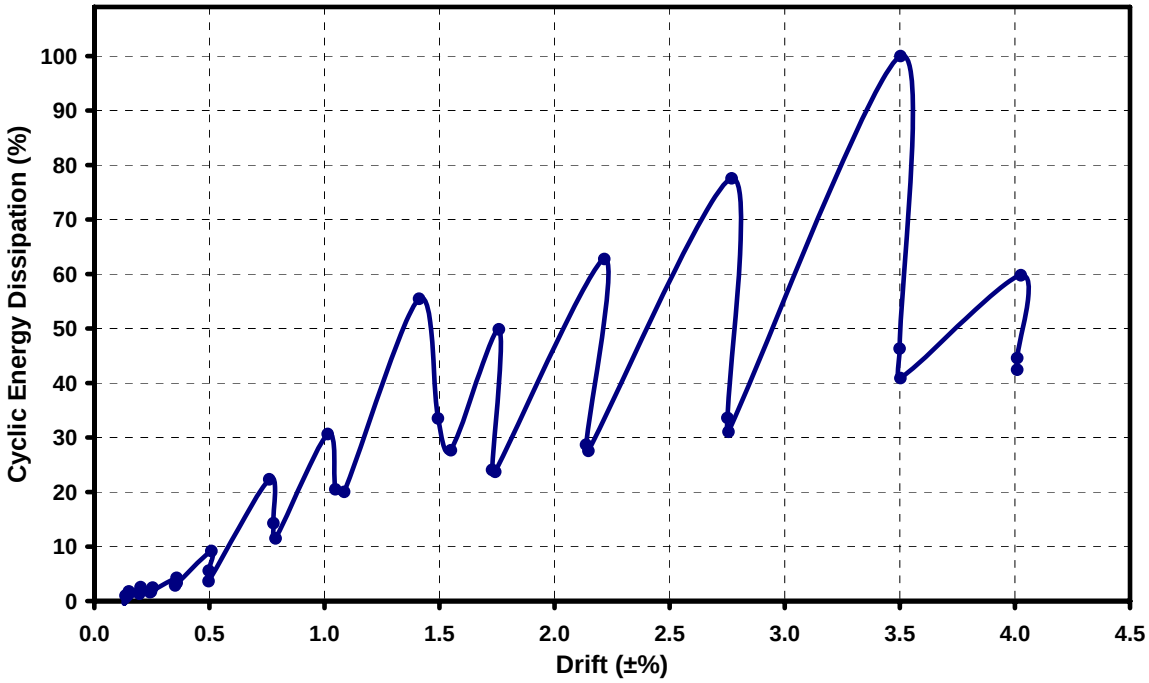

Figure 4.18. Normalized cyclic energy dissipation of US3-E-Control specimen

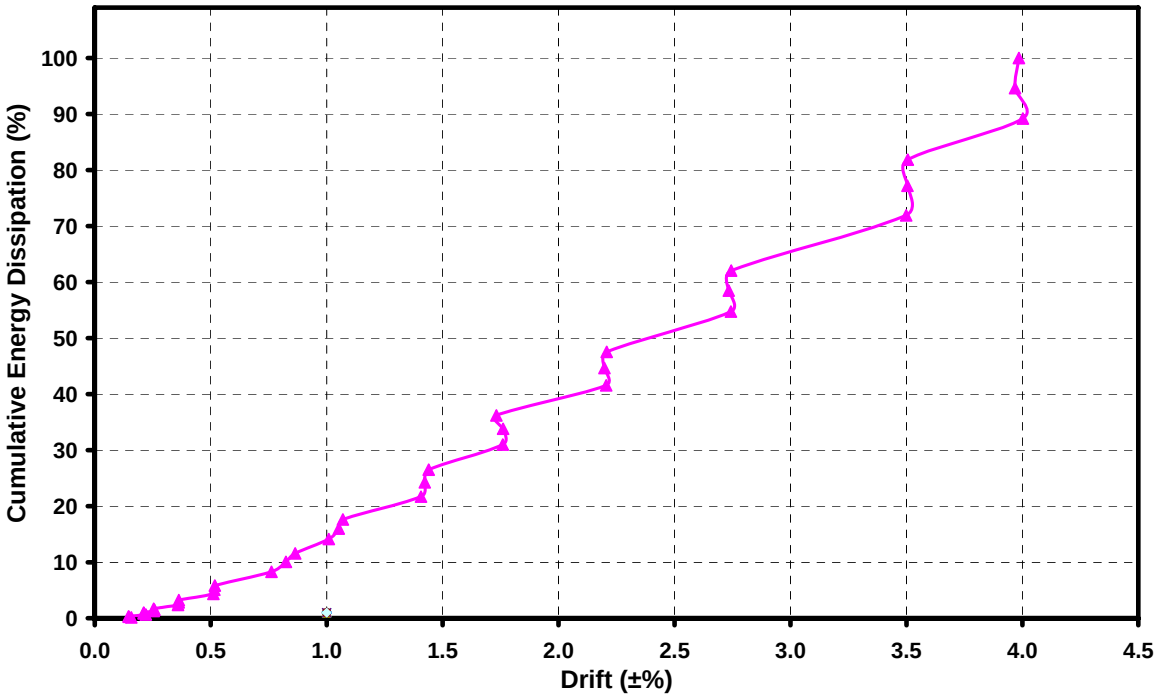

Figure 4.19. Normalized cumulative energy dissipation of US3-ES-Control specimen

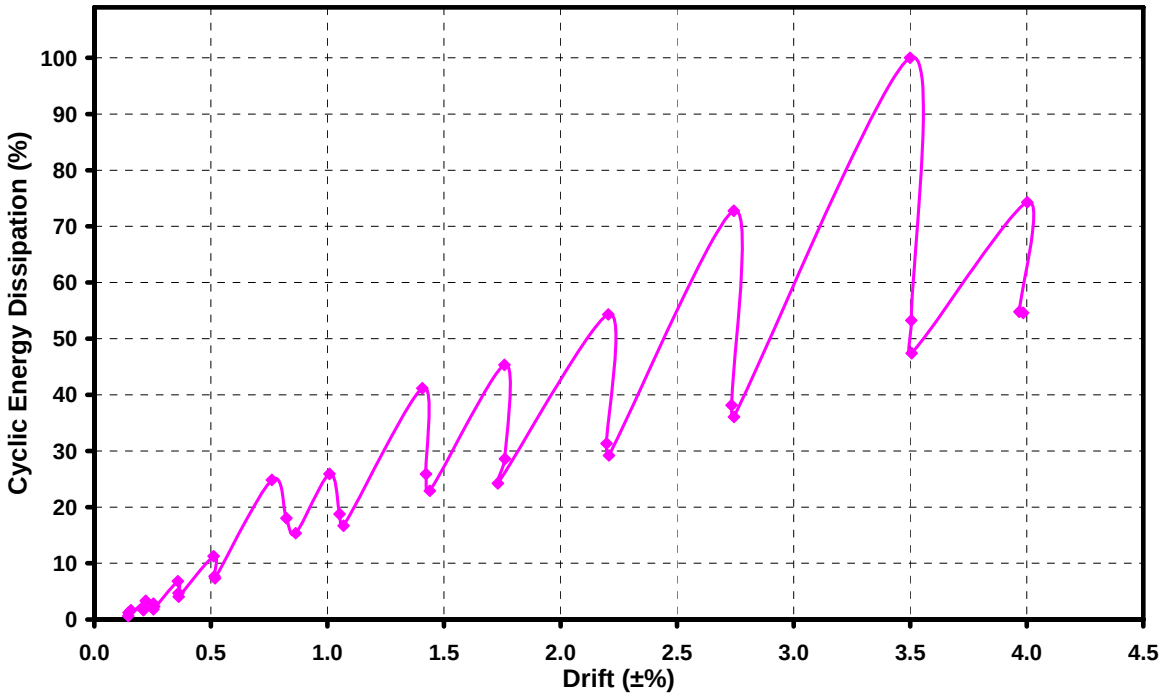

Figure 4.20. Normalized cyclic energy dissipation of US3-ES-Control specimen

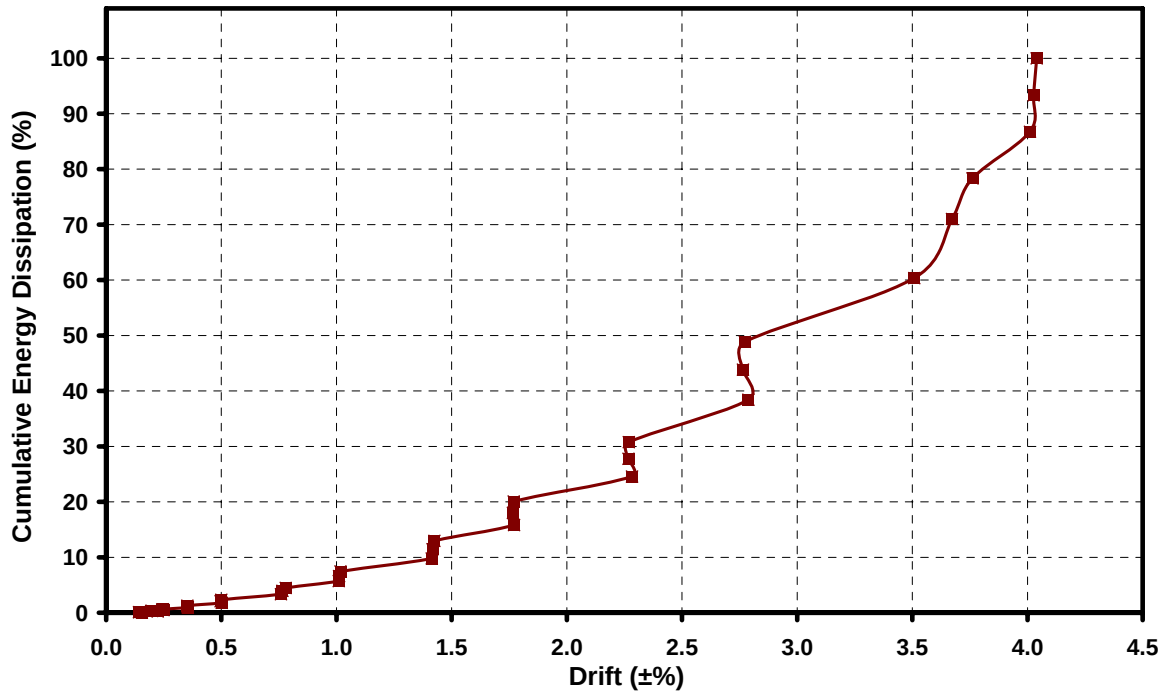

Figure 4.21. Normalized cumulative energy dissipation of US3-ES-FRP1 specimen

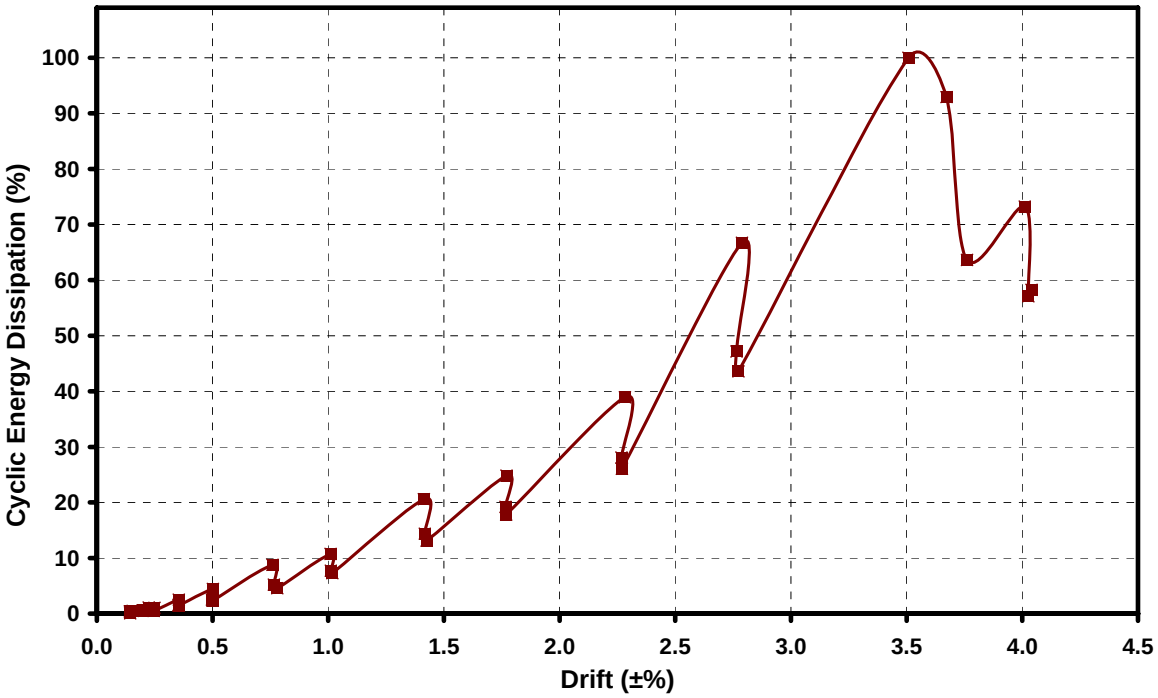

Figure 4.22. Normalized cyclic energy dissipation of US3-ES-FRP1 specimen

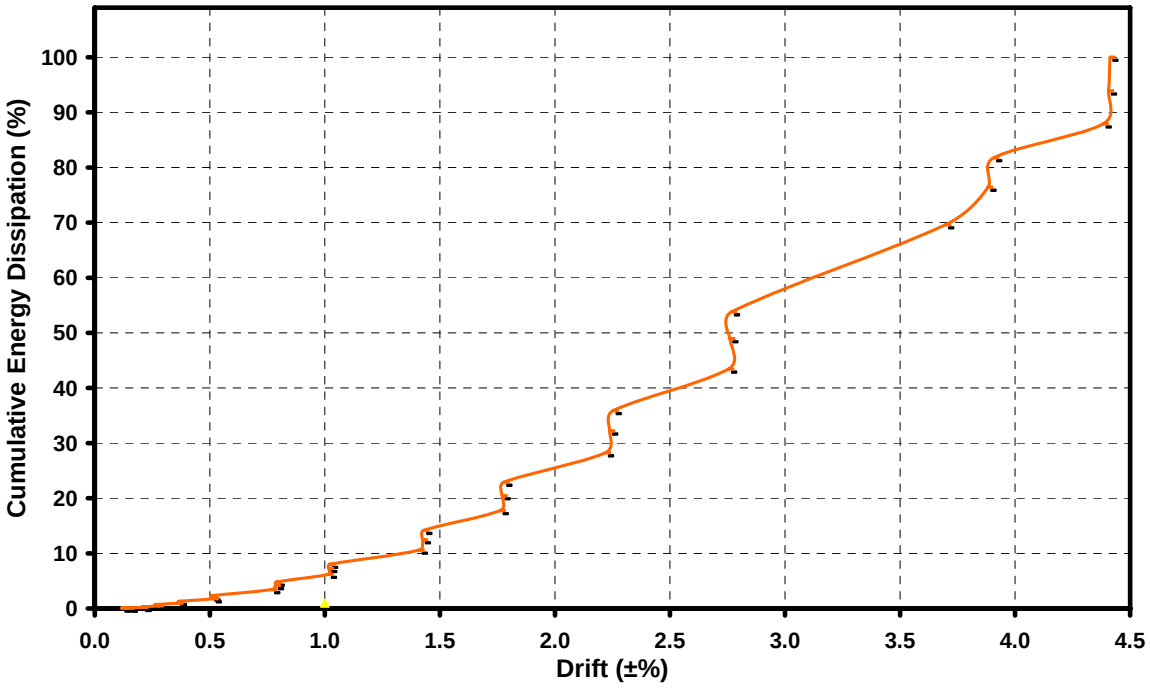

Figure 4.23. Normalized cumulative energy dissipation of US3-ES-FRP2 specimen

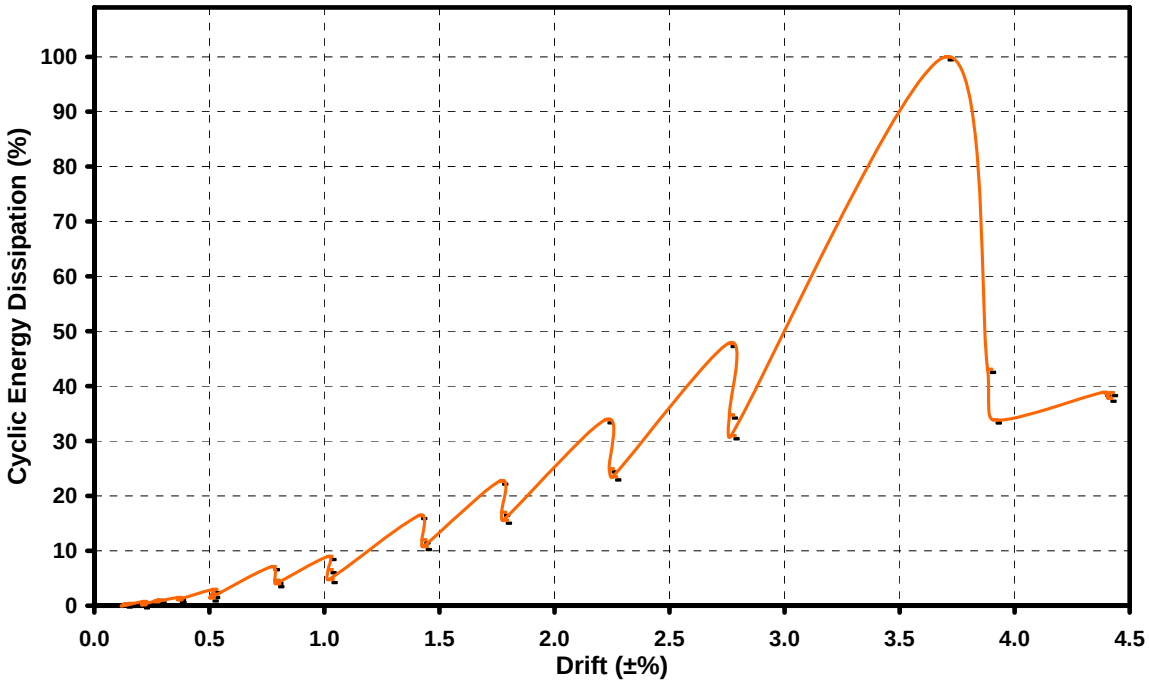

Figure 4.24. Normalized cyclic energy dissipation of US3-ES-FRP2 specimen

In Figure 4.25, the energy dissipation capacities of test specimens with respect to drift ratios are compared. For the control specimens, amounts of dissipated energy were not much different. As it was discussed before, in the push direction, there was no difference in failure modes and load capacities. Otherwise, only the difference could be observed in the pull direction due to contribution of floor slab on US3-ES-Control specimen.

In order to investigate the efficiency of the FRP retrofitting methodologies, energy dissipation capacities of US3-ES-FRP1 and US3-ES-FRP2 specimens should be compared with respect to results of US3-ES-Control specimen. At the first sight, improvements in the energy dissipation capacities were clearly inspected for both of the specimens. There are insignificant improvement (no more than 10%) in energy levels of FRP retrofitted specimens as compared to the control specimen.

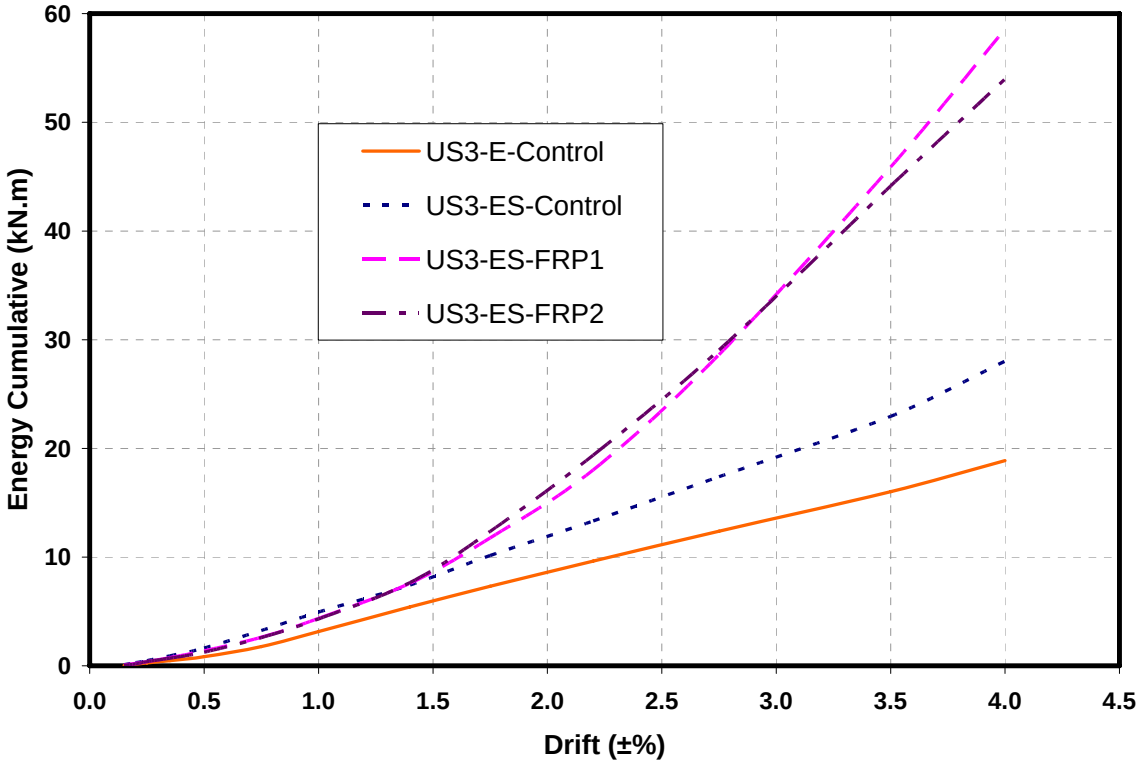

Figure 4.25. Comparative graph of cumulative energy dissipation

Table 4.2 summarizes the energy dissipation behavior of the specimens. It illustrates the amounts of cyclic dissipated energy. It is very helpful to see the differences of energy dissipation capacities for each cycle. It is possible to compare the cycles of test in terms of energy dissipation capacities both in their own hysteretic loops and among the other specimens.

Amount of cumulative dissipated energy after each drift level was tabulated in Table 4.3. By the help of this table, total energy dissipation can be compared any desired drift level individually.

Table 4.2. Dissipated energy (cyclic)

		Energy Dissipated Per Cycle (kN.m)												
Story Drift (%)		**0.15**	**0.20**	**0.25**	**0.35**	**0.50**	**0.75**	**1.00**	**1.40**	**1.75**	**2.20**	**2.75**	**3.50**	**4.00**
US3-E-Control	cycle 1	0.03	0.05	0.05	0.08	0.18	0.43	0.60	1.08	0.97	1.22	1.51	1.94	1.16
	cycle 2	0.02	0.03	0.03	0.06	0.11	0.28	0.40	0.65	0.47	0.56	0.65	0.90	0.87
	cycle 3	0.00	0.03	0.03	0.06	0.07	0.22	0.39	0.54	0.46	0.54	0.60	0.79	0.82
US3-ES-Control	cycle 1	0.05	0.09	0.08	0.19	0.31	0.69	0.72	1.14	1.25	1.50	2.01	2.77	2.06
	cycle 2	0.03	0.05	0.06	0.13	0.21	0.50	0.52	0.72	0.79	0.87	1.06	1.47	1.52
	cycle 3	0.02	0.05	0.05	0.11	0.20	0.43	0.46	0.63	0.67	0.81	1.00	1.31	1.51
US3-ES-FRP1	cycle 1	0.03	0.07	0.07	0.17	0.30	0.59	0.72	1.39	1.67	2.62	4.49	6.73	4.93
	cycle 2	0.03	0.04	0.06	0.11	0.17	0.35	0.52	0.97	1.29	1.89	3.17	6.25	3.84
	cycle 3	0.01	0.04	0.03	0.10	0.16	0.31	0.49	0.88	1.20	1.76	2.93	4.28	3.92
US3-ES-FRP2	cycle 1	0.03	0.06	0.09	0.13	0.25	0.61	0.76	1.40	1.93	2.89	4.07	8.53	3.31
	cycle 2	0.02	0.04	0.07	0.09	0.18	0.39	0.56	1.02	1.45	2.13	2.96	3.67	3.22
	cycle 3	-0.01	0.01	0.06	0.09	0.12	0.34	0.41	0.92	1.33	2.00	2.64	2.89	3.31

Table 4.3. Dissipated energy (cumulative)

	Cumulative Energy Dissipated (kN.m)												
Story Drift (%)	**0.15**	**0.20**	**0.25**	**0.35**	**0.50**	**0.75**	**1.00**	**1.40**	**1.75**	**2.20**	**2.75**	**3.50**	**4.00**
US3-E-Control	0.05	0.15	0.27	0.47	0.83	1.77	3.15	5.41	7.31	9.62	12.39	16.02	18.87
US3-ES-Control	0.10	0.28	0.48	0.91	1.63	3.25	4.95	7.43	10.15	13.33	17.40	22.95	28.03
US3-ES-FRP1	0.07	0.22	0.38	0.75	1.38	2.63	4.36	7.60	11.76	18.02	28.62	45.88	58.57
US3-ES-FRP2	0.05	0.17	0.39	0.70	1.25	2.59	4.32	7.66	12.37	19.38	29.06	44.14	53.98

4.5. Joint Shear Deformation

Shear failure of reinforced concrete structural elements or systems is highly undesired type of failure due its sudden and catastrophic nature. Such consideration is also valid for joints. Consequently, shear deformations of the joint should be evaluated carefully in order to control the mode of the failure of subassemblages.

Due to presence of transverse beams, typical (cross-type) joint shear deformation readings could not be achieved. Therefore, a new method was investigated in order to measure the joint shear deformation without readings of cross LVDTs. In this method, it was assumed that the horizontal shear force governs the joint shear behavior, that is to say, vertical shear forces can be negligible.

Shear deformation was calculated as the difference of top and bottom horizontal shear readings (LVDT #5 and LVDT #6) divided by distance between these LVDTs over the rotation of specimen (see Figure 4.26). Rotation of the specimen was calculated by the help of subtraction of bottom displacement readings from top displacement readings divided by the pin to pin story height.

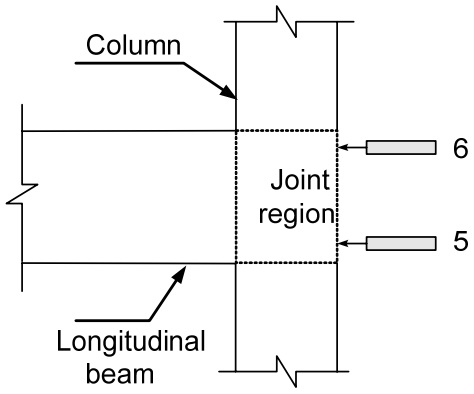

Figure 4.26. Shear deformation readings at joint region

Figure 4.27 illustrates the shear deformation versus lateral load behavior of US3-E-Control specimen. In the push direction of loading, load capacity was limited due to slippage of the rebars and therefore, the shear deformation was limited. Maximum shear deformation was only 0.004 rad. and it did not cause any failure. In the pull direction, longitudinal beam reached its flexural capacity and the yielding in the beam was observed.

Higher shear deformations was monitored in proportion to higher load capacity. However, such shear deformations (0.008 rad.) did not cause shear failures of the beam-column joint region.

US3-ES-Control specimen was much more critical in terms of shear forces, especially in the pull direction of loading (see Figure 4.28). In the push direction, the same failure of US3-E-Control was observed and load capacity was so limited due to slippage problem. Maximum shear deformation was detected as 0.003 rad. Such lesser shear deformation might occur due to increased ductility of the specimen from the floor slab contribution. In the pull direction of loading, 0.022 rad. of shear deformation was measured during the 4.00% drift level. Such amount of shear deformation expressed that the joint was close to its shear capacity. It is also possible to say that torsion originated from the slab reinforcement could cause an increase in the shear deformations.

For US3-ES-FRP1 specimen, shear deformations in the push direction was increased because of improved behavior by eliminating slippage problem (see Figure 4.29). Lateral load capacity increased significantly and therefore, the forced acted on a joint was enhanced. This caused higher shear deformations in the joint. In the pull direction, load capacity improved and also shear deformations were diminished from 0.022 radian to 0.019 radian. Whereas the shear deformation was not extremely critical for these specimens, this weakness was also improved.

Figure 4.30 illustrates the shear deformation versus lateral load response of US3-ES-FRP2 specimen. Shear deformations in the push direction of loading are increased with respect to those of first retrofitted specimen but it is so far from critical levels. In the pull direction of loading, shear deformations are close to other US3-ES specimens and they are also lower than the critical levels. It is possible to say that such deformations are not so effective in failure of beam-column joint specimens.

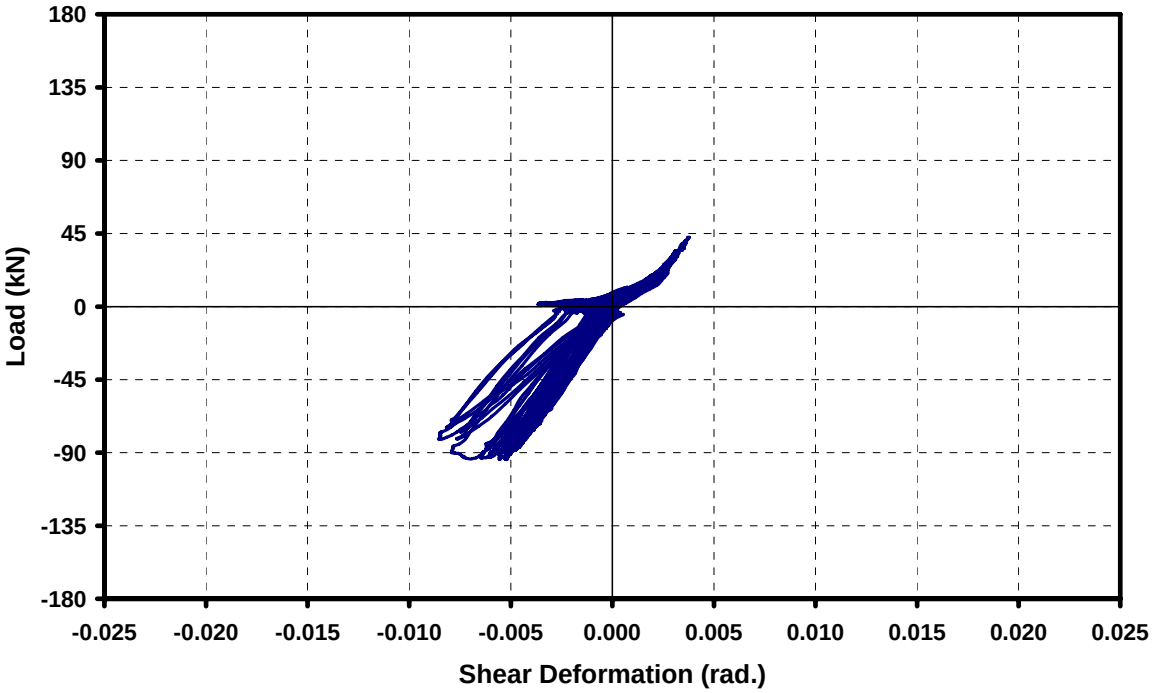

Figure 4.27. Shear deformation versus load graph of US3-E-Control specimen

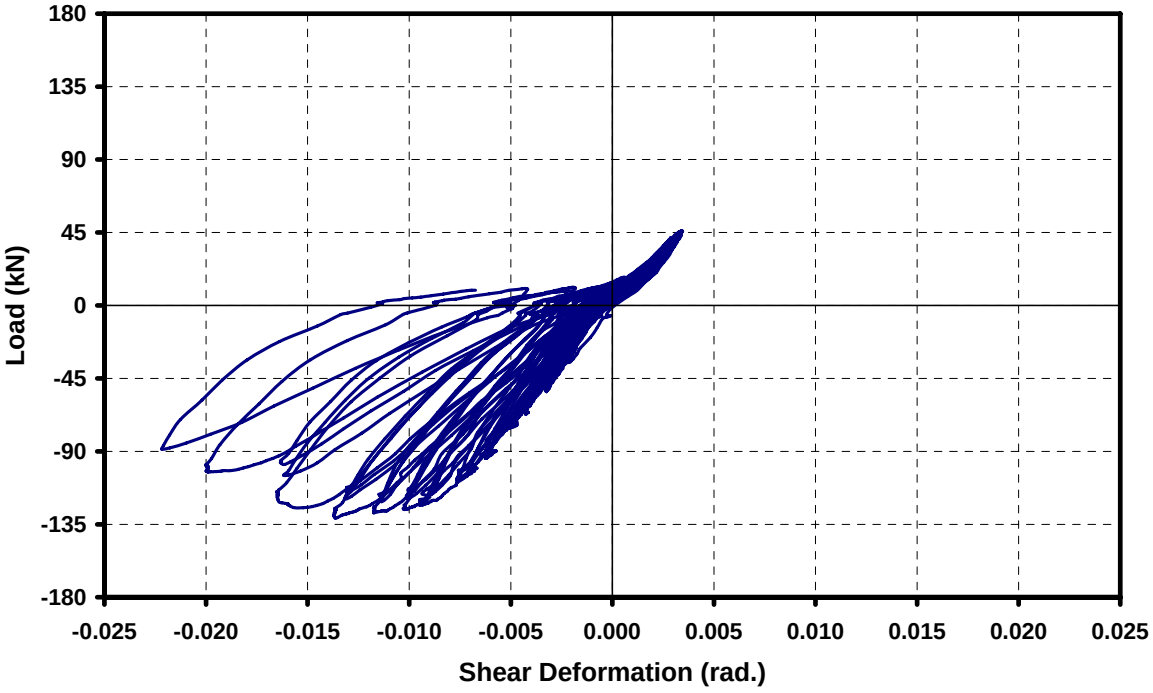

Figure 4.28. Shear deformation versus load graph of US3-ES-Control specimen

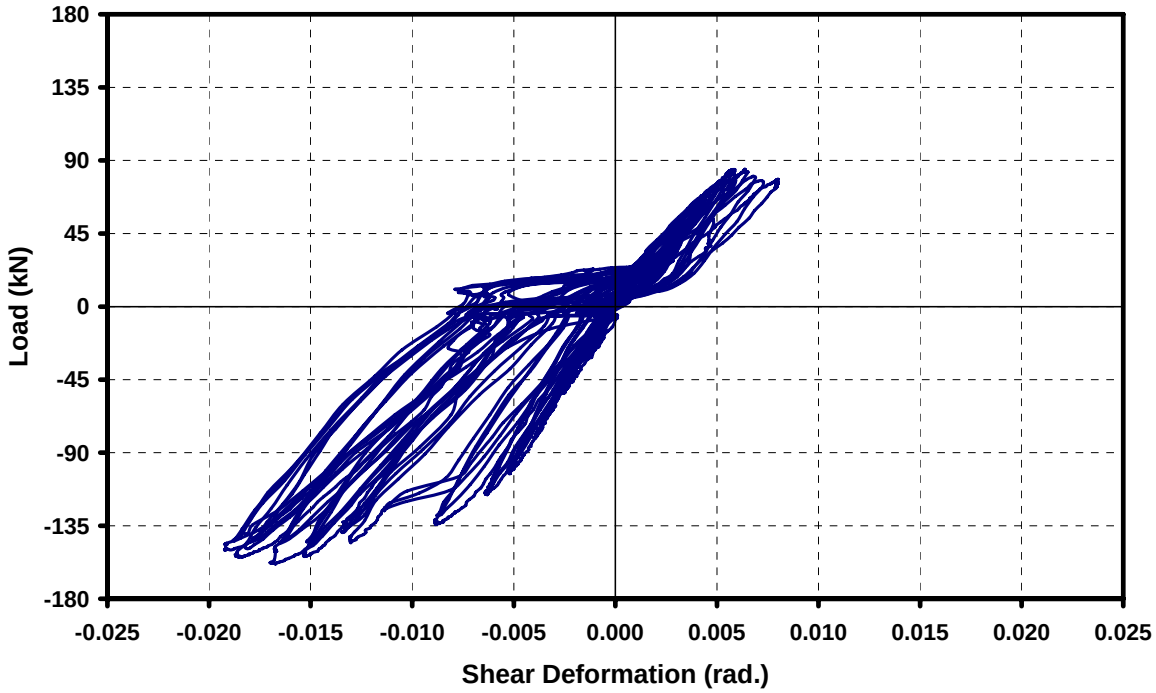

Figure 4.29. Shear deformation versus load graph of US3-ES-FRP1 specimen

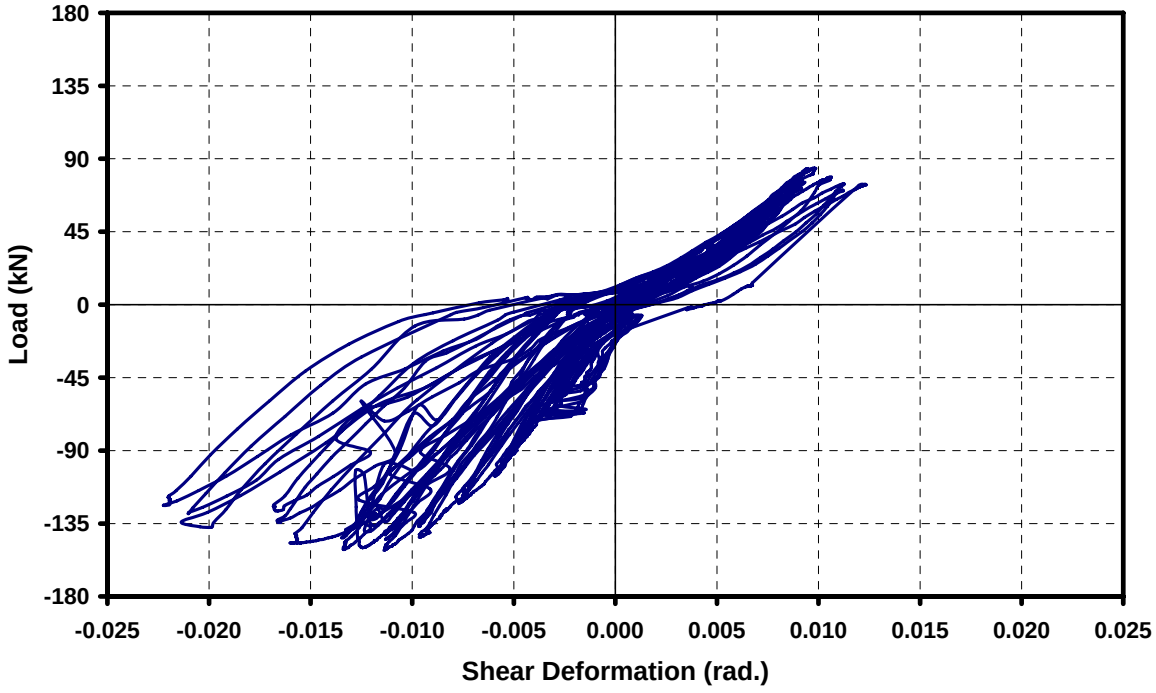

Figure 4.30. Shear deformation versus load graph of US3-ES-FRP2 specimen

Maximum values of shear deformation readings are given in the table 4.4 in order to compare the shear deformations of specimens. Whereas shear failure of joint for all specimens is not so critical in the push direction of loading, shear deformations in the pull direction are close to the limits of shear failure especially for the US3-ES-Control specimen. Load capacities of the FRP retrofitted specimens in the pull direction of loading were increased, but the shear deformations were limited and they did not exceed the 0.022 rad. by application of proper FRP retrofitting techniques. It is possible to say that the retrofitted specimens behaved better in terms of shear deformations with respect to US3-ES-Control specimen.

Table 4.4. Maximum shear deformations

Specimen	**Maximum Shear Deformation (Rad.)**	
	Push Direction	**Pull Direction**
US3-E-Control	0.004	0.008
US3-ES-Control	0.003	0.022
US3-ES-FRP1	0.008	0.019
US3-ES-FRP2	0.012	0.022

4.6. Slip versus Drift Relation

Typical construction details of pre-1970's buildings have a deficiency about the embedment length of beam longitudinal rebars. This insufficiency might result in catastrophic failures of joint regions especially under seismic action. During the experimental study, this deficiency was examined and the following results were monitored.

Figure 4.31 illustrates the inadequate embedment length of longitudinal beam. This deficiency was also applied to transverse beams, whereas these beams were in the transverse direction of loading. Such deficiency could only be effective in the push direction of loading as predicted easily. In the pull direction of loading, top rebars of beam would be in tension and they were anchored well.

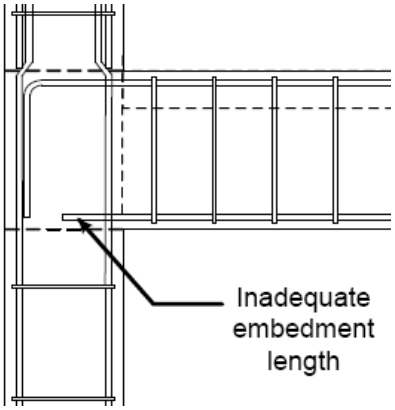

Figure 4.31. Typical details of inadequate embedment length of beam reinforcement

In order to measure the slippage of the rebar of longitudinal beam, a hole from the exterior side of the joint throughout the end of inadequate rebars was drilled. It was not an easy to apply method and therefore some small mistakes in determination of rebar location might occur during drilling holes due to working inside the joint you could not see. For that reason, slip readings of US3-E-Control specimen could not be accomplished before 1.75% drift level. Afterwards, location of LVDT was changed and proper data could be collected. For the US3-ES-FRP2 specimen, proper data could not be collected from the LVDT related to slip readings.

Figure 4.32 illustrates the slip versus drift ratio behavior of US3-E-Control specimen. As explained in load versus drift response of the specimen, up to a certain level of drift ratio (0.75%), or load level (45 kN), slippage could not be observed or it was limited. When the lateral load reached around 45 kN, slippage started and increased rapidly. It is possible to say the almost same algorithm for failure of US3-ES-Control specimen in the push direction. The same slip vs. drift relation can be seen in Figure 4.33.

For US3-ES-FRP1 specimen, slippage was prevented by application of CFRP belts. These belts limited the slippage of rebars up to 3.5% drift level. From this level, slippage increased rapidly and reached the 24 mm, namely, the maximum level of previous specimens (see Figure 4.34).

Whereas proper measurement was not achieved for US3-ES-FRP2 specimen, the reading at 3.50% drift level is almost the same with reading of US3-ES-FRP1 specimen.

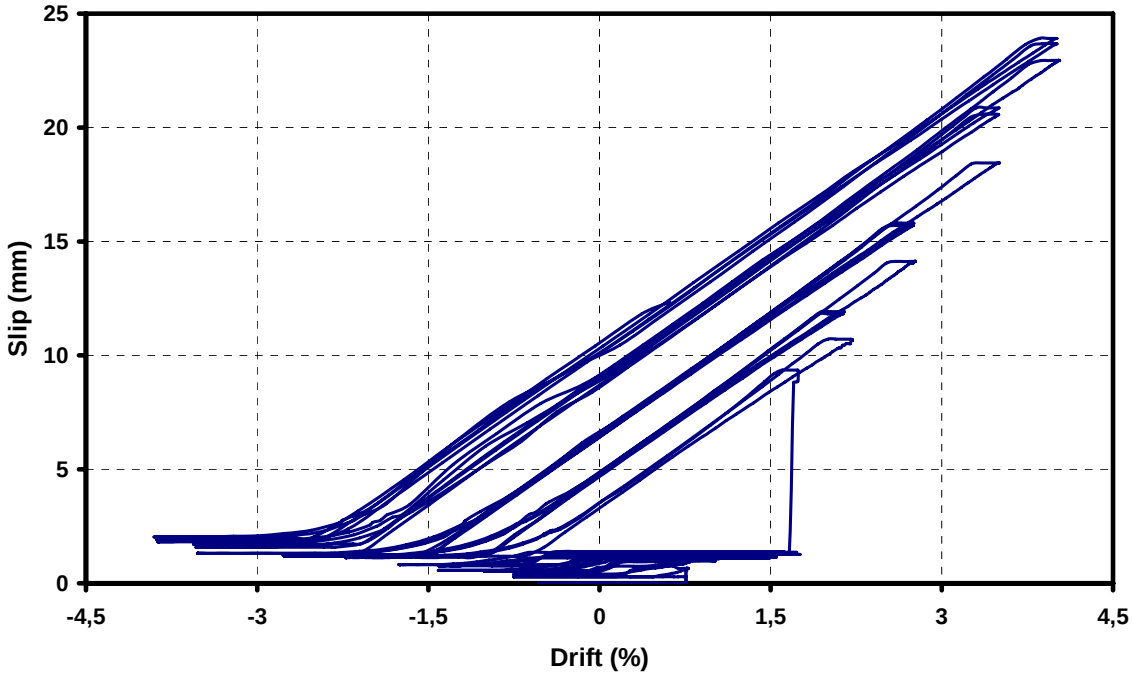

Figure 4.32. Slip versus drift ratio graph of US3-E-Control specimen

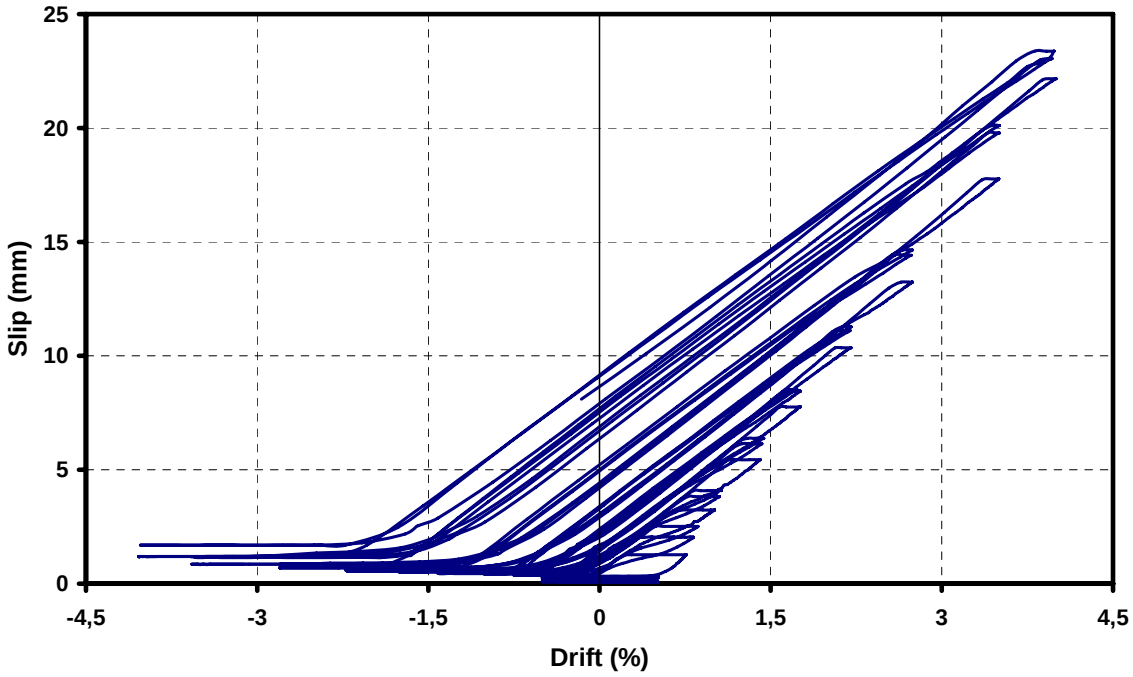

Figure 4.33. Slip versus drift ratio graph of US3-ES-Control specimen

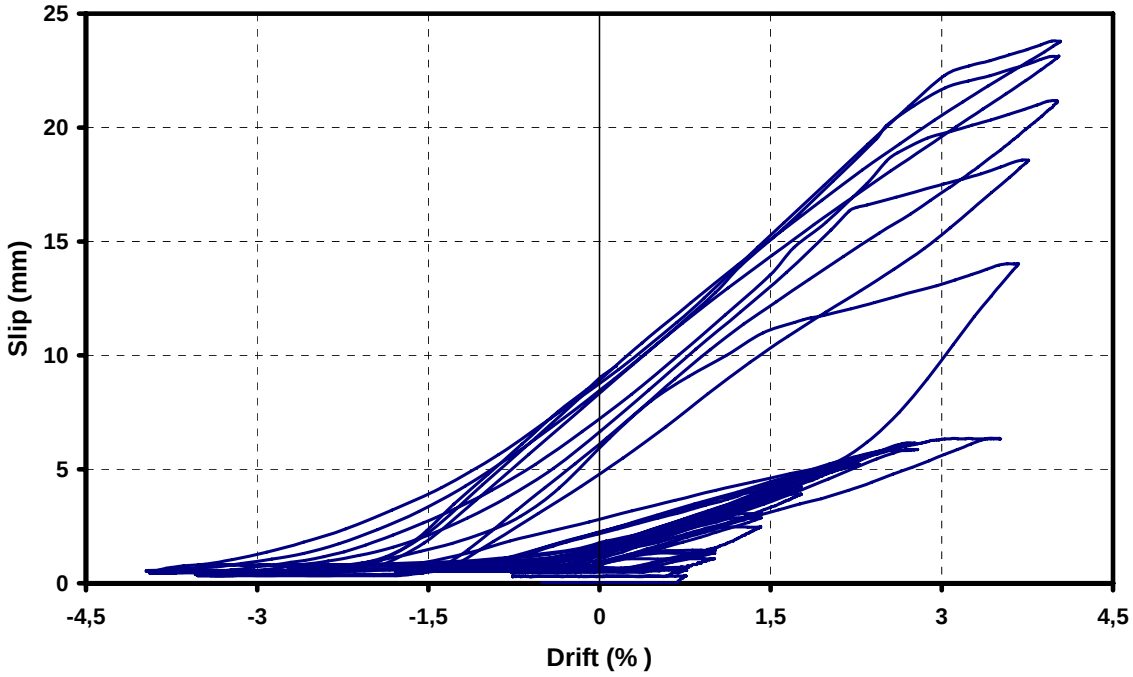

Figure 4.34. Slip versus drift ratio graph of US3-ES-FRP1 specimen

4.7. Strains on Reinforcement Bars

First of all, it should be expressed that strain data cannot be so reliable every time. Sometimes, straingauges can not express the proper data due to possible application mistakes caused by uneven surfaces and probable voltage errors on cables and connections and gauge itself. Furthermore, strain values sometimes cannot be used because they reached meaningless values due to excessive displacements. In the following strain data, some corrections were done and some part of the data was discarded due to the reasons above mentioned.

4.7.1. Strains on Beam Longitudinal Bars

Beams of subassemblages have 3Ø20 rebars as top reinforcement and 2Ø20 rebars as bottom reinforcement. Details of these rebars were given in the previous chapter. Strains on beams in the transverse directions were not measured because no significant strains would be expected in the transverse direction of loading.

Strain level of longitudinal beams was very important in determination of possible plastic hinge zones. Because of probable errors on strain gauges, two straingauges were mounted on the same level of re-bars in order to take an average value. Figure 4.35 illustrates the location strain gauges on longitudinal re-bars.

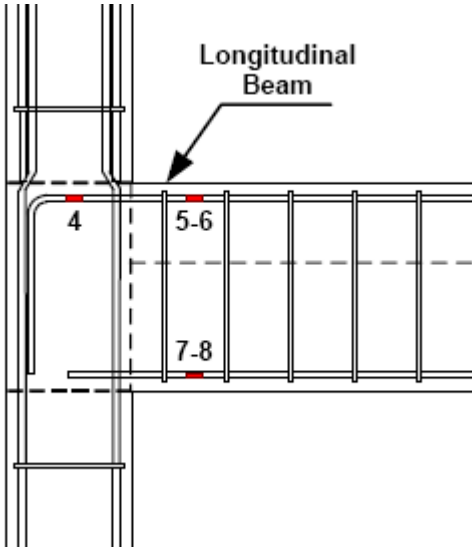

Figure 4.35. Location of strain gauges on longitudinal bars

The top bars of longitudinal beam were yielded in the pull direction of loading for US3-E-Control specimen. Figure 4.36 shows obviously this yielding behavior. Yielding strain level is around 2400 μs. In the push directions, the same reinforcement bars were under compression up to the drift level where load decreased due to slippage.

For the US3-ES-Control specimen, failure mode in the pull direction was more complex. Figure 4.37 illustrates the behavior of top rebars of longitudinal beam. It was rather different than those of US3-E-Control. Strain level was also close to 2400 μs but such strain level did not continued during the test and then decreased. This might stem from the bending of these rebars under tension and spalling of concrete at the exterior side of the joint. Bending of rebars and spalling of concrete might develop from the shear and torsional deformations of the joint.

In the push direction of loading, strain levels of top reinforcements were also positive, especially for the higher drift levels. As it was discussed on the previous parts, in this direction, load capacity decreased due to slippage problem. Afterwards, crack which

occurred due to slippage extended upward and reached very high levels. For the cracked section, equilibrium could be obtained with changing position of neutral axis. At that moment, upper reinforcement bars were also under tension and reached higher strain levels (1000 μs).

Strain values of FRP retrofitted (US3-ES-FRP1) specimen expressed excellent similarity with its own lateral load versus drift hysteresis. Strain level was lower than the expected yielding level of around 2000 μs (see Figure 4.38). Whereas the specimen could overcome higher lateral load levels, strain levels were lesser due to contribution of FRP sheets in flexural capacity of beam. In the push direction of loading, re-bars were under compression as explained before.

Bottom rebars were normally in tension (positive strains) under push direction of loading. Figure 4.39 illustrates the strain versus drift response of bottom rebars of longitudinal beam (US3-E-Control). After slippage occurred, the load capacity decreased suddenly and the strain values were also diminished. In the pull direction of loading, these reinforcements were in compression and negative strains were also observed.

Figure 4.40 illustrates the strain values of US3-ES-Control specimen. They were also similar to those of US3-E-Control, because of almost the same behavior of specimens in push directions due to slippage.

FRP wrapped specimen demonstrated an enhanced performance in push direction of loading and therefore strain levels increased highly (see Figure 4.41). Strain levels reached around yielding range. It was not possible to say that the yielding was exactly observed. Because yielding plateau could not be observed. It should be reminded that strain gauge data cannot be used after certain drift levels because it did not work properly. Otherwise, rebars were also under compression in pull direction of loading.

Strain gauge readings of US3-ES-FRP2 specimen are not reasonable and therefore these readings cannot be expressed.

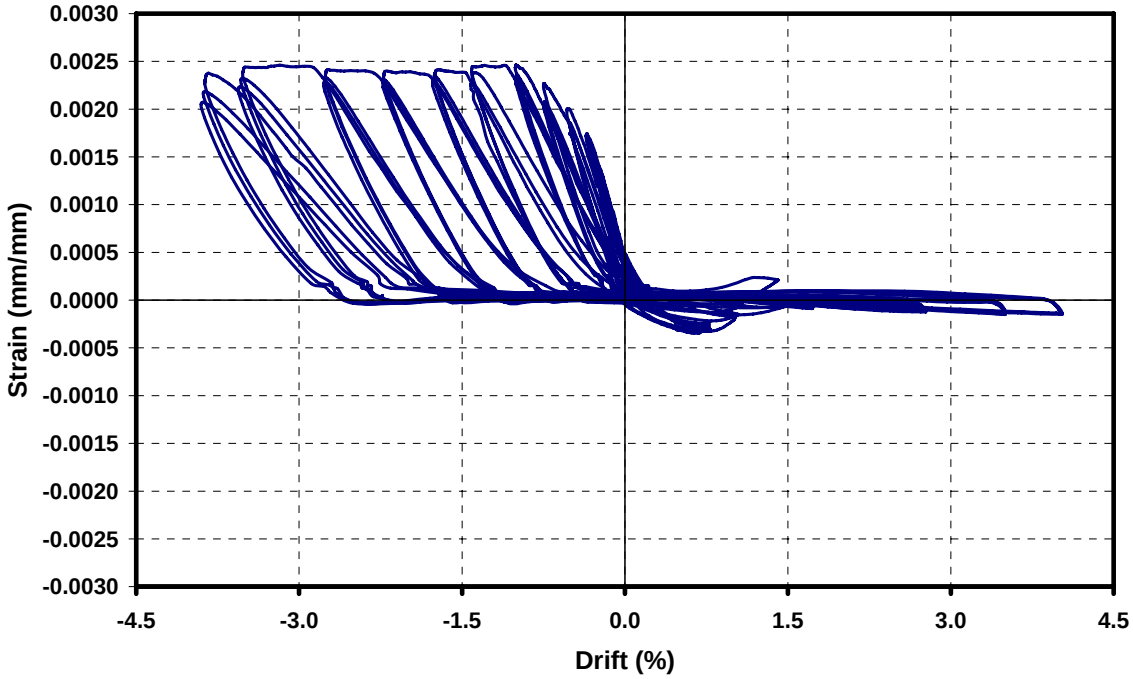

Figure 4.36. Strain versus drift graph of gauge #5 for US3-E-Control

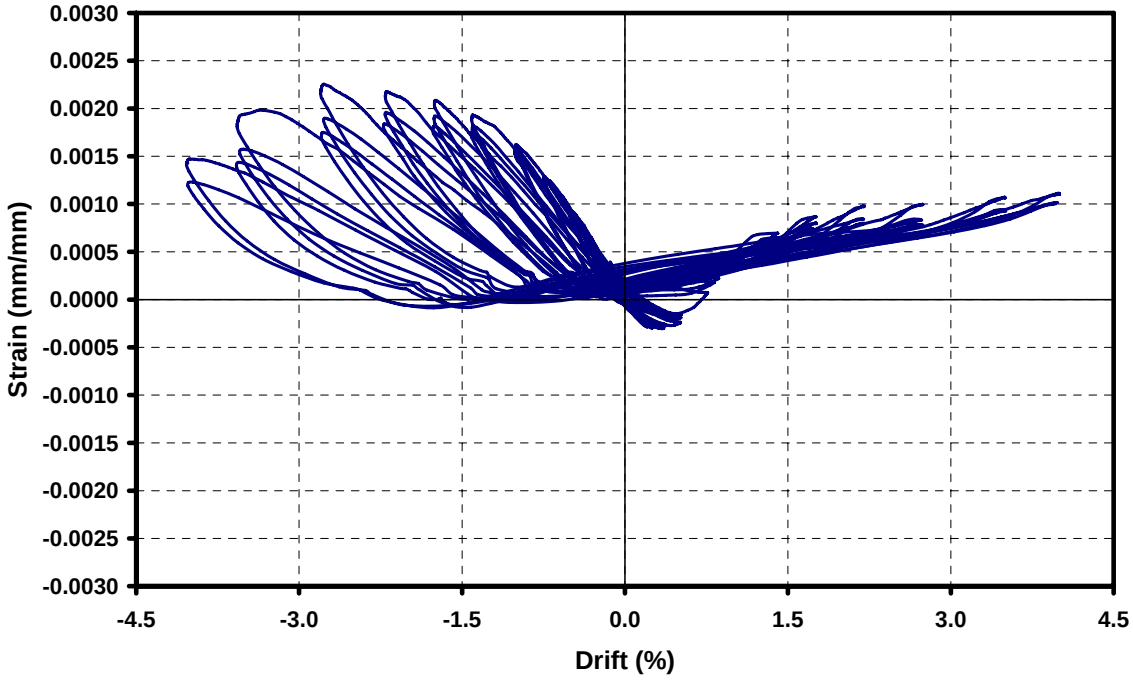

Figure 4.37. Strain versus drift graph of gauge #5 for US3-ES-Control

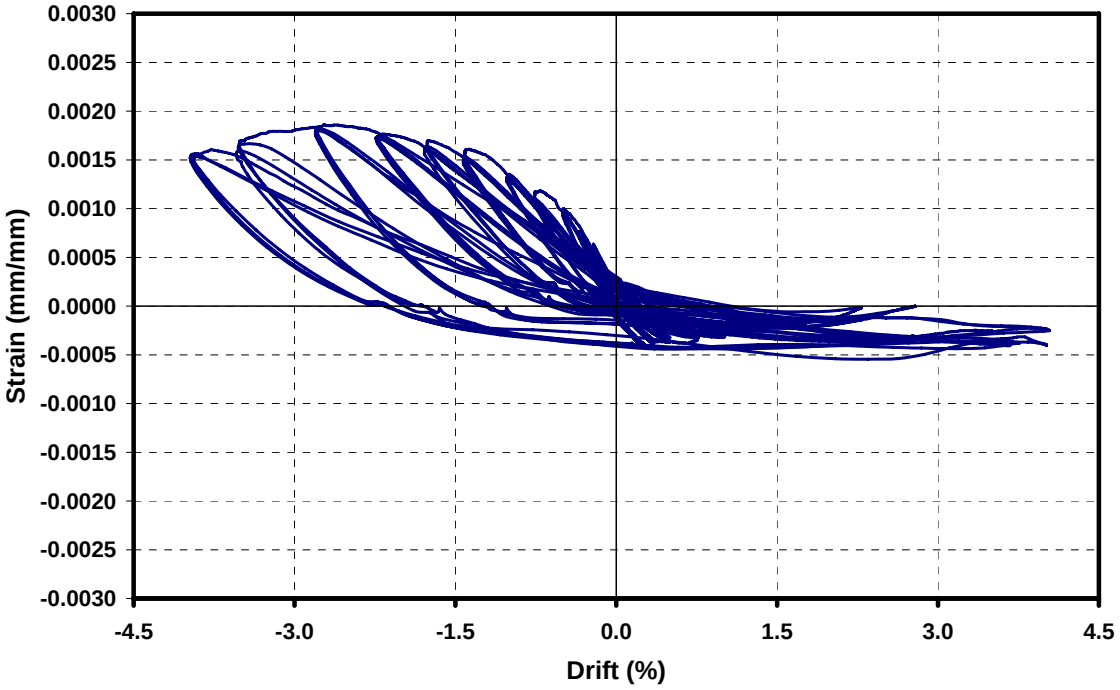

Figure 4.38. Strain versus drift graph of gauge #5 for US3-ES-FRP1

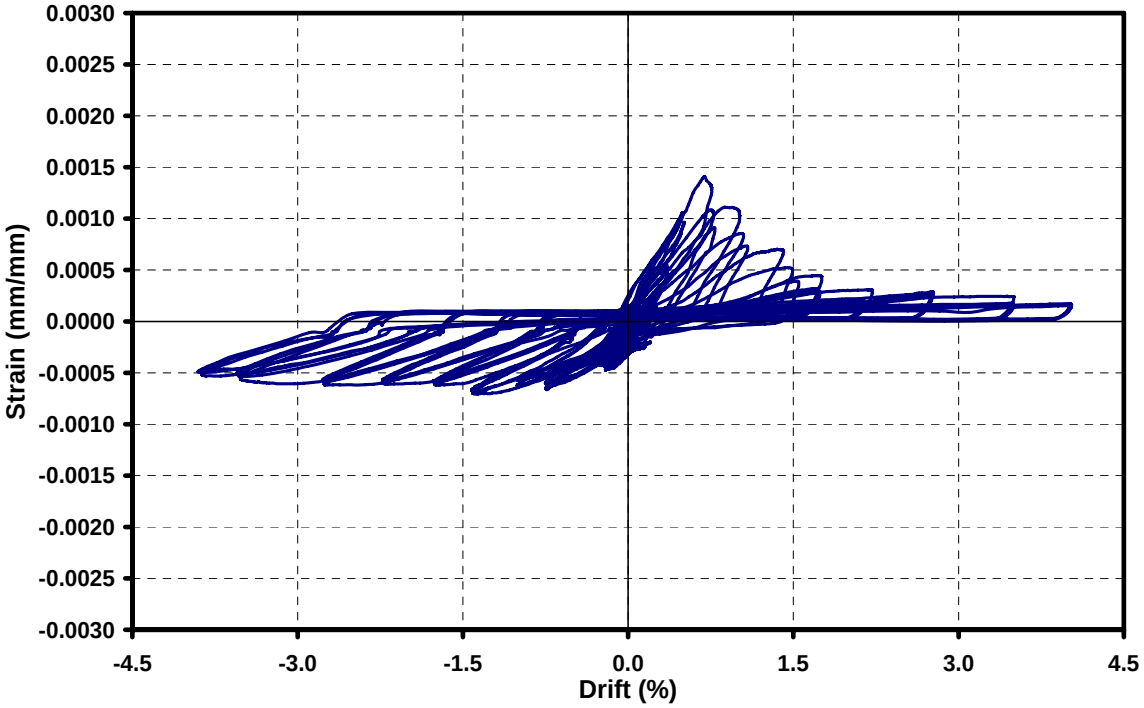

Figure 4.39. Strain versus drift graph of gauge #7 for US3-E-Control

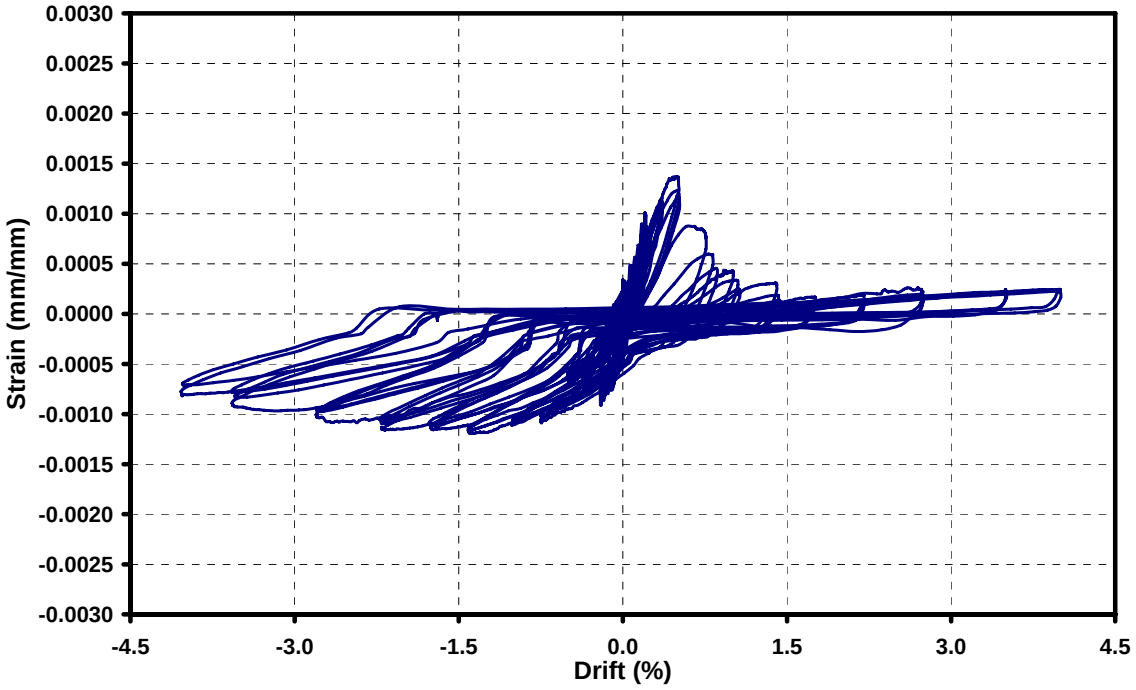

Figure 4.40. Strain versus drift graph of gauge #7 for US3-ES-Control

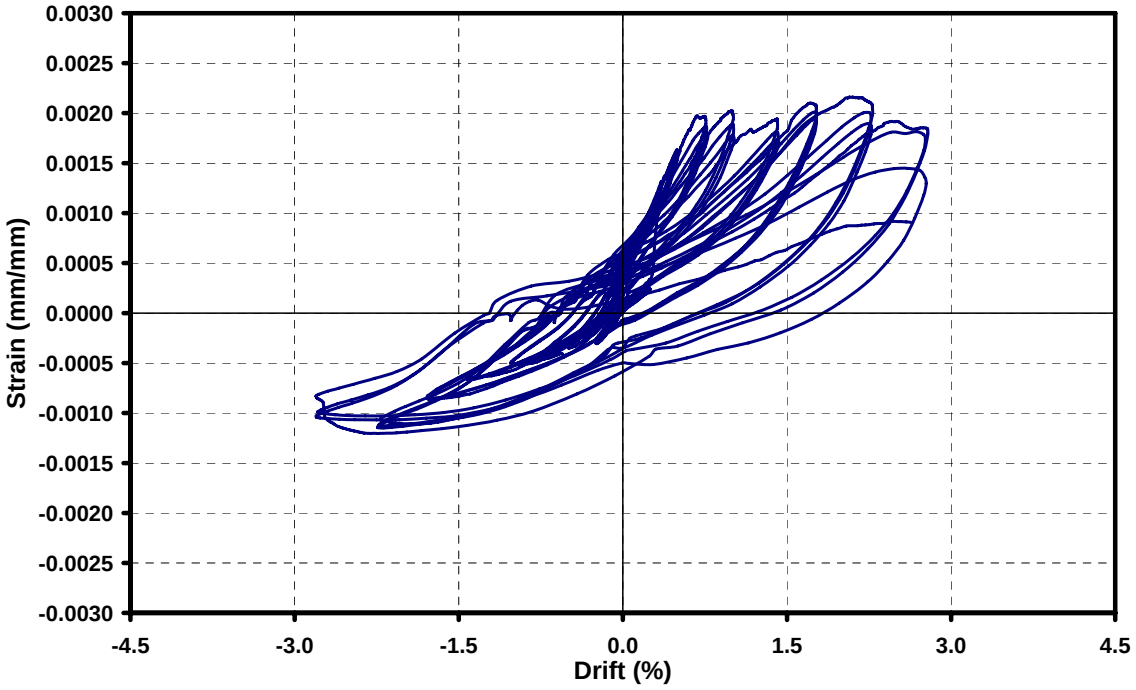

Figure 4.41. Strain versus drift graph of gauge #7 for US3-ES-FRP1

4.7.2. Strains on Stirrups

Strain level of beam stirrups was very essential in terms of shear forces. Shear forces might be critical in beams due to lack of required amount of stirrups in shear critical zones. For the columns, column cross section tried to expand due to axial load on the column. Stirrups prevented both the expansion of the column by confinement effect and avoided possible shear failure on columns.

Figure 4.42 illustrates the locations of strain gauges on stirrups both in columns and beams. In order to evaluate the forces acted on the transverse directions, strain gauges were mounted on stirrups located in longitudinal and transverse beams and columns. All stirrups were selected as Ø10 rebars. Details of locations of stirrups and strain gauges were also given in the previous chapter.

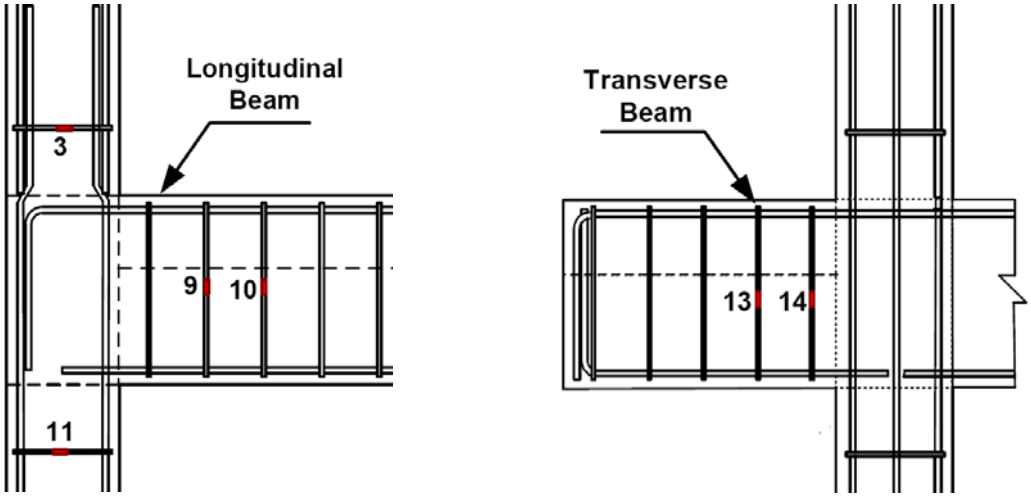

Figure 4.42. Location of strain gauges on stirrups

For US3-E-Control and US3-ES-Control specimens, strain values on longitudinal beam stirrups were not so high (see Figures 4.43 and 4.44). They were around 400 μs and this ratio was very far away from the yielding level. It was observed that higher shear deformations could cause higher strains on stirrups. For the US3-ES-FRP1 specimen, strain values were very high and close to yielding stage (see Figure 4.45). Such big strains could not be predicted for a transverse reinforcement. Therefore, strain data could be wrong. Observations of higher strains in the push direction of loading might be evidence of this error. Figure 4.46 illustrates the strains on such stirrup of US3-ES-FRP2 specimen.

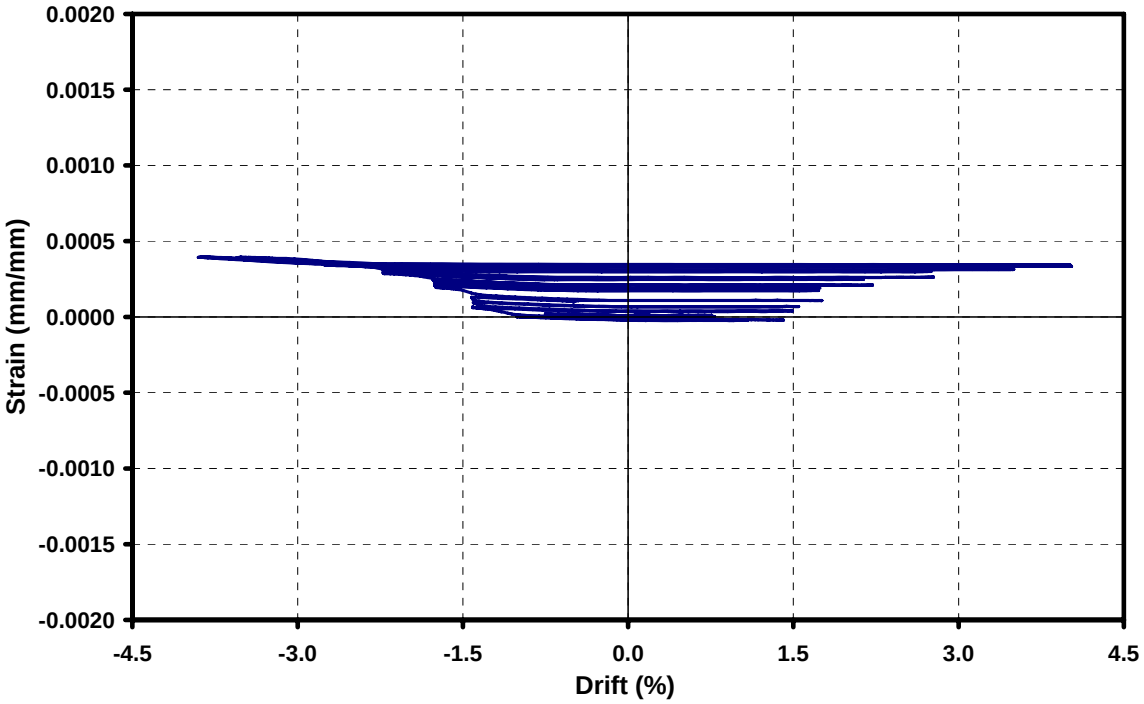

Figure 4.43. Strain versus drift graph of gauge #9 for US3-E-Control

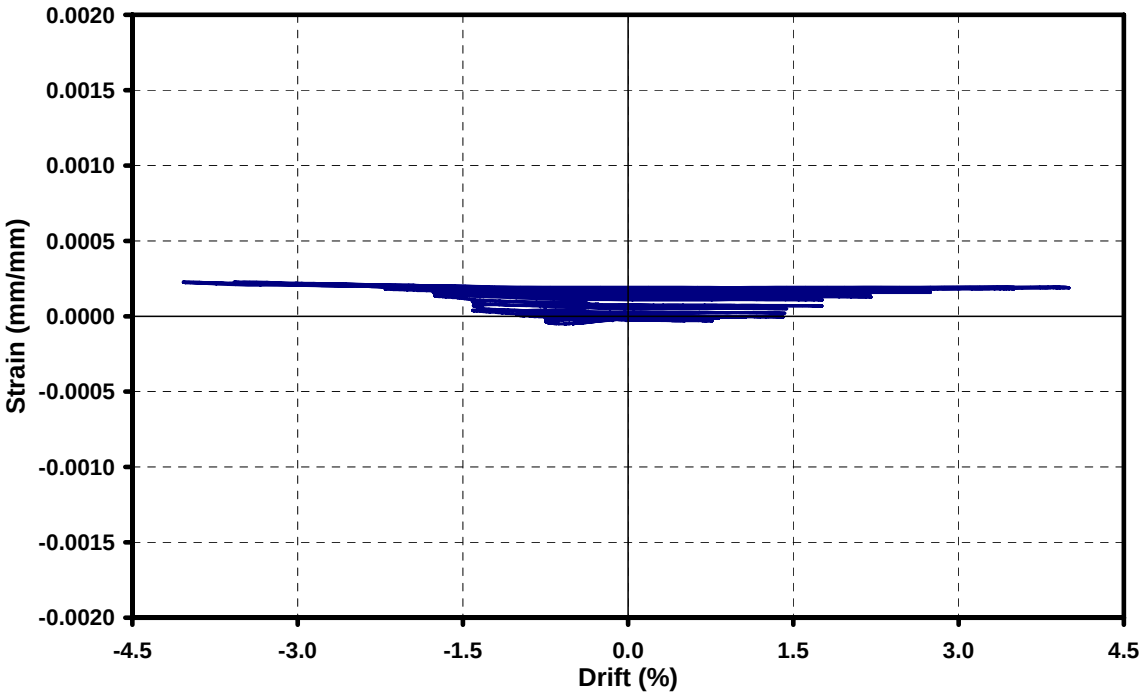

Figure 4.44. Strain versus drift graph of gauge #9 for US3-ES-Control

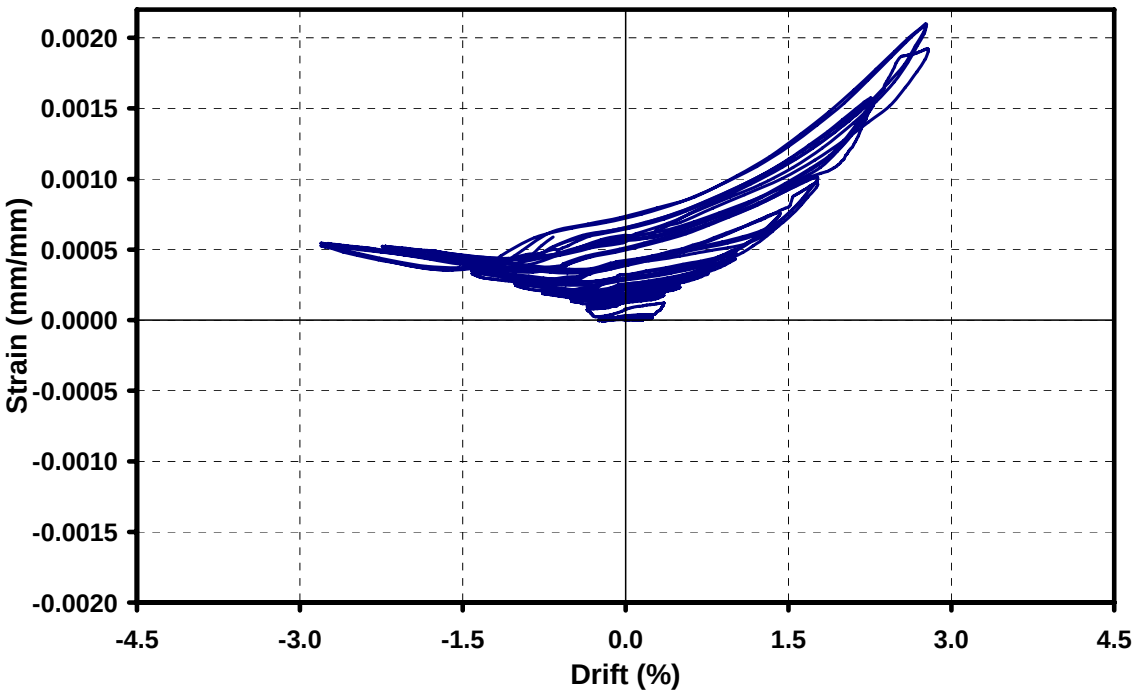

Figure 4.45. Strain versus drift graph of gauge #9 for US3-ES-FRP1

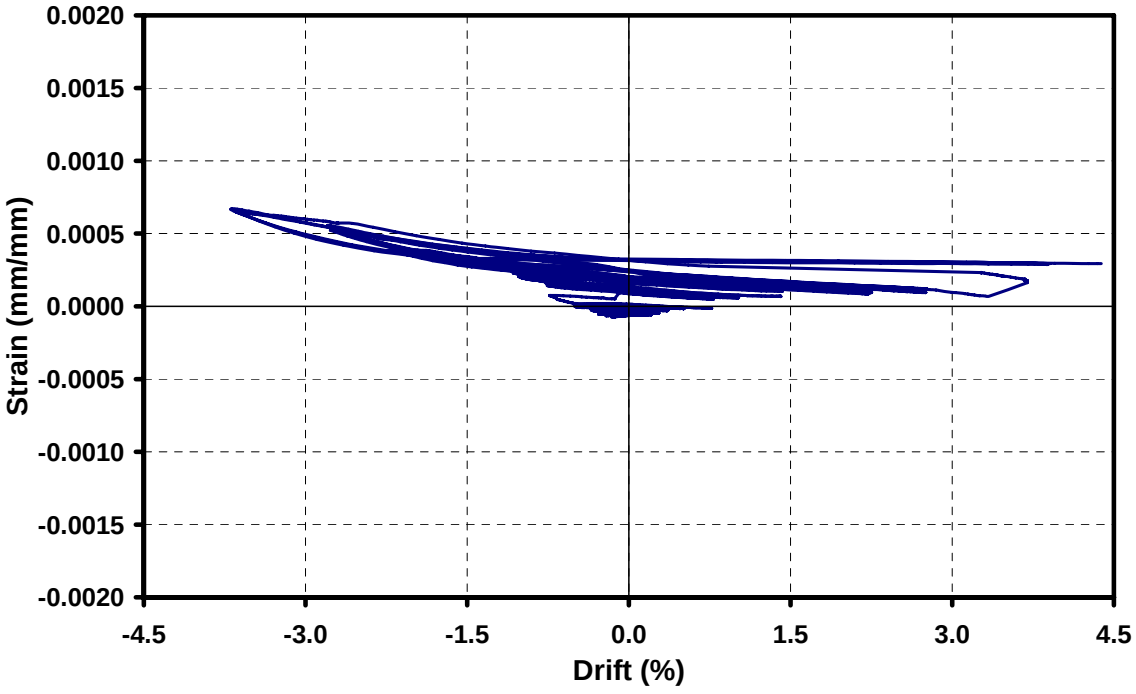

Figure 4.46. Strain versus drift graph of gauge #9 for US3-ES-FRP2

Transverse beam stirrups could be in tension due to shear deformation of the joint core and torsional forces which originated from the slab contribution. As shown in Figure 4.47, gauge #14 read smaller strains in this stirrup. This might stem from the shear deformations of this specimen (US3-E-Control) were lesser than the US3-ES-Control specimen. Otherwise, strain values of gauge #13 at US3-ES-Control reached very high levels (see Figure 4.48) due to excessive shear deformation and torsional crack. Torsional cracks occurred extensively in the zone where this stirrup was located.

Figure 4.49 illustrates the strain versus drift response of gauge #14 for US3-ES-FRP1 specimen. Maximum strain levels were also around 200 μs. CFRP strips on transverse beams and application of vertical and horizontal CFRP sheets on exterior side of the joint seems efficient to prevent the shear deformations and torsional cracks. Figure 4.50 shows the strain values of the stirrup for the US3-ES-FRP2 specimen.

Moreover, strains on stirrups located on the column were also not much more critical with respect to yielding strain level. Figure 4.51 illustrates the example of the strain gauge readings from US3-E-Control specimen.

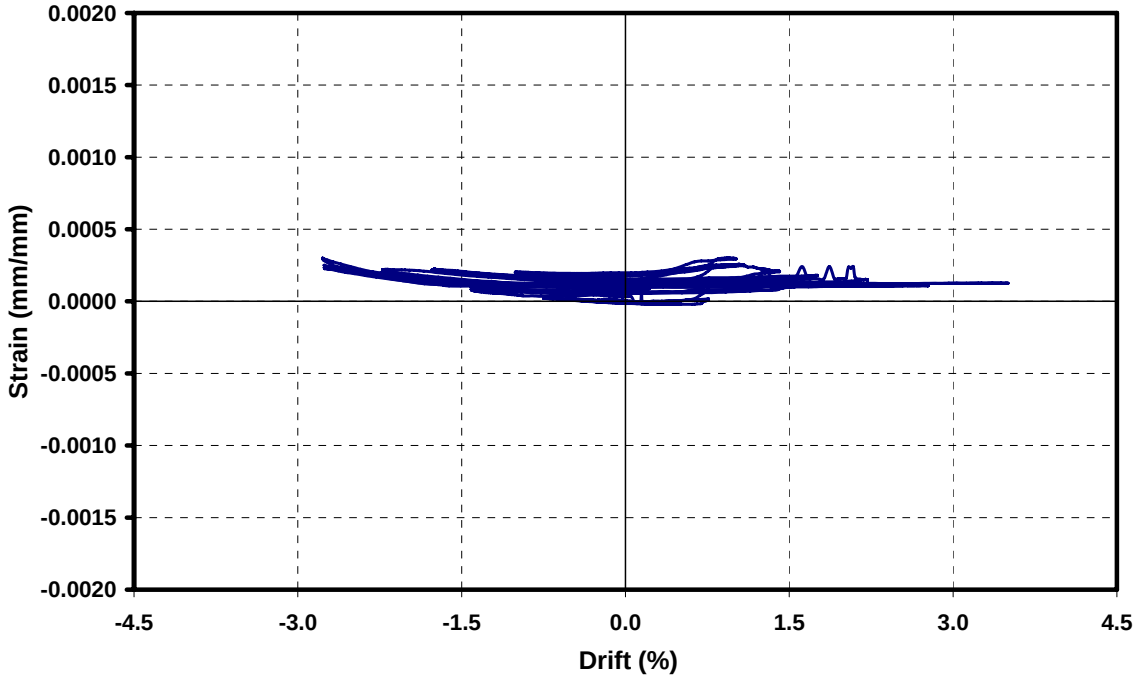

Figure 4.47. Strain versus drift graph of gauge #14 for US3-E-Control

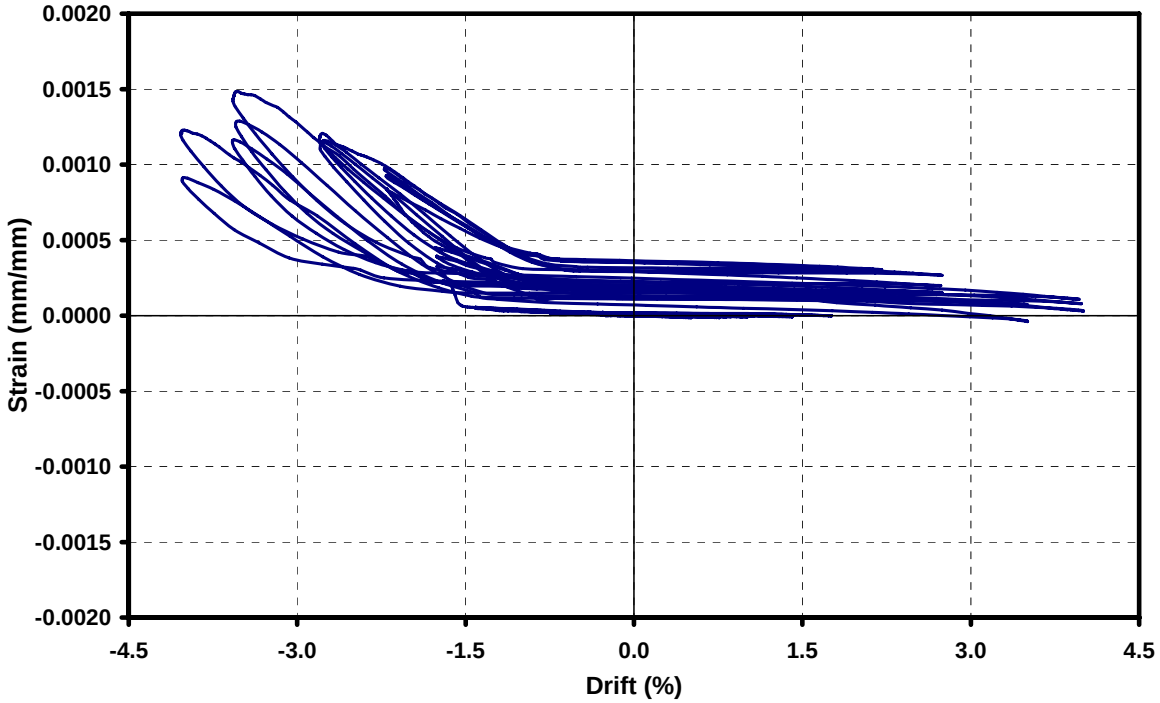

Figure 4.48. Strain versus drift graph of gauge #13 for US3-ES-Control

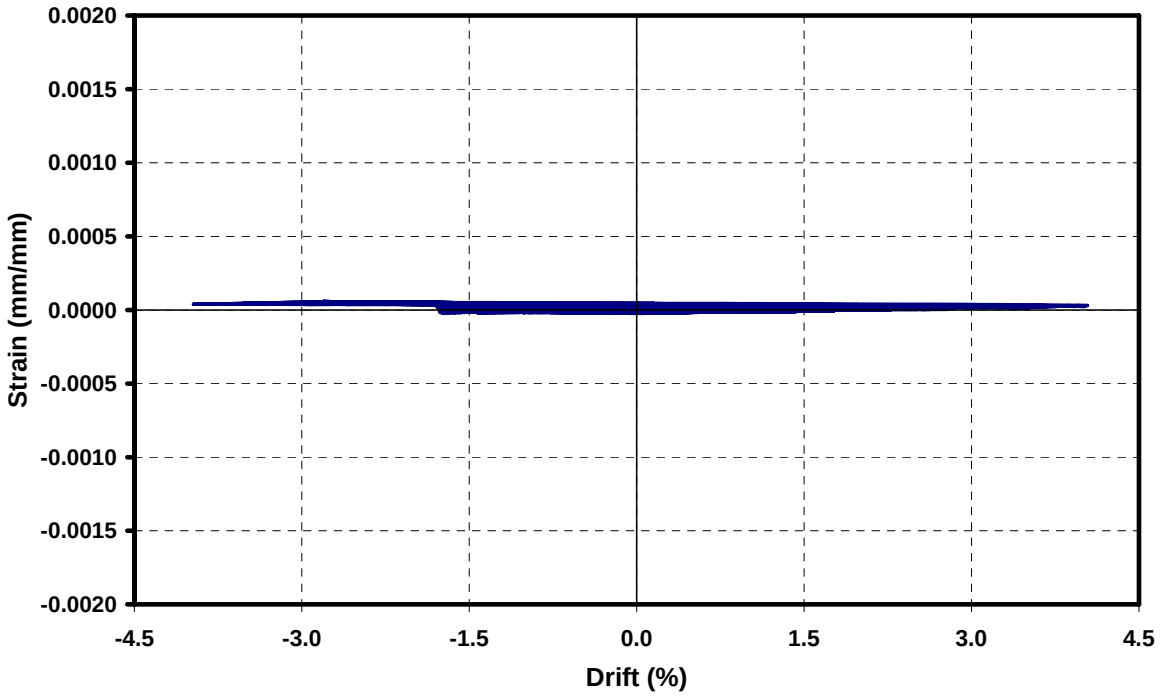

Figure 4.49. Strain versus drift graph of gauge #14 for US3-ES-FRP1

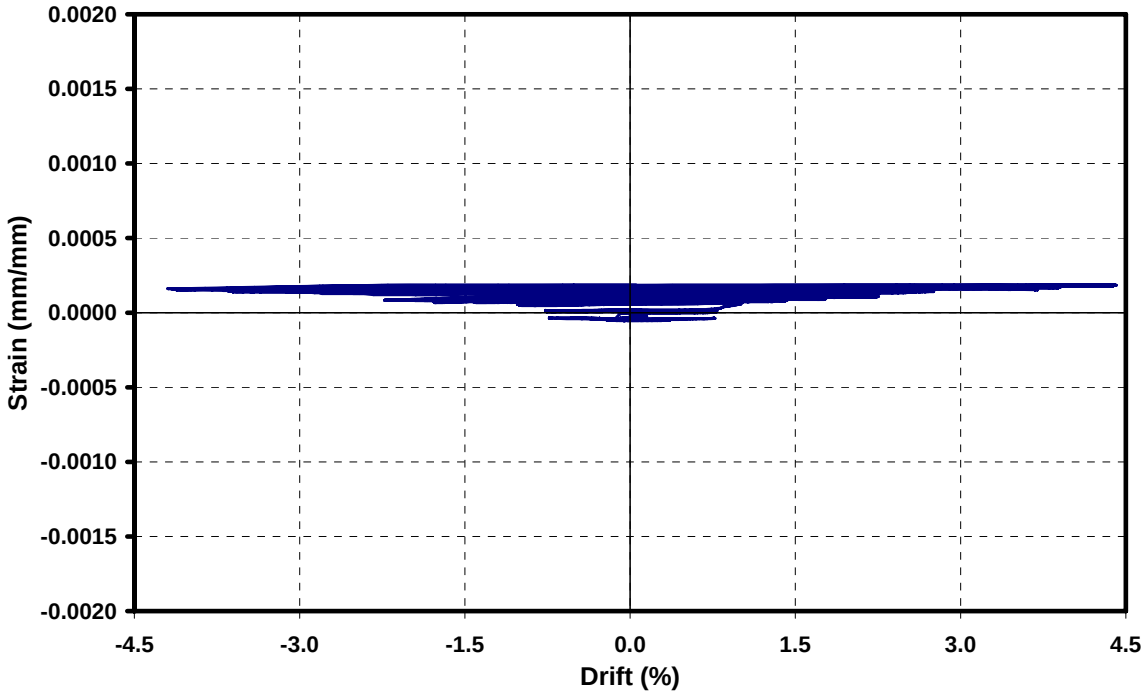

Figure 4.50. Strain versus drift graph of gauge #14 for US3-ES-FRP2

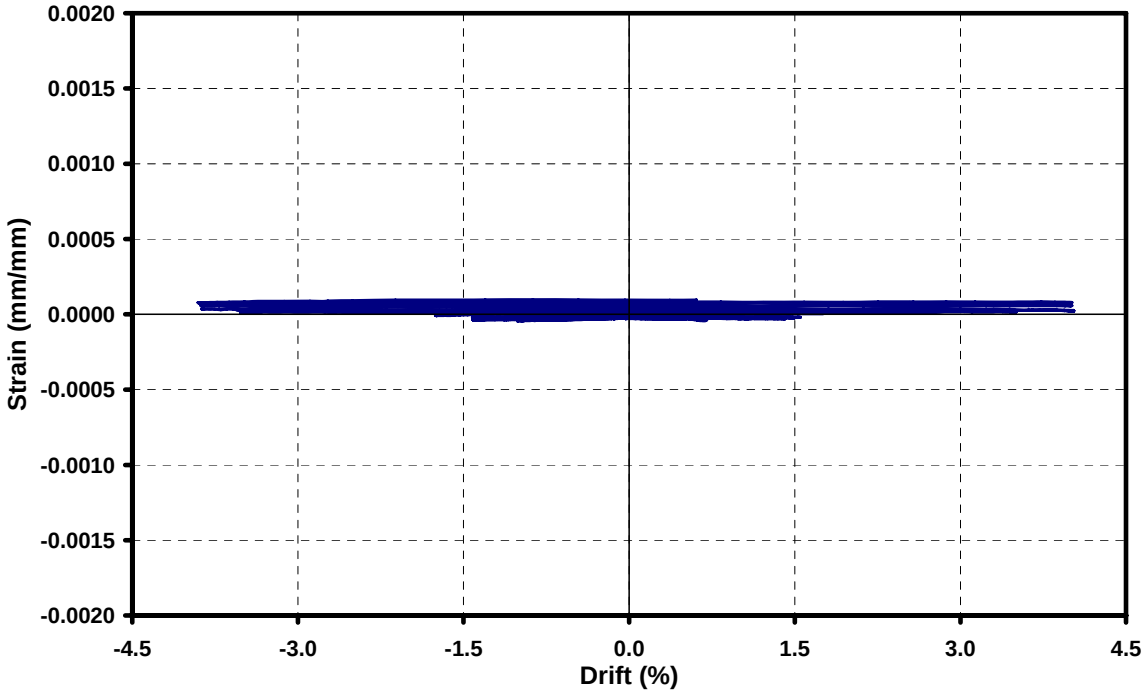

Figure 4.51. Strain versus drift graph of gauge #11 for US3-E-Control

4.7.3. Slab Bar Strains

Slab contribution is very important in determination of capacity of beam in both push and pull directions of loading, namely, under negative and positive moments. In order to estimate how much of the floor slab contribute in flexural capacity of the beam, strain gauges were mounted on rebars of floor slab. It was assumed only the rebars in the loading directions would work and therefore strains of these rebars were measured.

Slab rebars were located with an interval of 250 mm and they were selected as Ø10. Design details of reinforcements were given in the previous chapter. Locations of strain targets were given in Figure 4.52 once more.

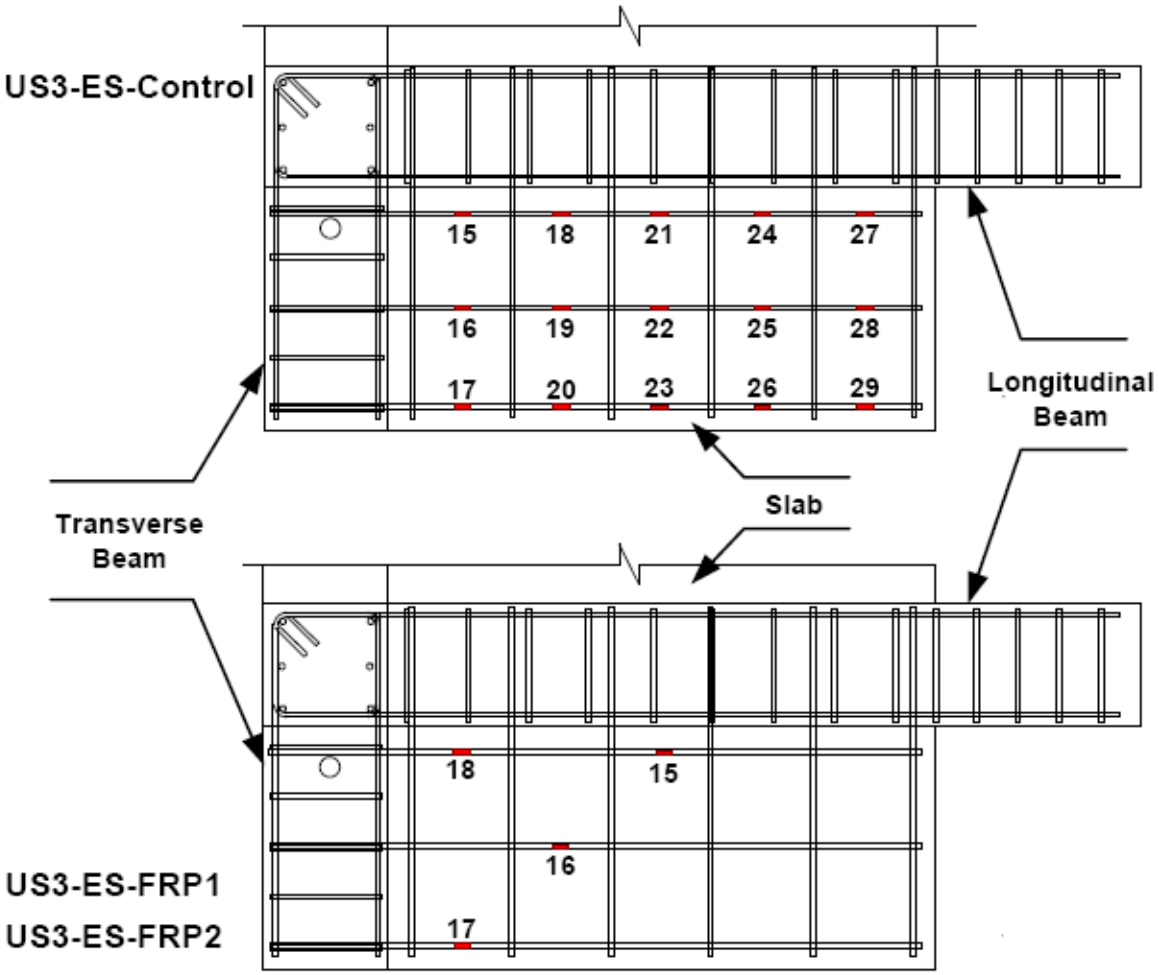

Figure 4.52. Location of strain gauges on rebars of floor slab

Figure 4.53 illustrates the cross section of longitudinal beam. Three lines of longitudinal slab reinforcements were identified as outer, middle and inner strips as shown in the figure.

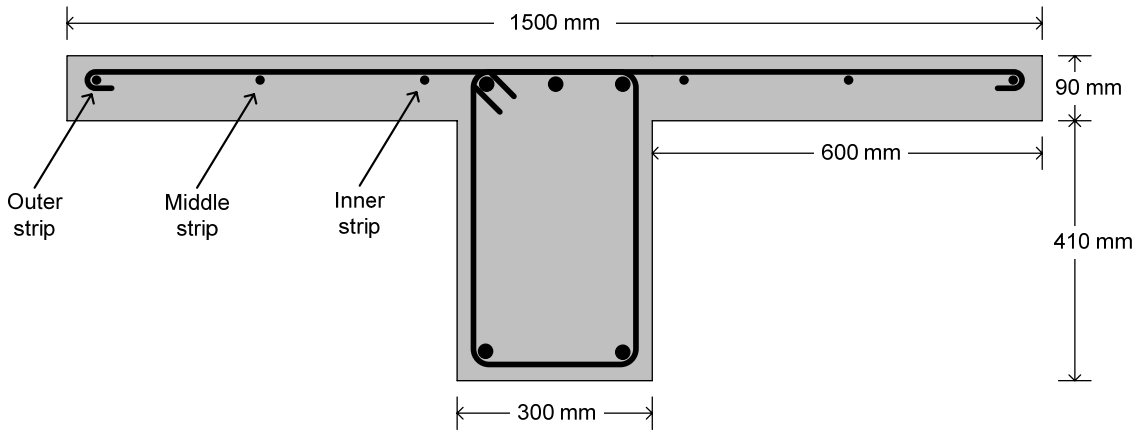

Figure 4.53. Distribution of slab reinforcement and their labels

As compared to US3-E control, for the US3-ES-Control specimen, contribution of the floor slab increased the capacity of the beam in pull direction of loading from 93 kN to 130 kN in terms of lateral load. In order to determine the contribution of slab rebars, strain gauges were mounted in all reinforcement in each interval (see Figure 4.52). However, some of the strain gauge data could not be realistic. Therefore, these data were neglected in evaluation of experimental results. Rest of the strain values were investigated carefully and some general remarks were drawn. First of all, strain values (strain gauge #23, #26, #29) were lesser on the exterior sides than those (strain gauge #18, #21, #24, #27) on the interior side (close to longitudinal beam) as it was expected. In the other direction, strain gauges read higher strain values when they were closer to transverse beam because the moment increased due to increased moment arm. Unfortunately, strain values could not be read properly for the middle strip of rebars, except strain gauge #25.

As examples of these strain gauge data, strain gauge #18 readings were illustrated in Figure 4.54. In the pull direction of loading, strain level reached more than 2000 μs and it was assumed as yield strain level. When the strain values of the inner strip were investigated carefully, it could be observed maximum strain values diminished from strain gauge #18 to #27. Maximum strain values of strain gauge #18, #21, #24 and #27 were 2200 μs, 1500 μs, 1100 μs and 400 μs respectively.

Whereas such detailed analysis could not be done for the middle strip of slab rebars, it is also possible to make a sufficient analysis for the outer strip. Maximum strain values of strain gauge #23, #26 and #29 were 1000 μs, 500 μs and 300 μs respectively. There are also diminishing strain values through end of the beam. Figure 4.55 illustrates the data of strain gauge #23 as an example.

For the CFRP retrofitted specimen (US3-ES-FRP1), all strain gauges on slab reinforcements worked almost properly. Figure 4.56-4.59 represent the strain versus drift relations of strain gauges #15, #16, #17 and #18, correspondingly. Similar stress distribution was also observed for this specimen. Maximum strain level was observed on the inner strip and this reached the yielding level. Strain gauges on middle and outer strips read smaller strains with respect to inner strip, or yielding level.

Figure 4.60 illustrates strain versus drift relation of strain gauge #16 for US3-ES-FRP2 specimen. It is clearly observed that strain levels are so similar with those of US3-ES-FRP1.

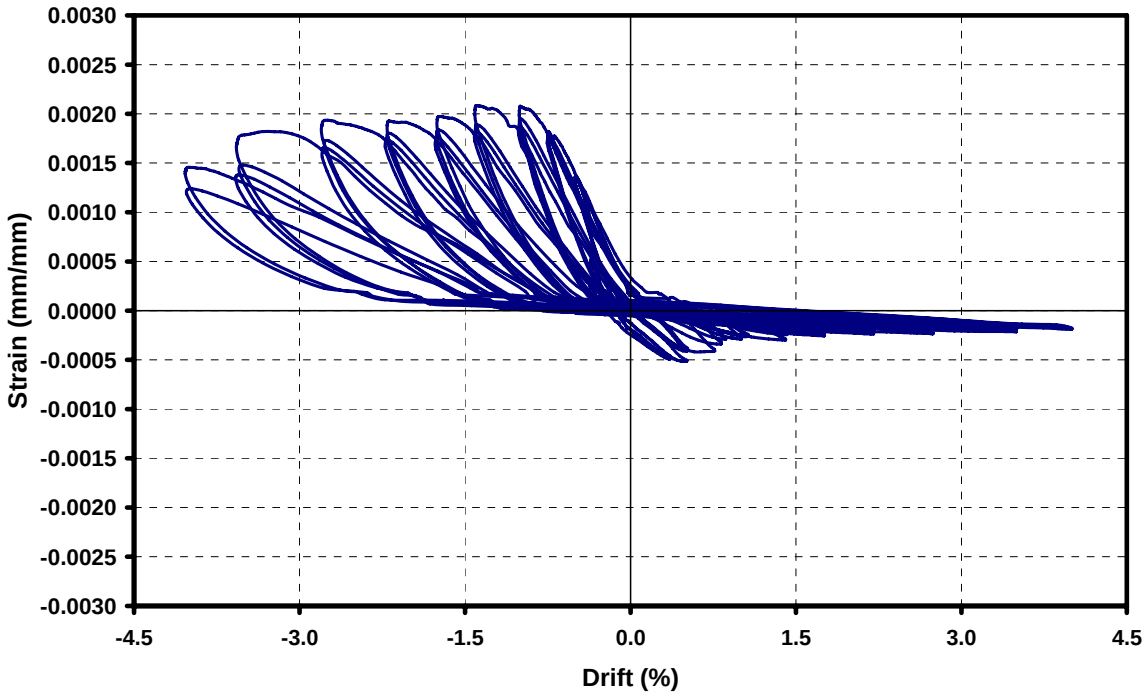

Figure 4.54. Strain versus drift graph of gauge #18 for US3-ES-Control

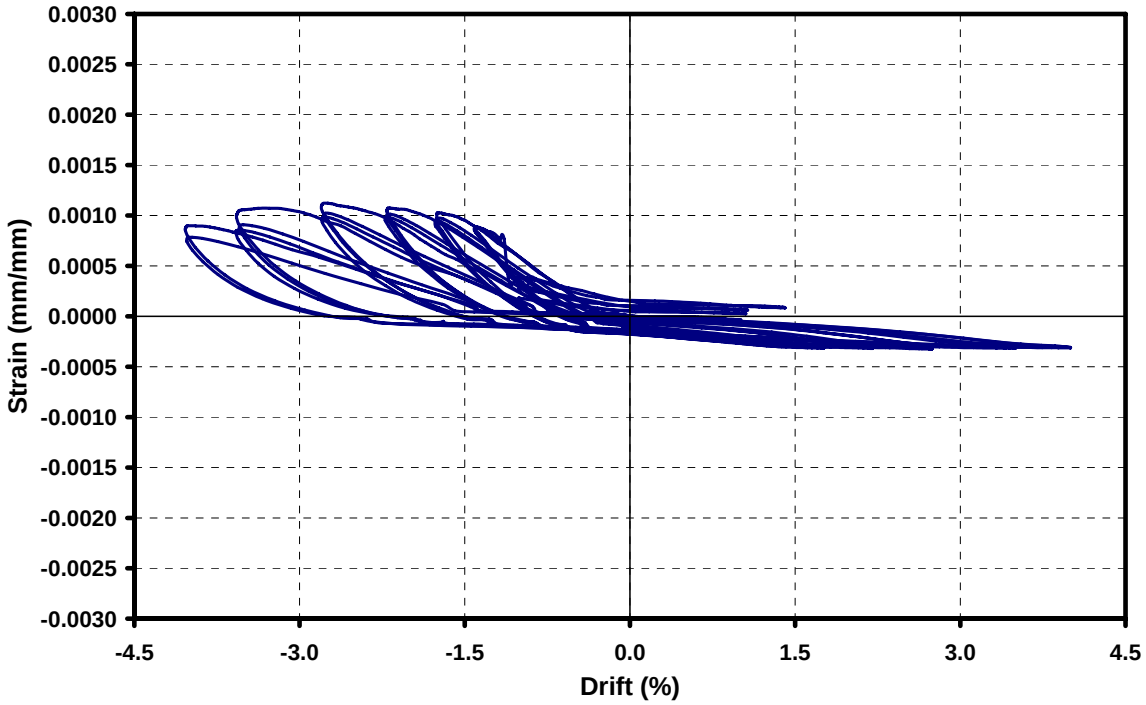

Figure 4.55. Strain versus drift graph of gauge #23 for US3-ES-Control

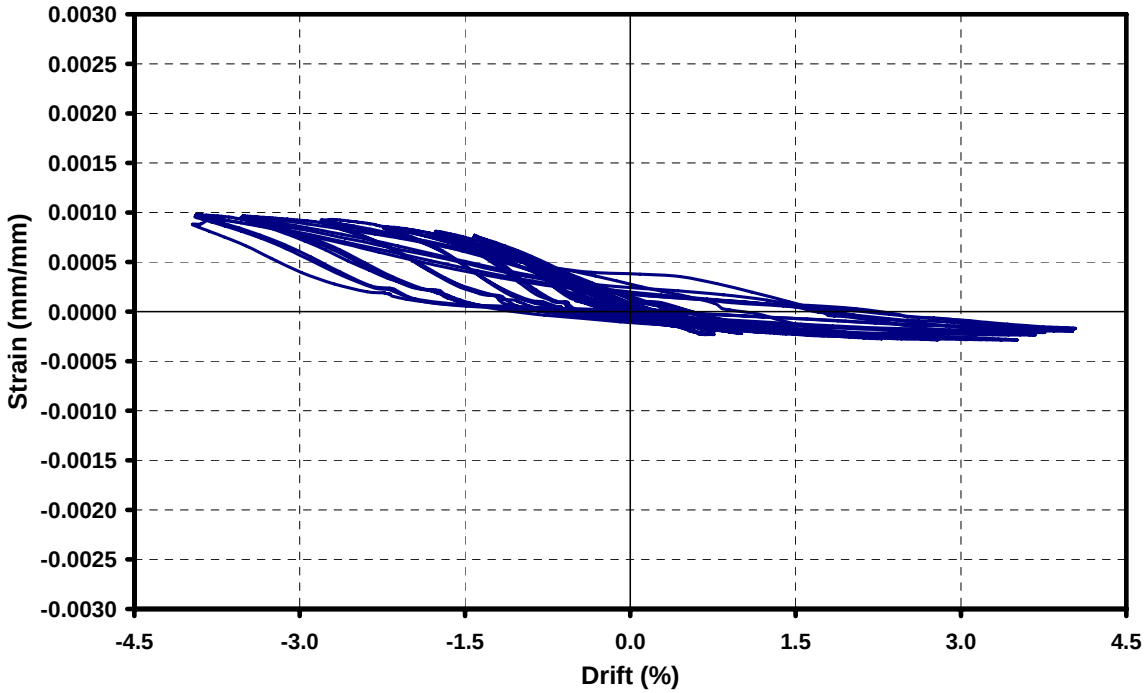

Figure 4.56. Strain versus drift graph of gauge #15 for US3-ES-FRP1

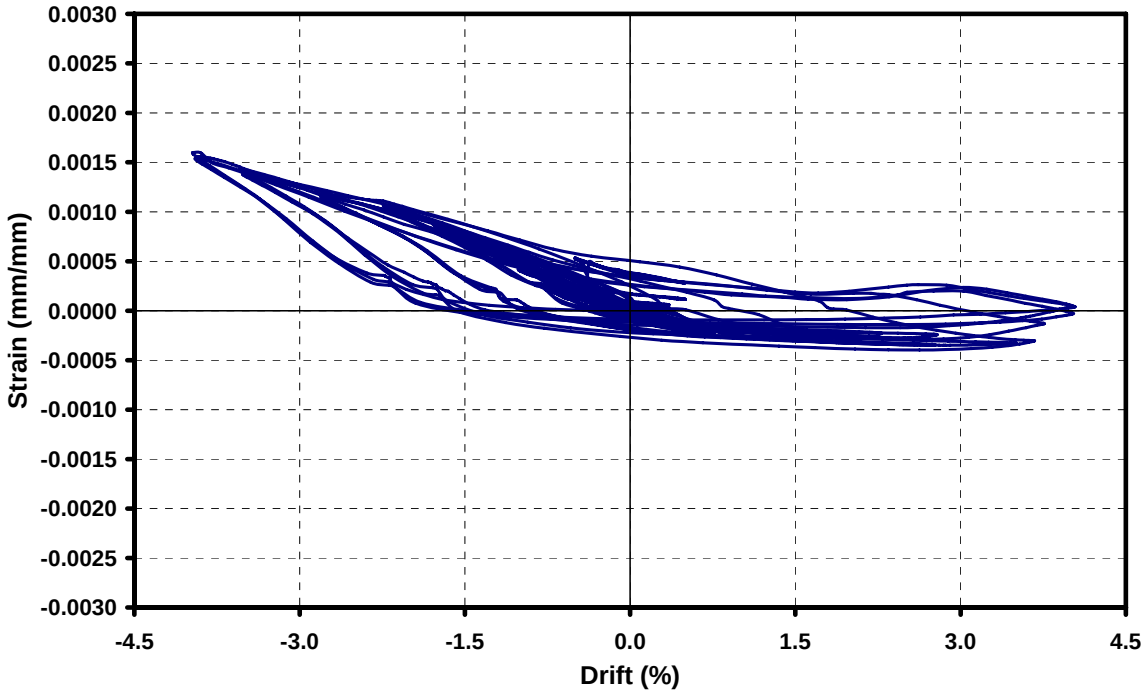

Figure 4.57. Strain versus drift graph of gauge #16 for US3-ES-FRP1

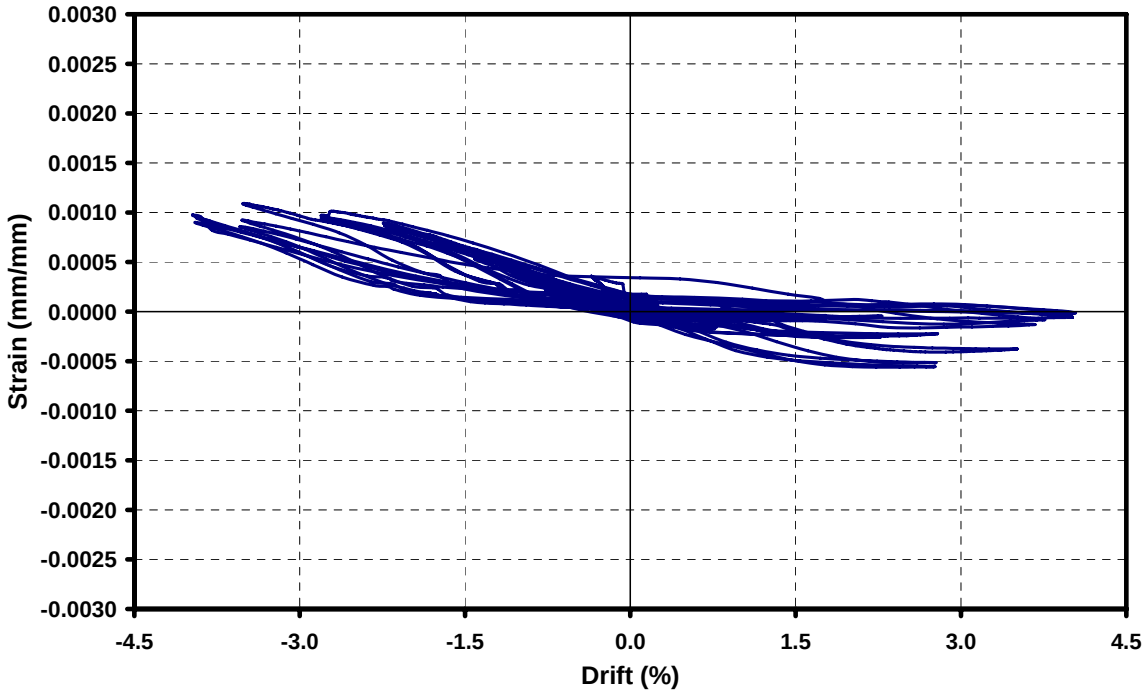

Figure 4.58. Strain versus drift graph of gauge #17 for US3-ES-FRP1

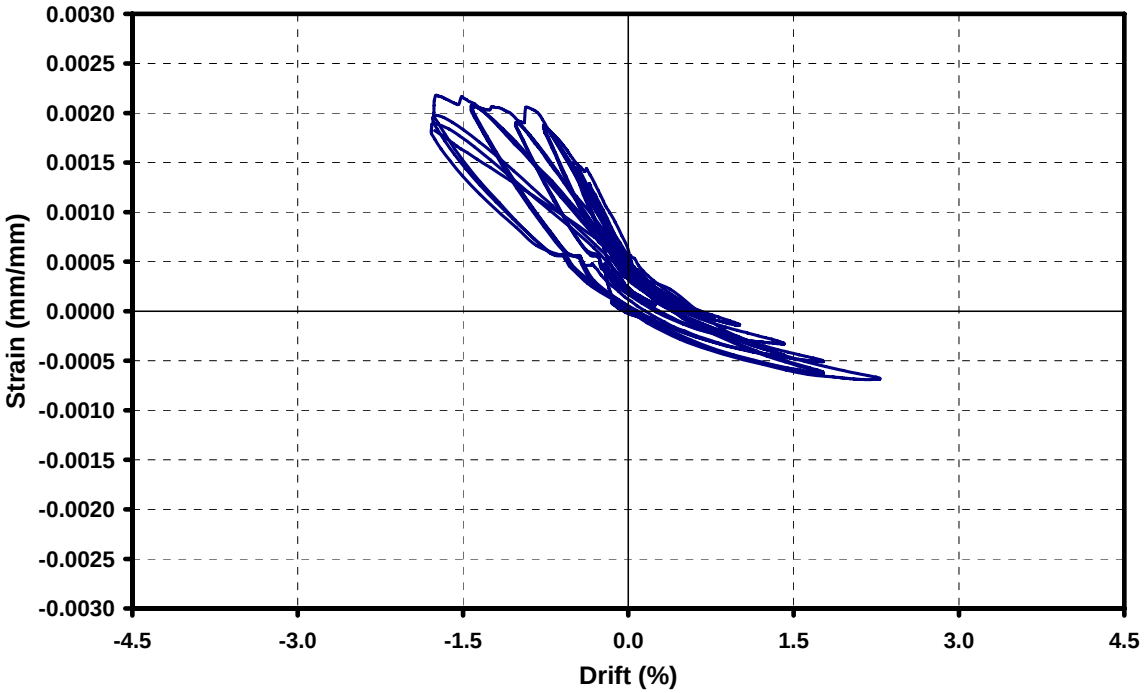

Figure 4.59. Strain versus drift graph of gauge #18 for US3-ES-FRP1

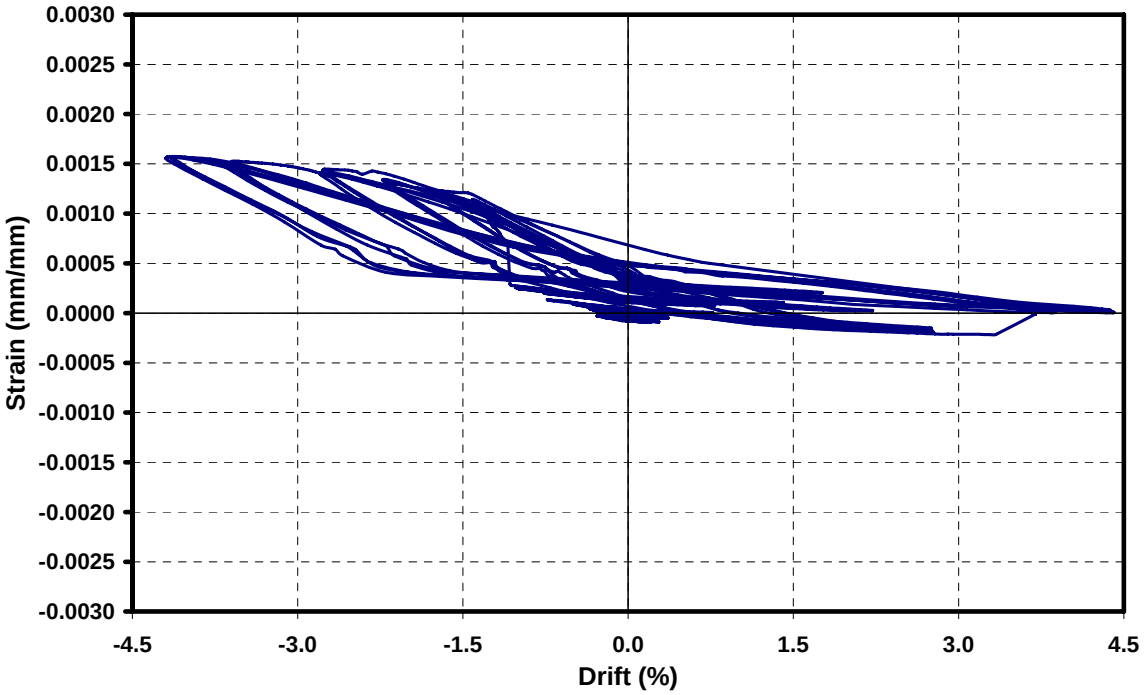

Figure 4.60. Strain versus drift graph of gauge #16 for US3-ES-FRP2

4.7.4. Column Bar Strains

Column bar strains are significant in terms of two main parameters. One is related to flexural capacity of the column, and the other is anchorage of column longitudinal bars with an inadequate lap splice just above the level of floor slab. In order to check these considerations, two strain gauges (straingauge #1 and #2) were mounted on two rebars at the same level on the spliced region. This strain levels should be the same if there is no slippage on these rebars. Furthermore,, strain level with respect to yielding level should be verified with a proper strain gauge reading (strain gauge #12). Figure 4.61 illustrates the locations of strain gauges.

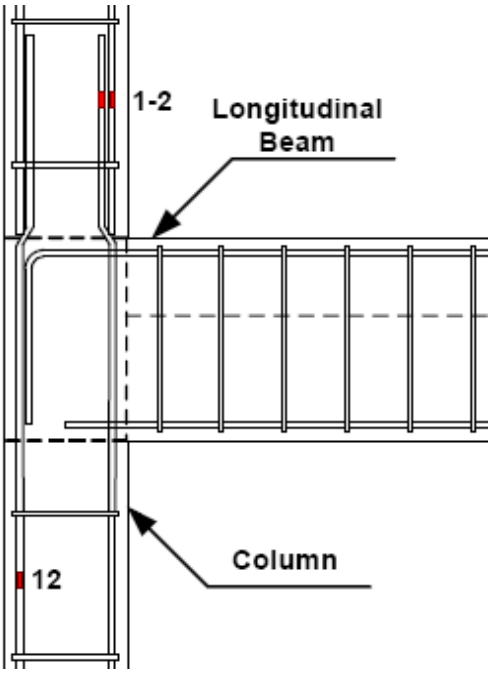

Figure 4.61. Location of strain gauges on longitudinal bars

Due to axial load on the column, there were initial strains on column rebars. In order to calculate the initial strain level, modulus of elasticity of the concrete was taken as 10% of the steel. According to these assumptions, initial strain due to 750 kN axial load was calculated as approximately 350 μs. this strain was added to the strain readings on the column longitudinal bars.

Figure 4.62 shows the strain versus drift relation of US3-ES-Control specimen as an example of all specimens. Typically, strain level of strain gauges was so limited due to

short moment arm and initial strain stemmed from axial load. In all specimens, difference in strain levels of column bars located at splice region was not observed. That is to say, slippage of rebars did not occur.

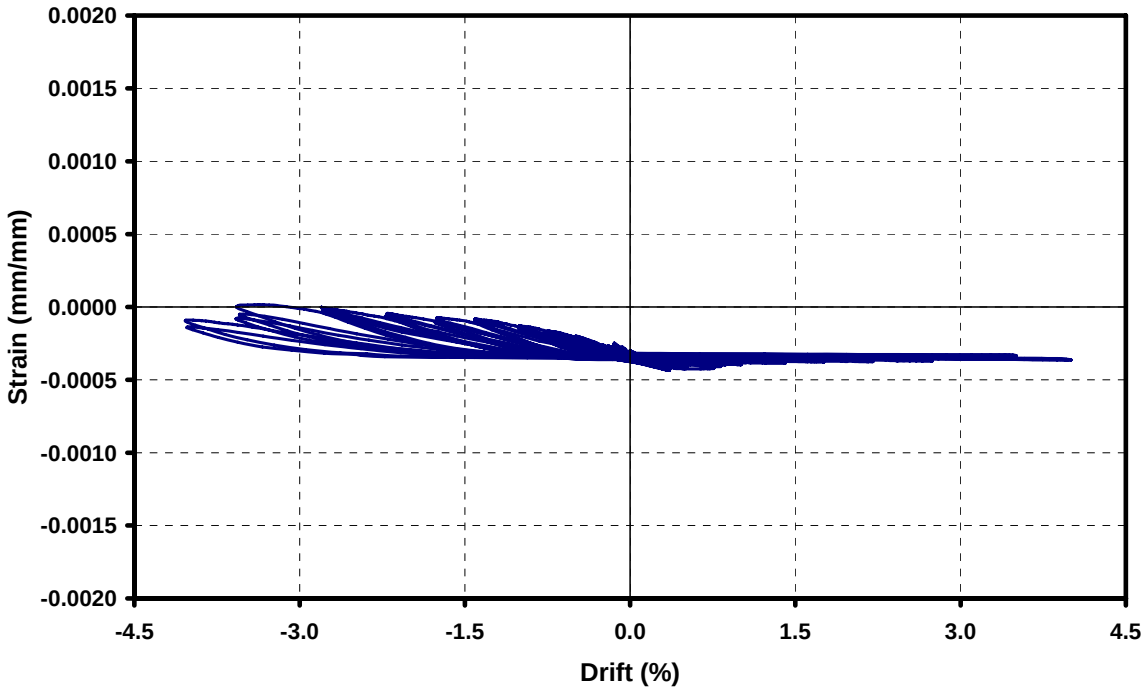

Figure 4.62. Strain versus drift graph of gauge #12 for US3-ES-Control

4.7.5. Strains on CFRP Sheets

In order to analyze the efficiency of CFRP sheets, the most proper method is examination of strain of these sheets by the help of strain gauge readings. According to the failure mode of US3-ES-Control specimen, critical locations of CFRP sheets, namely, the zones, where the higher tensile forces would be expected, were instrumented with strain gauges.

4.7.5.1. US3-ES-FRP1

Numerous strain gauges were applied to the US3-ES-FRP1 specimen and details of this application were illustrated in Figure 4.63. Table 4.5 summarizes maximum strain values read by strain gauges. By the help of these readings, utilization of these CFRP sheets can be defined and number of layers can be changed after proper analyses.

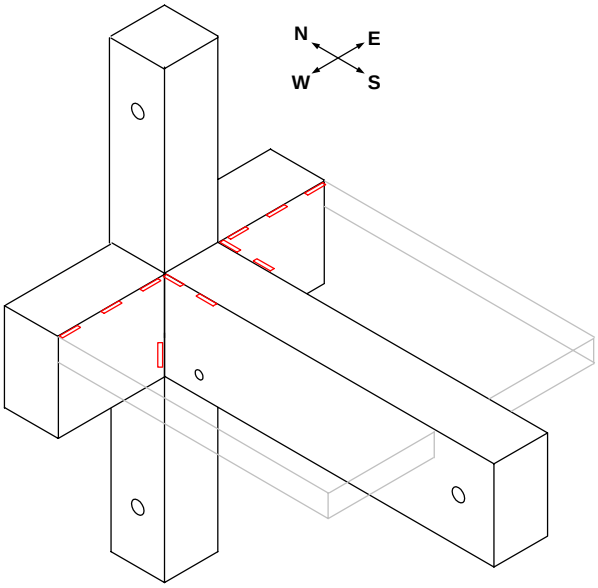

(a) 3-D View

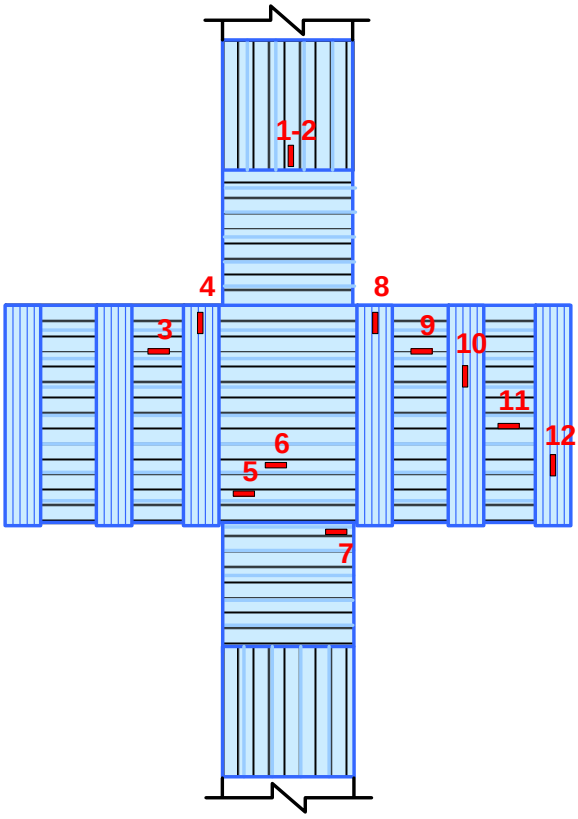

(b) North View

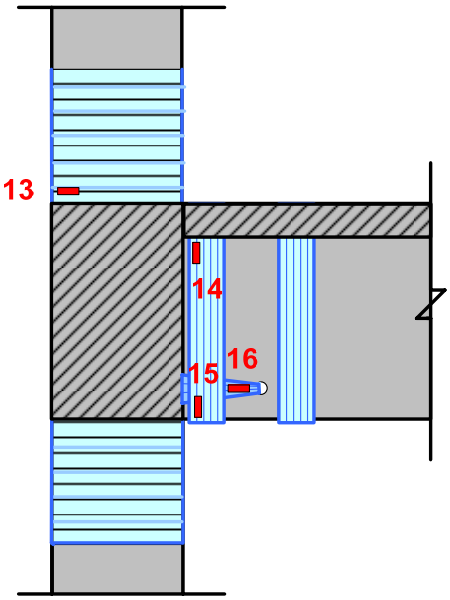

(c) West View

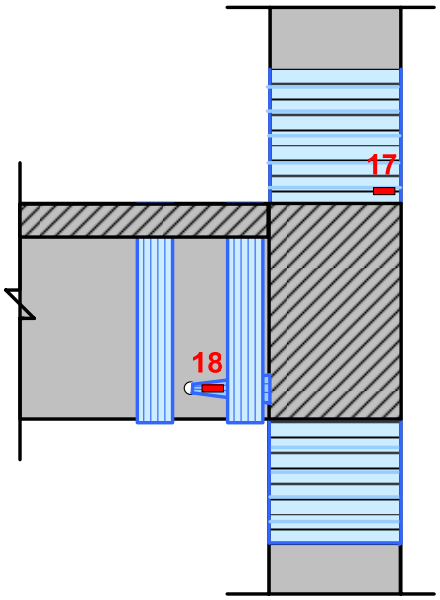

(d) East View

Figure 4.63. Locations of strain gauges on CFRP sheets for US3-ES-FRP1

Table 4.5. Strain gauge readings of US3-ES-FRP1

Gauge ID	Number of Layers	Maximum Strain Values (μs)	
		Compression	**Tension**
1	3	500	400
2	3	300	500
3	6	100	400
4	6	0	700
5	6	100	1100
6	6	300	1600
7	3	0	4700
8	6	0	1600
9	6	400	350
10	6	0	200
11	6	0	400
12	6	0	500
13	3	0	1300
14	6	100	1500
15	6	0	2400
16	6	0	6200
17	3	0	800
18	6	-	-

It is possible to draw some conclusions from these strain gauge data. First of all, maximum strain was measured at the belt layers as 6200 μs by strain gauge #16 (see Figure 4.67). Another strain gauge on the belt layers (strain gauge #18) did not work properly during the experiment. Therefore, this data have to be used for analysis. Such high strain confirmed that the belt layers came in very useful.

Secondly, maximum strain rates (strain gauges #13 and #17) at the layers which confined top column were around 1300 μs and 800 μs. These strains were not so critical; however, they confirmed that these CFRP sheets worked properly as confinement of top column. For the bottom column, the failure mode was different. The concrete block at the top of the bottom column was separated from the column due to slippage of the bottom rebars of longitudinal beam in the push direction of loading. The aim of confinement layers of bottom column was to prevent such separation and also to prevent separation of CFRP sheets used for flexural strengthening and slippage. The maximum strain value of strain gauge #7 was measured as 4700 μs.

FRP strips were applied at 8 different locations on both transverse and longitudinal beams. Details of these strips were given in the previous chapter and also Figure 4.63. Strips which are located close to the joint are named as inner strips; those located away from joint are named as outer strips both for transverse and longitudinal beams. Besides, the strips between these are named as middle strips for transverse beams.

These strips on longitudinal beam were applied in order to confine the beam, to prevent possible shear cracks and also to prevent possible debonding of FRP sheets applied for flexural strengthening. The inner strips (strain gauge 14&15) had the maximum strain values as 1500 μs and 2400 μs. The outer strip on longitudinal beam was not instrumented because it was not so important with respect to inner strip.

The strips on transverse beams were applied in order to confine the beams, to prevent possible shear cracks on joint and torsional cracks and also to prevent debonding of FRP sheets applied on north side of the specimen. The maximum strain value of the outer strip (strain gauge #12) was 500 μs. For the middle strip (strain gauge #10), the maximum strain value was 200 μs. It is possible that strain gauge did not work properly. The inner strips (strain gauge #4 and #8) reached maximum strain values as 700 μs and 1600 μs, respectively.

At the north side of the joint and transverse beams, FRP sheets were applied in order to prevent torsional crack and spalling of concrete at this side of the joint core due to bending of top rebars of longitudinal beam. Two strain gauges (#5 and #6) were mounted at this location. The maximum strain values were measured as 1100 μs and 1600 μs. Other maximum strain readings (straingauge #3, #9 and #11) were around 400 μs. The strain readings (strain gauges 1 and 2) on FRP sheets used for column flexure were around 500 μs again.

4.7.5.2. US3-ES-FRP2

Locations of strain gauges on FRP sheets and strain gauge readings for the US3-ES-FRP2 specimen, are given in Figure 4.65, and Table 4.6, respectively.

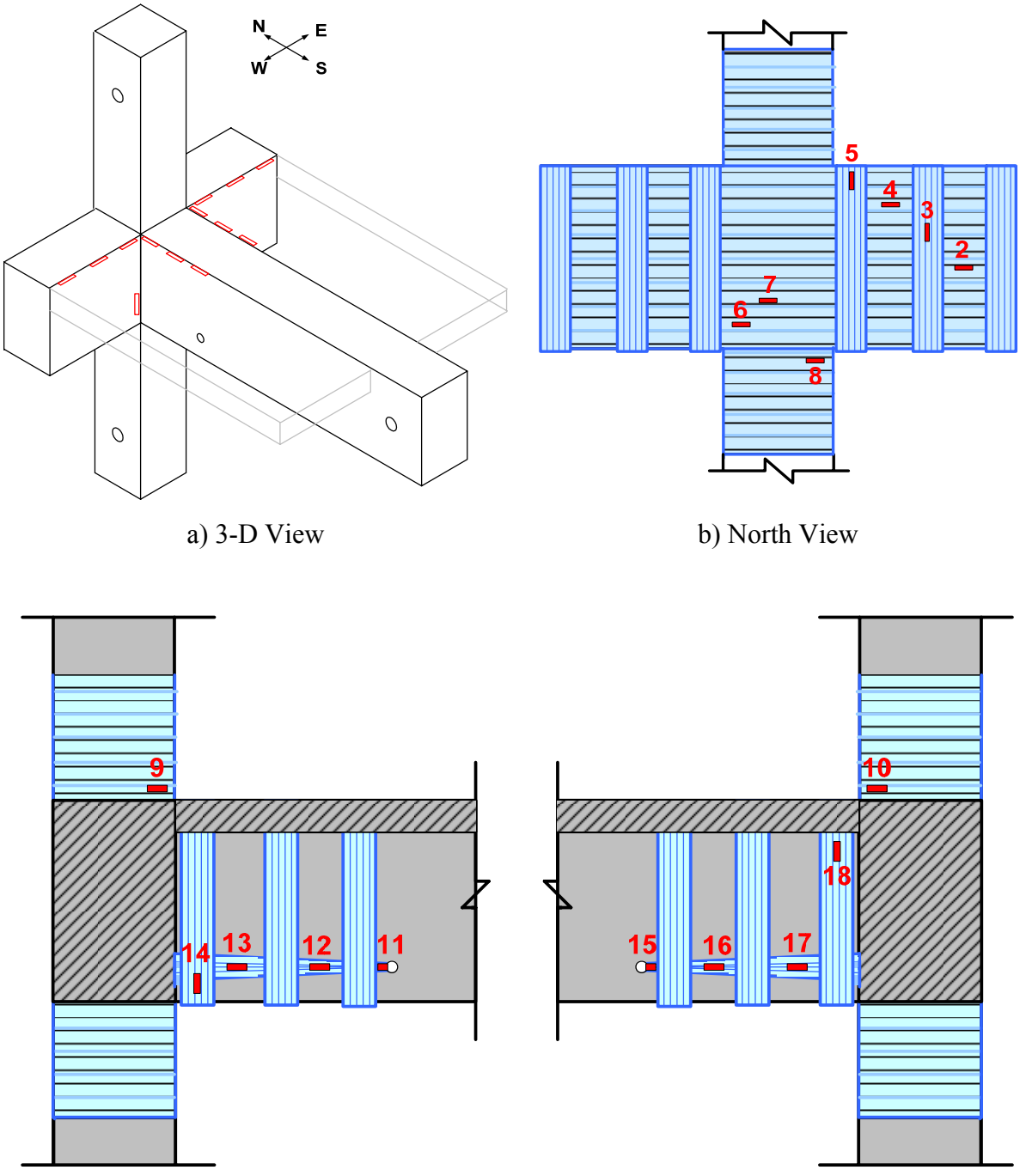

a) 3-D View

b) North View

c) West View

d) East View

Figure 4.64. Locations of strain gauges on CFRP sheets for US3-ES-FRP2

Table 4.6. Strain gauge readings of US3-ES-FRP2

Gauge ID	Number of Layers	Maximum Strain Values (μs)	
		Compression	**Tension**
1	6	100	100
2	6	50	100
3	6	50	150
4	6	250	650
5	6	150	1600
6	6	50	750
7	6	100	1300
8	3	400	700
9	3	50	1600
10	3	50	2200
11	6	200	3700
12	6	200	4700
13	6	600	600
14	6	100	1250
15	6	300	5200
16	6	250	3500
17	6	300	4400
18	6	500	2200

Strain readings exhibit very important conclusions on efficiency of CFRP sheets. Firstly, strain levels of CFRP belt layers are very high up to the slippage occurs. Afterwards, these readings fall down very sharply. This is an evidence of the rupture at the belt layers. The maximum strain was measured at the belt layers as 5200 μs by strain gauge #15. Such high strain confirmed that the belt layers work effectively up to the rupture strain of the CFRP sheets. Maximum strain of the strip which was located on the longitudinal beam was around 2200 μs. This strip works for the confinement as well as anchorage of the column flexural CFRP sheets.

FRP sheets used for confinement of the columns were also under high tensile forces. Maximum strain rates (strain gauges #9 and #10) at the layers which confined top column were around 1600 μs and 2200 μs, respectively. These layers were also used for anchorage of the L-shaped flexural sheets. For the bottom column, strain gauge did not work properly. Whereas the CFRP sheets ruptured, maximum strain level was around 700 μs. It must be higher than 5000 μs for the FRP rupture.

According to readings on CFRP strips at the transverse beams, only inner strips worked effectively. Other strips on the transverse beams were not subjected to high forces. CFRP sheets which were applied at the north (exterior) side of the joint and transverse beams were not subjected to high forces like in the first CFRP retrofitted specimen test.

Figures 4.65 and 4.66 show the strain versus drift relation on FRP belt for US3-ES-FRP1 and US3-ES-FRP2 specimens, respectively. In the first FRP retrofitted specimen, CFRP belt was not ruptured and therefore strain levels did not reached to zero. However, for the second specimen, CFRP belt was ruptured at 3.5% drift ratio and strain level reached almost zero.

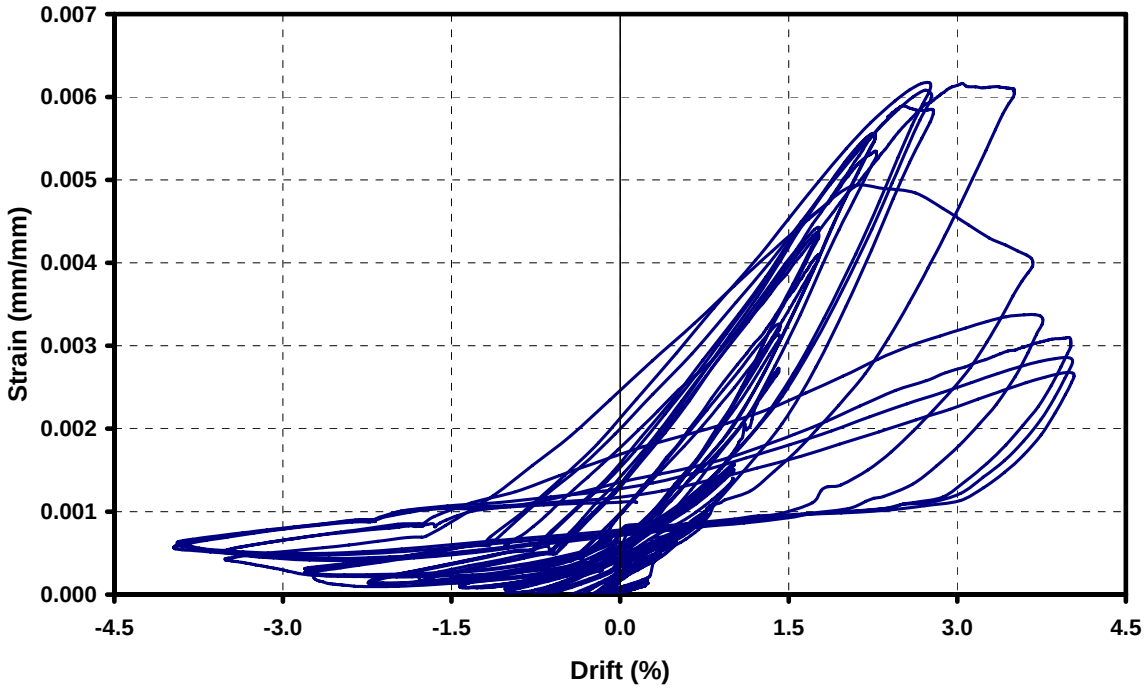

Figure 4.65. Strain versus drift graph of gauge on CFRP belt for US3-ES-FRP1

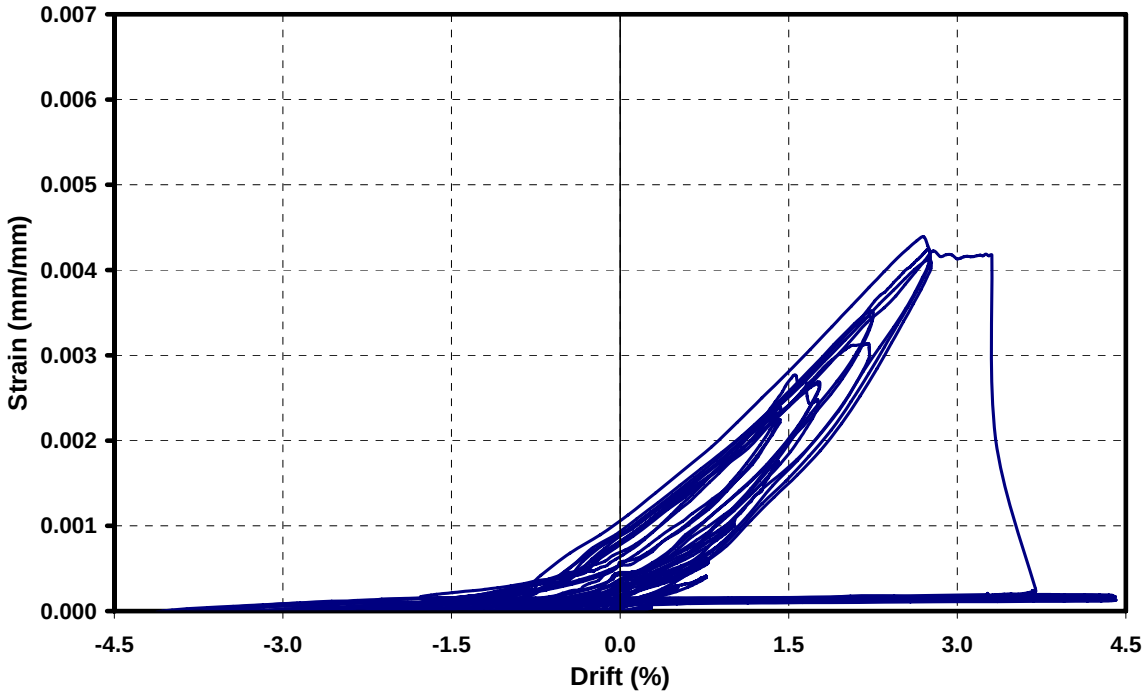

Figure 4.66. Strain versus drift graph of gauge on CFRP belt for US3-ES-FRP2

4.8. Comparison of Test Results between 2-D and 3-D specimens

The behavior of 2-D and 3-D control specimens is also discussed briefly, whereas they are not in the content of this thesis. 2-D specimen, US3-Control, is the beam-column joint specimen without transverse beams and floor slab. This specimen was produced and tested as a part of an ongoing NSF (grant no: OISE-0535294) and TUBITAK (grant no: ICTAG-I597-NSF103I026) research which has been conducted by Selçuk Altay (Ph.D. Candidate).

Figure 4.67 compares the backbone curves of these specimens. In the push direction of loading, slippage of the beam bottom reinforcement determine the failure mode of the joint. It can be obviously seen in the figure that the lateral load capacities are almost the same for all of the specimens and they exhibited similar behavior in push direction of loading.

However, in pull direction of loading, their load versus drift patterns differ from each other. At the initial drift levels, the tangent stiffness values (the slopes of the load versus displacement curves) of the specimens without floor slab are almost the same. After the

drift level of 0.75%, the load capacity of US3-Control specimen is decreased due to shear failure of the joint, whereas the US3-E-Control specimen shows a desired yielding behavior on longitudinal beam bars. Shear failure of the joint is prevented due to confinement effect of transverse beams. Furthermore, moment capacity of the beam of US3-ES-Control specimen was increased due to contribution of reinforcement of the floor slab and consequently the lateral load carrying capacity of the specimen was also increased.

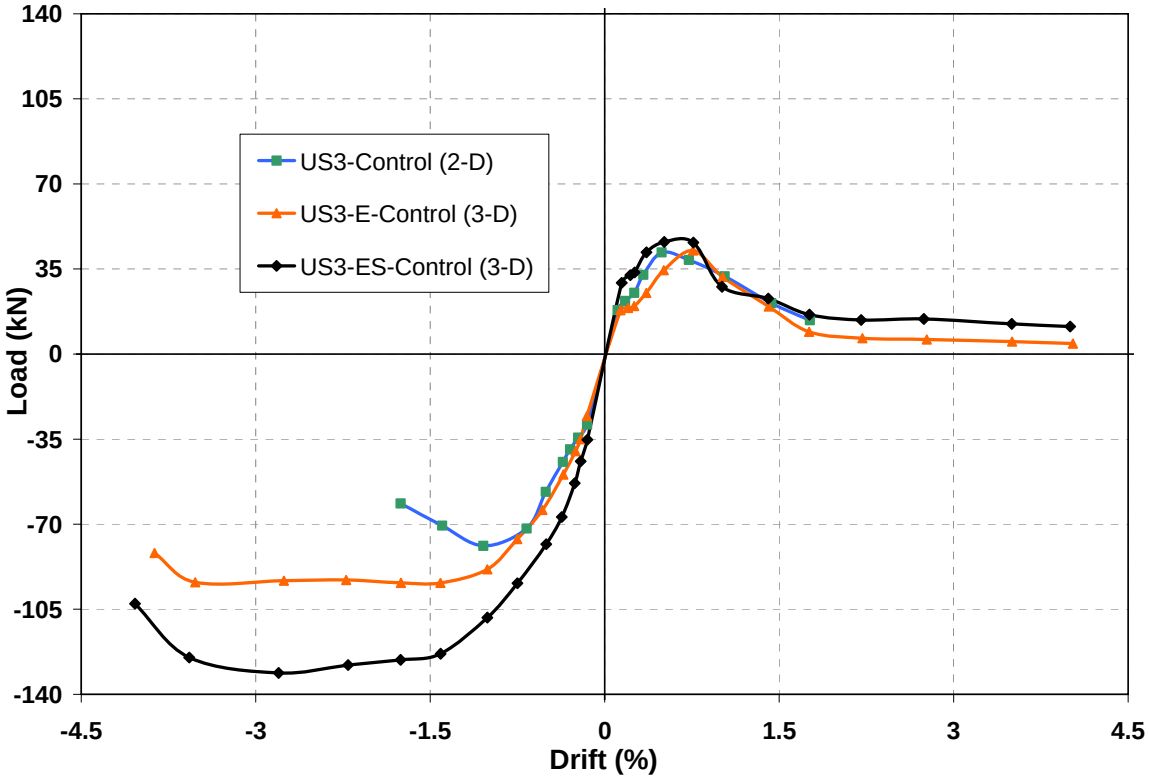

Figure 4.67 Comparison of test results of 2-D and 3-D specimens

5. SUMMARY AND CONCLUSIONS

5.1. Summary

Providing valuable test data on seismic performance of reinforced concrete exterior beam-column connections with and without floor slabs and determination of advanced retrofitting techniques are the primary motivation of the experimental study reported herein. In this experimental study, four reinforced concrete exterior beam-column subassemblies (three with slab and one without slab) were designed, constructed and tested under quasi-static cyclic lateral loading. Three of the subassemblies represented an exterior connection in a moment-resisting frame with a monolithic floor slab and transverse beams on two sides, and one symbolized a previously described exterior connection without floor slab, loaded in the longitudinal direction of the main (longitudinal) beam.

The tests specifically explored the effects of retrofitting techniques on seismically deficient beam-column-slab joints as well as the effect of floor slab and transverse beams on behavior of beam-column joints subjected to lateral earthquake loading. Performance of the test specimens was evaluated in terms of overall strength and stiffness, energy dissipation, joint shear deformation and strain behavior in various reinforcing bars.

Table 5.1 summarized the failure types of specimens in push and pull directions.

Table 5.1. Summary of failure types

Specimen	Failure Types	
	Push Direction	Pull Direction
US3-E-Control	Bond-Slip at 0.75% drift ratio No plastic hinging was observed, beam split from column at the beam-column interface.	Yielding at the beam top rebars at a distance of 150 mm away from the column surface.
US3-ES-Control	Bond-Slip at 0.75% drift ratio No plastic hinging was observed, beam split from column at the beam-column interface	Combined action of torsion, shear and anchorage, hinging did not occur.
US3-ES-FRP1	Bond-Slip at 3.50% drift ratio No plastic hinging was observed, beam split from column at a distance of 200 mm from column surface.	No significant strength degradation (less than 10%), hinging did not occur.
US3-ES-FRP2	Rupture of FRP (belt) at 3.50% drift ratio No plastic hinging, beam was split from column at the beam-column interface.	No significant strength degradation (less than 10%), hinging did not occur.

5.2. Conclusions

Shear deformations are very critical in the beam-column regions. In this experimental research, effect of transverse beams is evaluated and their confinement effect to prevent possible shear failure on the joint core could be seen obviously. It is concluded that shear deformations are limited and not so critical when transverse beams surround the joint core.

Effect of floor slab on behavior of beam-column joint could be observed as an increase in the moment carrying capacity of the beam. Therefore, calculated moment strength ratios between beams and columns could not be obtained and consequently desired yielding hierarchy could not be achieved when the contribution of the floor slab was neglected or underestimated. Lateral load was increased and therefore the shear forces acted on the joint increased. Finally, shear failure of the joint was observed in spite of yielding in the beam.

Bond-slip failure is observed as a sudden and catastrophic collapse of the joints. The failure also shows undesired behavior in terms of energy dissipation and stiffness degradation. Applied CFRP retrofitting methodologies were very effective in solving the slippage problem of beam bars which were inadequately embedded into joint core. According to test results, capacity of the beam-column joint increased approximately 100% after the retrofit with CFRP sheets.

In the overall behavior of the joint, lateral load capacities of CFRP retrofitting specimens were increased significantly. Rates of decrease in their stiffness degradation patterns were also improved. As a conclusion of these enhancements, energy dissipation capacity of the joint reached approximately twice of those of control specimens.

Finally, the research shows that application of CFRP retrofitting methods on a seismically deficient joint of a real structure can be easily achieved by using methodologies which were applied on the research.

During the experimental research, it was also observed that maximum strain level of CFRP sheets with epoxy resin were around 40% of the ultimate strain which were given by manufacturer.

5.3. Recommendations for Further Studies

During the experimental study, beam-column-slab subassemblies were tested in one direction only. Testing the specimens in two directions will be very helpful in understanding the behavior of beam-column joints under seismic action. Besides, having more experimental data on retrofitting methods will be useful in determination of more efficient rehabilitation of such seismically deficient structures.

In the next stage, tests on R/C frame specimens (with and without floor slab) after application of CFRP retrofitting will be very important in determination of efficiency of these retrofitting methods.

REFERENCES

ACI-ASCE Committee 315, 1957, "Manual of Standard Practice for Detailing Reinforced Concrete Structures", *American Concrete Institute*, Detroit.

ACI-ASCE Committee 315, 1965, "Manual of Standard Practice for Detailing Reinforced Concrete Structures", *American Concrete Institute*, Detroit.

ACI-ASCE Committee 318, 1956, "Building Code Requirements for Reinforced Concrete", *American Concrete Institute*, Detroit.

ACI-ASCE Committee 318, 1963, "Building Code Requirements for Reinforced Concrete", *American Concrete Institute*, Detroit.

ACI-ASCE Committee 318, 2002, "Building Code Requirements for Reinforced Concrete (ACI 318-02) and Commentary (ACI 318R-02)", *American Concrete Institute*, Farmington Hills, 443 pp.

ACI-ASCE Committee 352, 1985, "Recommendations for Design of Beam-Column Joints in Monolithic Reinforced Concrete Structures (ACI 352R-85)", *American Concrete Institute,* Detroit.

ACI-ASCE Committee 352, 2002, "Recommendations for Design of Beam-Column Joints in Monolithic Reinforced Concrete Structures (ACI 352R-02)", *American Concrete Institute.*

Aidoo, J., K. A. Harries and M. F. Petrou, 2006, "Full-Scale Experimental Investigation of Repair of Reinforced Concrete Interstate Bridge Using CFRP Materials", *Journal of Bridge Engineering*, ASCE, Vol. 11, No. 3, pp. 3550-358.

Alcocer S. and J. Jirsa, 1993, "Strength of Reinforced Concrete Frame Connections Rehabilitated by Jacketing", *ACI Structural Journal ,* Vol. 90, No. 3, pp. 249-261.

Altay, S., A. Parvin, C. Yalcin, and O. Kaya, 2007, "Evaluation of Existing Bond-Slip Models for R/C Joints," *the 9th Canadian Conference on Earthquake Engineering (9CCEE)* Ottawa, ON.

Antonopoulos, C. P. and T. C. Triantafillou, 2003, "Experimental Investigation of FRP-Strengthened RC Beam-Column Joints", *Journal of Composites for Construction*, ASCE, Vol. 7, No. 1, pp. 39-49.

Balsamo, A., A. Colombo, G. Manfredi, P. Negro and A. Prota, 2005, "Seismic Behavior of a Full-Scale RC Frame Repaired Using CFRP Laminates", *Engineering Structures,* Elsevier Ltd., Vol. 27, No. 5, pp. 769-780.

Beres, A., S. El-Borgi, R. White and P. Gergely, 1992, "Experimental Results of Repaired and Retrofitted Beam-Column Joint Tests in Lightly Reinforced Concrete Frame Buildings", *NCEER Report*, NCEER-92-0025.

Beres, A., S. P. Pessiki, R. N. White and P. Gergely, 1996, "Implications of Experiments on Seismic Behavior of Gravity Load Designed RC Beam-to-Column Connections", *Earthquake Spectra*, EERI, Vol. 12, No. 2, pp. 185-198.

Bonacci, J. and S. Pantazopoulou, 1993, "Parametric Investigation of Joint Mechanics", *ACI Structural Journal ,* Vol. 90, No. 1, pp. 61-71.

Chajes M. J., T. F. Januszka, D. R. Mertz, T. A. Thomson, and W. W. Finch, 1995, "Shear Strengthening of Reinforced Concrete Beams Using Externally Applied Composite Fabrics", *ACI Structural Journal ,* Vol. 92, No. 3, pp. 295-303.

Cheung, P. C., T. Paulay and R. Park, 1991, "New Zealand Tests on Full-Scale Reinforced Concrete Beam-Column-Slab Subassemblages Designed for Earthquake Resistance", *Design of Beam-Column Joints for Seismic Resistance (SP-123),* American Concrete Institute, Detroit, pp. 1-37.

Di Franco, M. A., D. Mitchell, P. Paultre, 1995, “Role of Spandrel Beams on Response of Slab-Beam-Column Connections”, *Journal of Structural Engineering,* ASCE, Vol. 121, No. 3, pp. 408-419.

Durrani, A. J. and H. E. Zerbe, 1987, “Seismic Resitance of R/C Exterior Connections with Floor Slab”, *Journal of Structural Engineering,* ASCE, Vol. 113, No. 8, pp. 1850-1864.

Durrani, A. J. and J. K. Wight, 1987, “Earthquake Resistance of Reinforced Concrete Interior Connections Including a Floor Slab”, *ACI Journal ,* Vol. 84, No. 5, pp. 400-406.

Ehsani, M. R. and J. K. Wight, 1985a, “Effect of Transverse Beam and Slab on Behavior of Reinforced Concrete Beam-to-Column Connections", *ACI Journal,* Vol. 82, No. 2, pp. 188-195.

Ehsani, M. R. and J. K. Wight, 1985b, “Exterior Reinforced Concrete Beam-to-Column Connections Subjected to Earthquake-type Loading”, *ACI Structural Journal,* Vol. 82, No. 4, pp. 492-499.

El-Amoury, T. and A. Ghobarah, 2002, “Seismic Rehabilitation of Beam-Column Joint Using CFRP Sheets”, *Engineering Structures,* Elsevier Ltd., Vol. 24, No. 11, pp. 1397-1407.

El-Salakawy, E. F., K. A. Soudki and M. A. Polak, 2004, “ Punching Shear Behavior of Flat Slabs Strengthened with Fiber Reinforced Polymer Laminates”, *Journal of Composites for Construction*, ASCE, Vol. 8, No. 5, pp. 384-392.

French, C. W. and A. Boroojerdi, 1987, “Contribution of R/C Floor Slabs in Resisting Lateral Loads”, *Journal of Structural Engineering,* ASCE, Vol. 115, No. 1, pp. 1-18.

French, C. W. and J. P. Moehle, 1991, "Effect of floor slab on behavior of slab-beam-column connections", *Design of Beam-Column Joints for Seismic Resistance (SP-123),* American Concrete Institute, Detroit, pp. 225-258.

Fujii, S. and S. Morita, 1991, "Comparison Between Interior and Exterior RC Beam-Column Joint Behavior", *Design of Beam-Column Joints for Seismic Resistance (SP-123),* American Concrete Institute, Detroit, pp. 97-123.

Gergely, J., C. P. Pantelides, R. J. Nuismer and L. D. Reaveley, 1998, "Bridge Pier Retrofit Using Fiber-Reinforced Plastic Composites", *Journal of Composites for Construction*, ASCE, Vol. 2, No. 4, pp. 165-174.

Gergely, J., C. P. Pantelides and L. D. Reaveley, 2000, "Shear Strengthening of RCT-Joint Using CFRP Composites", *Journal of Composites for Construction*, ASCE, Vol. 4, No. 2, pp. 56-64.

Ghobarah, A., T. S. Aziz, and A. Biddah 1997, "Rehabilitation of Reinforced Concrete Frame Connections Using Corrugated Steel Jacketing", *ACI Structural Journal,* Vol. 94, No. 3, pp. 282-294.

Ghobarah, A. and A. Said, 2002, "Shear Strengthening of Beam-Column Joints", *Engineering Structures,* Elsevier Ltd., Vol. 24, No. 7, pp. 881-888.

Ghobarah, A. and T. El-Amoury, 2005, "Shear Strengthening of RCT-Joint Using CFRP Composites", *Journal of Composites for Construction*, ASCE, Vol. 9, No. 5, pp. 408-416.

Goto, Y., O. Joh and T. Shibata, 1988, "Influence of Transverse Reinforcment in Beam Ends and Joints on the Behavior of R/C Beam-Column Subassemblages", *Proceeding of 9th WCEE,* Japan, Vol. 4, pp. 585-590.

Granata, P.J. and Parvin, A., 2001, "An Experimental Study on Kevlar Strengthening of Beam-Column Connections," *Composite Structures*, Vol. 53, No. 2, pp. 163-171.

Harajli, M. H. and K. A. Soudki, 2003, "Shear Strengthening of Interior Slab- Column Connections Using Carbon Reinforced Polymer Sheets", *Journal of Composites for Construction*, ASCE, Vol. 7, No. 2, pp. 145-153.

Harajli, M. H., K. A. Soudki and T. Kudsi, 2006, "Shear Strengthening of RCT-Joint Using CFRP Composites", *Journal of Composites for Construction*, ASCE, Vol. 10, No. 5, pp. 399-409.

Hwang, S. J and H. J Lee, 1999, "Analytical Model for Predicting Shear Strength of Exterior Reinforced Concrete Beam-Column Joint for Seismic Resistance", *ACI Structural Journal,* Vol. 96, No. 5, pp. 846-857.

Ichinose, T. 1991, "Interaction Between Bond at Beam Bars and Shear Reinforcement in RC Interior Joints", *Design of Beam-Column Joints for Seismic Resistance (SP-123),* American Concrete Institute, Detroit, pp. 379-399.

Kaku, T. and H. Asakusa, 1991, "Bond and Anchorage of Bars in Reinforced Concrete Beam-Column Joints", *Design of Beam-Column Joints for Seismic Resistance (SP-123),* American Concrete Institute, Detroit, pp. 401-423.

Kim, J, J. M. LaFave, 2007, "Key Influence Parameters for The Joint Shear Behavior of Reinforced Concrete (RC) Beam-Column Connections", *Engineering Structures,* Elsevier Ltd., Vol. 29, No. 10, pp. 2523-2539.

Kitayama, K., S. Otani and H. Aoyama 1991, "Development of Design Criteria for RC Interior Beam-Column Joints", *Design of Beam-Column Joints for Seismic Resistance (SP-123),* American Concrete Institute, Detroit, pp. 97-123.

Leon, R. T., 1991, "Towards New Bond and Anchorage Provisions for Interior Joints", *Design of Beam-Column Joints for Seismic Resistance (SP-123),* American Concrete Institute, Detroit, pp. 425-441.

Malek A. M. and H. Saadatmanesh, 1998, "Analytical Study of Reinforced Concrete Beams Strengthened with Web-Bonded Fiber Reinforced Plastic Plates or Fabrics", *ACI Structural Journal,* Vol. 95, No. 3, pp. 343-352.

Meinheit, D. F. and J. O. Jirsa, 1981, "Shear Strength of RC Beam-Column Connections", *Journal of Structural Division*, ASCE, Vol. 107, No. 11, pp. 2227-2244.

Moehle, J. P., 2000, "State of Research on Seismic Retrofit of Concrete Building Structures in the US", *US-Japan Symposium and Workshop on Seismic Retrofit of Concrete Structures*.

Mukherjee, A. and M. Joshi, 2005, "FRPC Reinforced Concrete Beam-Column Joints Under Cyclic Excitation", *Composite Structures,* Elsevier Ltd., Vol. 70, No. 2, pp. 185-199.

Pantazopoulou S. J. and C. W. French, 2001, "Slab Participation in Practical Earthquake Design of Reinforced Concrete Frames", *ACI Structural Journal,* Vol. 98, No. 4, pp. 479-489.

Park, R., 1989, "Evaluation of Ductility of Structures and Structural Assemblages from Laboratory Testing", *Bulletin of the New Zealand National Society for Earthquake Engineering,* Vol. 22, No. 3, pp. 155-166.

Paulay, T., R. Park, and M. J. N. Pristley, 1978, "Reinforced Concrete Beam-Column Joints under Seismic Actions", *ACI Journal ,* Vol. 75, No. 11, pp. 585-593.

Paulay, T. and M. J. N. Pristley, 1992, *Seismic Design of Reinforced Concrete and Masonry Buildings,* John Wiley & Sons, New York.

Prota, A., A. Nanni, G. Manfredi and E. Cosenza, 2000, "Seismic Upgrade of Beam-Column Joints with FRP Reinforcement", *Industria Italiana del Cemento*, November 2000.

Saadatmanesh, H., M. R. Ehsani, and L. Jin, 1996, "Seismic Strengthening of Circular Bridge Pier Models with Fiber Composites", *ACI Structural Journal,* Vol. 93, No. 6, pp. 639-647.

Sezen, H., K. J. Elwood, ; A. S. Whittaker, K. M. Mosalam, J. W. Wallace, J. F. Stanton, 2000, "Structural engineering reconnaissance of the August 17, 1999 earthquake: Kocaeli (Izmit), Turkey", *PEER Report,* Pacific Earthquake Engineering Research Center, University of California, Berkeley, No. 2000/09, 154 pp.

Sin, M., 2004, Performance of Reinforced Concrete Edge Beam-Column-Slab Connections Subjected to Earthquake Loading, Ph.D. Dissertation, University of Illinois at Urbana, Champaign.

Teng, J. G. (Editor), 2001, FRP composites in civil engineering: proceedings of the International Conference on FRP Composites in Civil Engineering, Elsevier, New York.

Triantafillou T. C., 1998, "Shear Strengthening of Reinforced Concrete Beams Using Epoxy-Bonded FRP Composites", *ACI Structural Journal,* Vol. 95, No. 2, pp. 107-115.

REFERENCES NOT CITED

Abdel-Fattah, B. and J. K. Wight, 1987, "Study of Moving Beam Plastic Hinging Zones for Earthquake-resistant Design of R/C Buildings", *ACI Structural Journal,* Vol. 84, No. 1, pp. 31-39.

Abrams, D. P., 1987, "Scale Relations for Reinforced Concrete Beam-Column Joints", *ACI Structural Journal,* Vol. 84, No. 6, pp. 502-512.

Durrani, A. J. and J. K. Wight, 1985, "Behavior of Interior Beam-to-Column Connections Under Earthquake Type Loading", *ACI Journal ,* Vol. 82, No. 3, pp. 343-349.

Ehsani, M. R., A. E. Moussa, and C. R. Vallennilla, 1987, "Comparison of Inelastic Behavior of Reinforced Ordinary- and High-Strength Concrete Frames", *ACI Structural Journal,* Vol. 84, No. 17, pp. 161-169.

Ichimasu, H., 1993, "RC Slabs Strengthened by Bonded Carbon FRP Plates: Part 1--Laboratory Study", *Special Publication-138,* American Concrete Institute, Detroit, pp. 933-956.

Kaku, T. and H. Asakusa, 1991, "Ductility Estimation of Exterior Beam-Column Subassemblages in Reinforced Concrete Frames", *Design of Beam-Column Joints for Seismic Resistance (SP-123),* American Concrete Institute, Detroit, pp. 167-186.

Leon, R. and J. O. Jirsa, 1986, "Bidirectional Loading of R.C. Beam-Column Joints", *Earthquake Spectra*, EERI, Vol. 2, No. 3, pp. 537-560.

Paulay, T., 1986, "A Critique of the Special Provisions for Seismic Design of the Building Code Requirements for Reinforced Concrete (ACI 318-83)", *ACI Journal ,* Vol. 83, No. 2, pp. 274-283.

Vecchio, F. J. and M. P. Collins, 1986, “The modified compression field theory for reinforced concrete elements subjected to shear”, *ACI Structural Journal ,* Vol. 83, No. 2, pp. 219-231.